Single-unit studies of visual motion processing in cat extrastriate areas

Helmholtz  Institute

School for Autonomous Systems Research

Cover design: Robert van Sluis

Single-unit studies of visual motion processing in cat extrastriate areas

Enkel-cel studies van visuele bewegingsverwerking in extrastriate gebieden van de kat
(met een samenvatting in het Nederlands)

Proefschrift

ter verkrijging van de graad van doctor aan de Universiteit Utrecht op gezag van de Rector Magnificus, Prof. Dr W.H. Gispen, ingevolge het besluit van het College voor Promoties in het openbaar te verdedigen op vrijdag, 13 juni 2003 des middags te 12.45 uur

door

Ildikó Vajda
geboren op 27 september 1972 te Kula

promotor:	Prof. Dr Ir W.A.P.F.L. van de Grind
copromotor:	Dr Ir M.J.M. Lankheet
	Faculteit Biologie

Universiteit Utrecht

beoordelingscommissie:	Dr J.E.J. Duysens
	Prof. Dr J.J. Koenderink
	Dr A.J. van Doorn
	Dr J. van Pelt
	Prof. Dr U. Eysel
opponenten:	Prof. Dr J.J. Koenderink
	Dr A.J. van Doorn
	Dr J. van Pelt
	Prof. Dr C.J. Erkelens
	Prof Dr V.A. Lamme

CIP-DATA KONINKLIJKE BIBLIOTHEEK, DEN HAAG
Vajda, Ildikó
Single-unit recordings of visual motion processing in cat extrastriate areas/
Ildikó Vajda.-Utrecht: Universiteit Utrecht, Faculteit Biologie
Thesis Universiteit Utrecht.-with ref.-With summary in Dutch.
ISBN 90-393-3403-X
Subject headings: cat visual cortex/single-unit

When the arrow is in a place just its own size, it is at rest.
At every moment of its flight, the arrow is in a place just its own size.
Therefore, at every moment of its flight, the arrow is at rest.

(Zeno)

Contents

Introduction

General Introduction

Proper processing of visual motion information is critical for our everyday behavior. Just think of our ability to avoid undesirable collisions or the ease with which we segregate moving objects from their background. It is evident, that motion detection is crucial for non-human animals as well: avoiding predators or hunting for food would be impossible without a reliable motion processing system. Actually, one can hardly imagine a life without the ability to use motion information for interacting with the environment. Indeed, no animal with vision has been found that lacks a mechanism for motion processing (Nakayama, 1985).

Revealing the operational mechanisms of motion perception has been a great intellectual challenge for a long time, from Euclid and Aristotle (ca. 300 B.C.), through Ptolemy (ca. 150 A.C), Leonardo da Vinci (ca. 1500 A.C.) and Purkinje (nineteenth century), just to mention some of the more notable thinkers, to the present time.

Probably because of his pioneering role in the foundations of neural models of vision, Exner's work is considered to be the first 'modern' approach to motion perception. He was the first to show that motion is a fundamental visual dimension and to suggest that the brain somehow computes direction and velocity of moving objects. Since then, scientists have been debating over which variables of visual motion are being processed when and where along the visual pathway(s). One of the key features of motion sensitivity is direction selectivity. Much attention has been devoted to the mechanisms of neuronal direction selectivity. Even before the first direction selective neurons were found, Exner proposed a model to explain how a cell could become direction selective. Early in the 20th century the first single cell recordings were made (Adrian, 1928) and this technique was subsequently applied to the study of visual systems (Hartline, 1938; Kuffler, 1953; Barlow, 1953). Based on experiments on insects, Reichardt suggested a model of motion detection (Reichardt, 1961), which has been adopted and modified by many others (e.g. Van Santen & Sperling, 1985; Adelson & Bergen, 1985) and which is still a starting point of many psychophysical, computational and physiological studies.

This thesis builds upon these traditions and combines the physiological and model-based approach to study motion vision in the cat brain. Single cell (single-unit) responses to moving random textured patterns are measured in two higher motion processing areas. Results are compared between the two areas and with those of the previously studied primary visual cortex and are put in the framework of a simple motion detection unit.

Motion stimuli and motion detection models

In theory, any moving object can serve as a stimulus in motion vision studies. However, different features of an image may interact and thereby alter the animal's ability to perceive different aspects of the moving image. Perceived speed, for example, depends on contrast (Stone & Thompson, 1992), pattern (Smith & Edgar,

1990) and color (Cavanagh et al., 1984) of the stimulus. For studying basic motion vision, one wants to avoid such complicating side-effects. Therefore simple, well-defined stimuli are favored in such studies. Moving line stimuli or sinusoidally modulated luminance gratings are examples of such elementary stimuli.

From about 1830, investigators experimented with stroboscopic or 'apparent' motion, that is motion seen in a sequence of systematically differing static images. Plateau understood that there are spatiotemporal limits to such apparent motion and experimented with instruments displaying series of stills to quantify these limits (Wade, 1998). By the end of the nineteenth century, Exner went to the limit of simplicity and studied such apparent motion with two brief sparks shifted slightly in time and position. This led to his discovery that motion is an elementary sensation. In the early 20th century, Exner's pupil Wertheimer (1912) founded Gestalt psychology on this finding that apparent motion is always seen 'as a whole', as a Gestalt, rather than as consisting of its elements (e.g. two sparks). Motion is not 'calculated' from displacement over time, but perceived directly and signalled through specialised motion channels in the nervous system, much like color, tone, or pain.

Nowadays, since the advent of a powerful movie-industry and with the availability of computer monitor screens, apparent motion is the major way to display moving stimuli. A landmark in studying apparent motion was the introduction of random dot cinematograms (Julesz, 1971), that originated from the development of monocularly perfectly camouflaged targets for studying stereopsis. Nowadays, there are many versions of these random dot cinematograms, one of which is the moving Random Pixel Array (RPA), that has been used in all studies in this thesis (Fig. 1). Like all other random dot cinematograms, moving RPAs have a random spatial distribution of pixel elements. In an RPA these pixels are of equal size, but of different luminance, either darker or lighter than the average luminance. Because of this randomness, it is not plausible that the visual system is recognizing and tracking patterns in images. Instead, when the pixels of an RPA are shifted in position during successive frames, the visual system matches corresponding elements in different frames, that is: it solves the 'motion correspondence problem' and extracts motion from the displaced pixels. Because there are also myriads of possible false matches of pixels between frames, the visual system has to signal those with 'common fate' (same spatiotemporal displacement) to detect the overall coherent motion. This requires a kind of spatiotemporal correlation that is at the heart of global motion detection in random textures. It is this basic operation of motion vision that can best be studied with moving RPAs.

Since Reichardt's correlation model, a whole range of motion detection models have been proposed (Van Santen & Sperling, 1985; Watson & Ahumada, 1985; Adelson & Bergen, 1985; Zanker, 1994a,b). All of these models fulfill the three requirements of motion detection: the image must be sampled at more than one retinal position, the samples must be processed asymmetrically in time and they should be combined in a non-linear fashion (Clifford & Ibbotson, 2003; Borst &

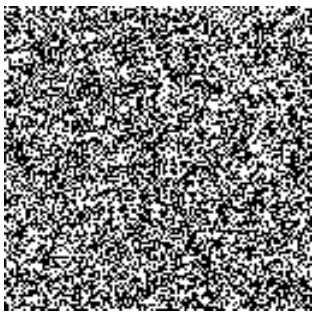

Fig. 1. Image of a Random Pixel Array (RPA), consisting of 128x128 black and white pixels, that are randomly distributed.

Egelhaaf, 1989). The first requirement is a consequence of the definition of motion itself. Displacement is a vector of nonzero magnitude, which requires representation by (at least) two spatially segregated points. Temporal asymmetry is crucial, because in a symmetrical detector, inputs would be interchangeable, therefore the sequence of excitation would be ambiguous, hence no motion direction could be signalled. Non-linear processing of the input signal is required to retain information about the temporal sequence of excitation (Borst & Egelhaaf, 1989).

Motion detection models can roughly be divided into two main groups: gradient models and correlation-type models. Originating from studies of computer vision, the gradient schemes of motion detection were applied later to biological vision of motion. Marr and Ullman (1981) proposed a discrete version of such a gradient model, by which a direct estimate of the local velocity could be obtained by dividing the temporal luminance gradient by the spatial luminance gradient of the image. It seems unlikely that the known cell types in the retina or cortex perform the computational steps in the model (Nakayama, 1985). Moreover such a model acts like a speedometer and therefore does not easily explain the percept of two motions at the same time and position, as when two transparently moving RPAs are viewed. The first correlation-type of movement detector was deduced from experiments on the insect's optomotor response (Reichardt, 1961). Its basic working unit is the bilocal detector, which is shown in Figure 2.

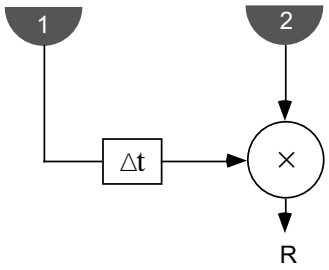

Fig. 2. Schematic drawing of the bilocal type of motion detector. The detector consists of two spatially segregated inputs (1 and 2), that are correlated. The signal from input 1 is delayed compared to input 2 by a delay ($\triangle$t) and if the signals arrive at the same time at the correlation stage, which is a multiplication ($\times$), the detector will signal rightward motion (R).

It is composed of two spatially segregated (or partially overlapping) Receptive Fields (RFs). Signals from the receptive fields arrive simultaneously at the site of interaction if the signal from one of the fields (1) is delayed by a time ($\triangle$t) that is needed for the moving object to travel from the position of the first to that of the second receptive field. At the site of interaction ($\times$), correlation of the signals takes place by multiplication and in the case of coinciding signals, it results in a large response amplitude. If the temporal sequence of the stimulation is reversed (opposite motion direction), signals at the multiplier do not coincide and small response amplitudes result. A local detector like in Figure 2 will also have response components due to correlated input signals that are independent of motion, like background luminance. In order to eliminate such bias-signals that are not related to motion, Reichardt proposed a motion detector model, that is composed of two mirror-symmetrical subunits (bilocal detectors), each with its own delay and multiplication stage. The output signals of the subunits are subtracted and in the case of a fully balanced correlation model, this leads to equal response amplitudes for motions in opposite directions, but with different signs. The subtraction eliminates any bias-signals that are common to both receptive fields.

In a Reichardt-detector, the two receptive fields were not spatial filters, but functioned merely to sample the visual field at two points. Due to this lack of filtering, aliasing might occur when moving sinusoidal gratings are used as stimuli. By introducing spatial frequency selective receptive fields Van Santen and Sperling eliminated the aliasing problem (Van Santen & Sperling, 1985). Adelson and Bergen (1985) proposed an incarnation of the multiplicative two-RF model in which pairs of space-time oriented receptive fields with different zones of excitation and inhibition (quadrature pairs) were used. This makes the response independent of stimulus phase. Their energy model and its variants received much attention in the past years, because certain simple and complex cells in cat area 17 (Emerson et al., 1992; Emerson, 1987; Emerson & Huang, 1997) and monkey V1 (DeValois et al., 1998) have directional properties which can easily be explained by some form of the energy model. Several other models, mostly variants of the original Reichardt-detector (e.g. Watson & Ahumada, 1985; Barlow & Levick, 1965; Zanker, 1994a,b) will not be discussed. Contrary to the detailed explanatory purposes of these more elaborate motion detection models, the bilocal detector that we use in the chapters to come, is merely adopted as a tool of thought. It provides a very convenient and conceptually simple scheme to interpret low-level single-cell response data to stimuli like a moving RPA, and it captures the main principle of more elaborate models, a delayed coincidence operation.

Visual motion processing in the cat

Subcortical level

The cat is a visual animal, like primates, including man. This is one of the reasons for the popularity of the cat in studies of visual information processing. As a result there is overwhelmingly detailed knowledge of anatomy and function of the cat visual system. Yet, the fundamental processes of motion vision have not been studied in much detail. Especially the processes beyond the primary visual cortex, the topic of my study, need to be analysed in more detail in order to understand motion vision in the cat and other similarly 'visual' mammals. For a detailed description of the cat visual system, the reader is referred to textbooks (e.g. Orban,1984; Payne & Peters, 2002). Here I will merely review some of the background facts that are used without further explanation in the chapters to follow.

The first stages of visual information processing are to be found in the three cell layers and two 'plexiform' layers in the **retinae** of the cat. After transduction by photoreceptors (rods and cones), light information is passed on to bipolar cells and from there to ganglion cells, but at both transmission stages there are elaborate lateral connections and interactions with horizontal cells and amacrine cells of various types. The ganglion cells represent the output of the retinae and their axons project through the optic nerves. In the cat retinae, different morphological and functional classes of ganglion cells exist. The morphologically different α, β, and γ cells are the origin of functionally distinct Y, X and W signals. X-cells have small receptive fields, exhibit linear spatial summation, have low flicker fusion frequencies, slower conducting axons and sustained light-evoked responses (Enroth-Cugell & Robson, 1966). Y-cells are bigger and have large receptive fields, non-linear spatial summation, high flicker fusion frequencies, faster conducting axons and transient responses. Because of these differences it has been suggested that X-cells serve spatial resolution and pattern recognition, while Y-cells are involved in mediating motion information (Stone, 1983). The third major type of ganglion cells, the W-cells, comprises a very heterogeneous group of cells, with many different types of RFs (Stone & Hoffmann, 1972) that can be either linear or non-linear (Sur & Sherman, 1982). W-cells have slow conduction axons (slower than X-cells) and are assumed to play a role in ambient vision (Orban, 1984).

The RF's of X and Y cells have a circular-symmetric center-surround organization (Kuffler, 1953). They can have an On-center Off-surround spatial organization or reversely an Off-center On-surround organization. An On-response is defined as an enhancement of firing during a light stimulus, while an Off-response consists of a suppression of firing during light on and a discharge after switching the light stimulus off (Hubel, 1988). Some W-cells have the same layout as X and Y-cells, although many of them have mixed On-Off centers or are selective for color (Orban, 1984).

As a result of their RF organizations, X- and Y-ganglion cells respond best to light or dark spots, presented to their RF center and/or surround. These cells do therefore respond to moving RPAs, but not in a direction selective manner. They are the main sources of information for the striate and extrastriate cortical areas discussed in this thesis.

The axons of ganglion cells run through the optic tract and terminate in a **thalamic relay**, that consists of the dorsal Lateral Geniculate Nucleus (dLGN), the Medial Interlaminar Nucleus (MIN) of the dLGN and the retino-recipient zone of the Lateral Pulvinar (LP) complex (Guillery et al., 1980). The **dLGN** has six layers. Different ganglion cell types terminate in different layers of the dLGN: fibres carrying Y-signals enter layers A, A1 or C_m (these are called the magnocellular layers), fibres carrying X-signals enter layers A and A1, while W-fibres enter the parvocellular complex (C_p) of layers (C1, C2, C3). Medial from the laminated portion of dLGN is the MIN, that consists of 3 layers (Guillery et al., 1980). Y-fibres going to the MIN terminate in layers 1 or 2, W-fibres in layer 3, while X-fiber innervation of MIN has been inconsistently described (Payne & Peters, 2002). All retinal fibres establish orderly point to point maps in the dLGN. RFs of dLGN cells have center-surround organization, like retinal ganglion cells. Two types of X and Y geniculate cells have been found: the lagged and the non-lagged ones (Mastronarde, 1987; Humphrey & Weller, 1988). Lagged cells show a significant delay in their firing compared to the retinal input. Both types of geniculate cells project to the cortex and they are good candidates for the generation of directional selectivity of cortical cells, where, as we have seen, differences in temporal properties of the inputs is needed.

The **retinal recipient zone of the LP** is also called the geniculate wing. It has a much coarser retinotopic organization than the dLGN and MIN. It is believed that predominantly W-type retinal ganglion cells project to the geniculate wing, and that the geniculate wing is part of a direct retino-pulvinar-cortical relay (Stone, 1983). In the cat, and contrary to the primate, only about 50 % of the retinal fibres project to the dLGN, while the other 50% project to the **Superior Colliculus** (SC). The SC receives input from the whole visual field of the contralateral eye predominantly from Y and W cells. It receives little if any input from X-type retinal ganglion cells. While Y-cell axons are branches of axons projecting to the dLGN, W-cells project directly. Y and W cells appear to activate different subgroups of SC cells.

Geniculocortical projection stream

From the dLGN, MIN, geniculate wing and SC, signals travel further toward the cortex. From the dLGN and MIN, this path is called the geniculocortical projection. In the same way that different ganglion cell types have different dLGN and MIN layers as targets, cells originating from different layers of the dLGN and MIN have different cortical targets. Laminae A and A1 project to area 17, but also to area 18. In area 17, this projection accounts for 94% of the thalamic input, in area 18 it is only 47% (Hollander & Vanegas, 1977). Lamina C projects to area 17, area 18 and area 19.

It constitutes 4% of the thalamic input to area 17, and about 20% to area 18 and area 19. The parvocellular C laminae project also to area 17, 18 and 19. They account for less than 5% of the input to area 17 and 18, but about 20% to area 19. MIN projects mainly to area 18 and 19 and accounts for approximately 25% of the input to area 18 and 40% of the input to area 19. The geniculate wing projects only to area 19 and accounts for approximately 20% of the input to area 19 (Payne & Peters, 2002).

In terms of X-, Y- and W-projections, X-cells from layers A and A1 are the major components of geniculate input to area 17, while Y-cells from laminae A, A1 and C project to both area 17 and area 18. Y-cells from the MIN project strongly to area 18 and probably also to the suprasylvian gyrus. W-cells from the parvocellular laminae and the MIN send axons to areas 17 and 18, suprasylvian areas, but primarily to area 19.

Extrageniculocortical projection stream

The predominantly W-cells from the retinal recipient zone of the LP, project to area 19, area 21a and to the lateral suprasylvian areas. Cells from a more medial part of the LP, that receives strong projections from the SC, project to area 19 and the lateral suprasylvian areas.

The described thalamocortical connections and projection streams are important for all chapters of this thesis, but predominantly for chapters 2 and 4. There, functional properties of area 18 and PMLS cells are debated based on found similarities or differences in cell responses. Comparisons to area 17 wil also be made, mainly in chapters 1 and 3.

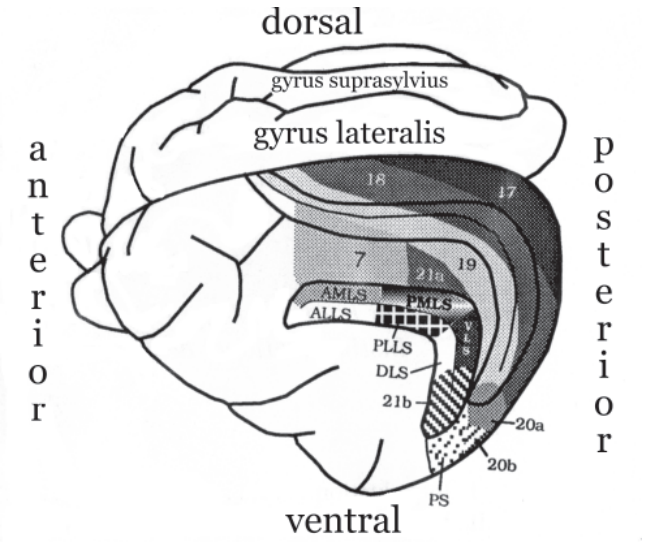

Fig. 3. Cortical areas of the cat visual system. Sulci containing visual areas have been opened. PMLS, posteromedial lateral suprasylvian visual area; PLLS, posterolateral suprasylvian visual area; AMLS, anteromedial lateral suprasylvian visual area; ALLS, anterolateral suprasylvian visual area; DLS, dorsolateral ventral suprasylvian visual area; PS, posterior suprasylvian visual area. Adapted from Salin and Bullier (1995).

Cortical level

The **primary visual area (area 17)** is the most studied visual cortex region in the cat. Figure 3 gives an impression of the division of the cat's brain in separate cortical areas. On the basis of histological criteria area 17 is divided in six layers. 80% of the neuronal population of area 17 consists of pyramidal cells and stellate cells, both of which are excitatory (non-GABA-ergic) (Gabbott & Somogyi, 1986). The remaining 20% is composed of GABA-ergic cells. The thickest layer is layer 4 and is subdivided in two sublayers (4A and 4B). Layer 4A input is dominated by dLGN fibres carrying Y-signals, whereas 4B receives input from X signals. Signals from dLGN enter layer 4A of area 17 and from there they are transmitted further in the layer, upward into the superficial layers and downward into the deep layers. Signals entering layer 4B are transmitted to the deeper layers and from there back to layer 4 or layer 2 and 3.

Functionally, the two main types of cells in area 17 are so-called simple and complex cells (Hubel & Wiesel, 1962). Simple cells consist of excitatory and inhibitory domain(s), lying parallel next to each other. In complex cells, the On and Off regions overlap. Both types respond to properly oriented lines. Contrary to most simple cells that prefer flashed stimuli, however, a complex cell responds best if a properly oriented line is swept across its RF. Wherever it is positioned in the RF, a complex cell will fire. Many complex cells have a preferred direction of motion, to which they respond more vigorously than to e.g. the opposite ('null') direction of motion. An ordinary simple or complex cell usually exhibits length summation: the longer the stimulus, the better the response, until the line length equals that of the RF. There are however so-called end-stopped (complex) cells, where lengthening the stimulus line beyond the RF results in a weaker response. Area 17 contains a straightforward, point-to-point representation of the contralateral visual field and a narrow strip of the ipsilateral hemifields (Orban, 1984).

The cytoarchitecture of **area 18** is very similar to that of area 17, though overall, area 18 is thicker than area 17 (particularly layer 3). Like area 17, it contains simple and complex cells. At corresponding eccentricities, area 18 cells have larger RFs than area 17 cells. They are also tuned to lower spatial frequencies and to higher velocities than area 17 cells at corresponding eccentricities (Orban et al., 1981). Lesion studies showed that this area is involved in motion perception (e.g. Pasternak & Maunsell, 1992). The transformation of the visual field is more complicated in area 18 than in area 17. Area 18 neurons have mostly been studied together with area 17 neurons, since they lie next to each other (see Fig. 3). There is even still some discussion about whether these two areas together represent the primary visual cortex or whether only area 17 can be considered as the primary recipient of most subcortical input. Because area 17 receives most of its input from the X-pathway and area 18 from the Y-pathway, these two areas may play a different role. Simple cells have been very extensively studied in both areas, however, complex cells in area 18 have still largely unknown properties and functions. One of the aims of this thesis is to

shed more light on their spatial and temporal RF properties and response characteristics and thereby to gain more insight into their functional roles.

The **Posteromedial Lateral Suprasylvian Region (PMLS)** is one of the lateral suprasylvian areas, described by Hubel and Wiesel (1969) and Clare and Bishop (1954). In this brain region, cells have more complicated RF structures (see discussion in chapter 4) and the majority is directionally selective (Dreher et al., 1992). Therefore, in contradistinction to area 18, PMLS undoubtedly represents a higher level of visual information processing. More than 90% of the cells are of the complex type. At corresponding eccentricities, the RF sizes are larger than in area 17 and area 18. The representation of the visual field in PMLS is incomplete and transformed in a more complicated manner than in area 18. Recording single-cell activities in PMLS of anaesthetised animals is quite difficult: neuronal activity at such a high level of processing depends critically on the exact level of anaesthesia and the general physiological condition of the animal. Partly due to this problem, studies of cell properties in this area are very scarce.

Cortical connections

Part of the feedforward connections between the thalamus and the cerebral cortex has been described above. In addition, most of the connections between the thalamus and cortex are reciprocal (Scannel et al., 1999). They are either feeding connections (arriving at another layer of the thalamus than from which they receive input) or coupling connections (reciprocal connections, departing from and terminating in the same layers). Corticocortical connections are also reciprocal (Symonds & Rosenquist, 1984a,b; Salin & Bullier, 1995) and either feeding or coupling. Almost all visual areas in the cat are interconnected and these connections have a highly complicated pattern (for more detail and maps of connections see Scannel et al., 1995; 1999). Strong connectivity exsists between area 17 and area 18 and between area 18 and PMLS (Scannel et al., 1999). Feedforward connections are visuotopically organized, while feedback connections are not (Salin & Bullier, 1995).

Outline of the thesis

All results in this thesis are based on single-unit recordings from area 18 and PMLS in the cat extrastriate cortex. Complex cells in these areas have been studied using moving RPAs. Different chapters deal with different aspects of motion detection mechanisms.

In chapter 1, the separability of complex cell responses to RPAs of varying pixel size and velocity are studied. Previous studies, that used moving sinusoidally modulated luminance gratings, reported separable tuning for spatial frequency and temporal frequency of the moving gratings. Separability means that the spatial and

temporal response properties are not mutually dependent, that is: the temporal properties of the response are invariant for changes of the spatial properties of the stimulus and vice versa. This has also been suggested for area 18 simple and complex cells. However, complex cells also respond directionally selective to motion of RPAs i.e. they are able to solve the motion correspondence problem for random textures.

It therefore remains to be seen if they are also temporal frequency rather than velocity tuned for RPAs and if separability holds for this broadband stimulus. In the experiments of chapter 1, I used RPAs moving in the preferred direction of each cell. The pixel size and velocity of the patterns were varied randomly from trial to trial. Average firing rates were then plotted in a two-dimensional graph as a function of pixel size and velocity. In such a graph velocity tuning would lead to either circular RF profiles or RF profiles that are oriented along one of the main axes (the pixel size or the velocity axis) while temporal frequency tuning would result in oriented RFs along a diagonal. In the first case, we speak of independent tuning for pixel size and velocity, in the last case of a mutual dependence. By fitting our data to both predictions (one for perfect independence and one for perfect dependence), we tested whether area 18 complex cells are velocity or temporal frequency tuned. For 96% of the cells the hypothesis of velocity tuning fitted the responses significantly better than the alternative. Our population of area 18 complex cells belongs to the so-called special complex cells and we suggest that these cells are true motion detectors rather then neurons coding for temporal frequency.

In chapter 2, we compared the temporal dynamics and latencies of directionally selective responses in area 18 and PMLS. These two extrastriate areas are known to be involved in motion perception and they are strongly interconnected. In addition, they share a common extrageniculate input from the thalamus, which, as reviewed above, is mediated by the fast-conducting Y-pathway. The RFs of complex cells in PMLS are more elaborate and are much larger at corresponding eccentricities than in area 18. It is not possible from these facts alone to guess the functional role of the connectivity between these areas. Since both areas are involved in motion perception, the question arises whether direction selectivity arises in parallel in these two areas or whether for example direction selectivity in PMLS depends on the direction selectivity in area 18, from which it receives feedforward input. In chapter 2, I try to answer these questions, by measuring complex cell latencies and by characterizing the temporal dynamics of their directionally selective responses. Our results do not support a hierarchical model of motion processing: we found largely overlapping response latencies and quite similar temporal dynamics of directionally selective responses. Contrary to area 18, a small subset of cells in PMLS was tuned to reversals of motion directions, that is they changed their preferred directions (for example from right to left) in time. Together, these findings suggest that motion information is processed in parallel in these areas and is most likely based on input from Y-fibres.

In chapter 3, we return to the basic mechanisms of motion detection and study the spatiotemporal requirements for motion detection in area 18 and PMLS complex cells. We were interested to see whether the spatiotemporal limitations for motion detection of RPA's are similar in these two areas. Moreover, we wanted to compare this to the results obtained by Van Wezel (Van Wezel et al., 1997) in area 17, with the same stimulus paradigm. Pixel size, velocity and motion direction were optimized for each neuron and responses to different combinations of spatial displacement and temporal delay were measured. Small values of spatial displacements and delays represent smooth motion, while increasingly larger values make the moving RPA become gradually jerkier (non-smooth motion). Some cells preferred non-smooth motion, others preferred smooth motion of the RPAs. Previously studied area 17 complex cells also showed preference for non-smooth motion (Van Wezel et al., 1997). In our experiments, the grain size of the RPA determined largely in which category a cell would fall: smaller grain sizes favoured preference for non-smooth motion. On the other hand, in PMLS, all cells preferred the smoothest motion, even when grain size was very small. Complex cells in area 18 have quite a broad velocity tuning (chapter 2). In order to find out whether this results from variations in either spatial displacement, temporal delay or both, we studied the response of a subset of area 18 complex cells to a wider range of step and delay combinations. Optimal displacement proved to be independent of temporal delay, suggesting that the velocity tuning of these neurons did not depend on inseparable tuning of spatial displacement and temporal delay.

Chapter 4 describes the temporal interactions of responses to different motion steps in direction selective complex cells in area 18 and PMLS. The method of motion reverse correlation (Borghuis et al., 2003) allowed us to measure and analyse responses to pairs of temporally separated motion directions. To be able to analyse and interpret the so-called second order temporal response profile, we made a prediction from the first order reverse correlation data, and the assumption of linearity (superposition). By comparing these linear predictions with the measured profile, we could pinpoint non-linear suppression or facilitation due to combinations of two motion directions. Area 18 cells formed a homogeneous group: they exhibited facilitatory non-linear interactions for similar motion directions and suppressive interactions for opposite directions. PMLS complex cells, on the other hand, did not form a homogenous group: those cells that did show non-linear interactions, showed the opposite effects to that in area 18, that is, opposite directions were facilitatory and similar directions inhibitory.

Based on these results we assume that area 18 complex cells play an important role in local motion coherence detection, where integration of equal direction information in time is required. PMLS complex cells, on the other hand, are probably involved in tasks where motion opponency is important. Such tasks include enhancement of motion contrast, and object-background or object-object segregation.

References

Adelson, E. H., Bergen, J. R. (1985). Spatiotemporal energy models for the perception of motion. *J Opt Soc Am A*. **2**: 284-99.

Adrian, E. D. (1928) The basis of sensation. New York: W. W. Norton & Company Inc.

Barlow, H. B. (1953). Summation and inhibition in the frog's retina. *Journal of Physiology London*. **119**: 69-88.

Barlow, H. B., Levick, W. R. (1965). The mechanism of directionally selective units in rabbit's retina. *Journal of Physiology*. **178**: 477-504.

Borghuis, B. G., Perge, J. A., Vajda, I., Van Wezel, R. J., Van de Grind, W. A., Lankheet, M. J. (2003). The motion reverse correlation (MRC) method: A linear systems approach in the motion domain. *J Neurosci Methods*. **123**: 153-66.

Borst, A., Egelhaaf, M. (1989). Principles of visual motion detection. *Trends Neurosci*. **12**: 297-306.

Cavanagh, P., Tyler, C. W., Favreau, O. E. (1984). Perceived velocity of moving chromatic gratings. *J Opt Soc Am A*. **1**: 893-9.

Clare, M. H., Bishop, G. H. (1954). Responses from an association area secondarily activated from optic cortex. *Journal of Neurophysiology*. **17**: 271-7.

Clifford, C. W. G., Ibbotson, M. R. (2003). Fundamental mechanisms of visual motion detection: models, cells and functions. *Progress in Neurobiology*. **68**: 409-37.

De Valois, R. L., Cottaris, N. P. (1998). Inputs to directionally selective simple cells in macaque striate cortex. *Proc Natl Acad Sci U S A*. **95**: 14488-93.

Dreher, B., Michalski, A., Cleland, B. G., Burke, W. (1992). Effects of selective pressure block of Y-type optic nerve fibers on the receptive-field properties of neurons in area 18 of the visual cortex of the cat. *Vis Neurosci*. **9**: 65-78.

Emerson, R. C., Citron, M. C., Vaughn, W. J., Klein, S. A. (1987). Nonlinear directionally selective subunits in complex cells of cat striate cortex. *J Neurophysiol*. **58**: 33-65.

Emerson, R. C., Huang, M. C. (1997). Quadrature subunits in directionally selective simple cells: counterphase and drifting grating responses. *Vis Neurosci*. **14**: 373-85.

Emerson, R. C., Korenberg, M. J., Citron, M. C. (1992). Identification of complex-cell intensive nonlinearities in a cascade model of cat visual cortex. *Biol Cybern*. **66**: 291-300.

Enroth-Cugell, C., Robson, J. G. (1966). The contrast sensitivity of retinal ganlgion cells of the cat. *Journal of Physiology*. **187**: 517-22.

Exner, S. (1894) Entwurf zu einer physiologischen Erklärung der physischen Erscheinungen. Vienna: Deuticke.

Gabbott, P. L., Somogyi, P. (1986). Quantitative distribution of GABA-immunoreactive neurons in the visual cortex (area 17) of the cat. *Exp Brain Res*. **61**: 323-31.

Guillery, R. W., Geisert, E. E., Jr., Polley, E. H., Mason, C. A. (1980). An analysis of the retinal afferents to the cat's medial interlaminar nucleus and to its rostral thalamic extension, the "geniculate wing". *J Comp Neurol.* **194**: 117-42.

Hartline, H. K. (1938). The response of single optic nerve fibers of the vertebrate eye to illumination of the retina. *American Journal of Physiology.* **121**: 400-15.

Hollander, H., Vanegas, H. (1977). The projection from the lateral geniculate nucleus onto the visual cortex in the cat. A quantitative study with horseradish-peroxidase. *J Comp Neurol.* **173**: 519-36.

Hubel, D. H. (1988) Eye, brain, and vision. New York: Scientific American Library.

Hubel, D. H., Wiesel, T. N. (1962). Receptive fields, binocular interaction and functional architecture in the cat's visual cortex. *J.Physiol.* **160**: 106-54.

Hubel, D. H., Wiesel, T. N. (1969). Visual area of the lateral suprasylvian gyrus (Clare-Bishop area) of the cat. *J Physiol.* **202**: 251-60.

Humphrey, A. L., Weller, R. E. (1988). Functionally distinct groups of X-cells in the lateral geniculate nucleus of the cat. *J Comp Neurol.* **268**: 429-47.

Julesz, B. (1971) Foundations of Cyclopean Perception. Chicago: University of Chicago Press.

Kuffler, S. W. (1953). Discharge patterns and functional organization of mammalian retina. *Journal of Neurophysiology.* **16**: 37-68.

Marr, D., Ullman, S. (1981). Directional selectivity and its use in early visual processing. *Proc R Soc Lond B Biol Sci.* **211**: 151-80.

Mastronarde, D. N. (1987). Two classes of single-input X-cells in cat lateral geniculate nucleus. II. Retinal inputs and the generation of receptive-field properties. *J Neurophysiol.* **57**: 381-413.

Nakayama, K. (1985). Biological image motion processing: a review. *Vision Res.* **25**: 625-60.

Orban, G. A. (1984) Neuronal operations in the visual cortex: studies of brain function. Berlin: Springer.

Orban, G. A., Kennedy, H., Maes, H. (1981). Response to movement of neurons in areas 17 and 18 of the cat: velocity sensitivity. *J Neurophysiol.* **45**: 1043-58.

Pasternak, T., Maunsell, J. H. (1992). Spatiotemporal sensitivity following lesions of area 18 in the cat. *J Neurosci.* **12**: 4521-9.

Payne, B. R., Peters, A. (2002) The cat primary visual cortex. London: Academic Press.

Reichardt, W. (1961) Auto-correlation, a principle for the evaluation of sensory information by the central nervous system. In: Sensory Communication (Rosenblith, W. A., ed.), pp. 303-17. New York: Wiley.

Salin, P. A., Bullier, J. (1995). Corticocortical connections in the visual system: structure and function. *Physiol Rev.* **75**: 107-54.

Scannell, J. W., Blakemore, C., Young, M. P. (1995). Analysis of connectivity in the cat cerebral cortex. *J Neurosci.* **15**: 1463-83.

Scannell, J. W., Burns, G. A., Hilgetag, C. C., O'Neil, M. A., Young, M. P. (1999). The connectional organization of the cortico-thalamic system of the cat. *Cereb Cortex*. **9**: 277-99.

Smith, A. T., Edgar, G. K. (1990). The influence of spatial frequency on perceived temporal frequency and perceived speed. *Vision Res*. **30**: 1467-74.

Stone, J. (1983) Parallel processing in the visual system. New York, London: Plenum Press.

Stone, J., Hoffmann, K. P. (1972). Very slow-conducting ganglion cells in the cat's retina: a major, new functional type? *Brain Res*. **43**: 610-6.

Stone, L. S., Thompson, P. (1992). Human speed perception is contrast dependent. *Vision Res*. **32**: 1535-49.

Sur, M., Sherman, S. M. (1982). Linear and nonlinear W-cells in C-laminae of the cat's lateral geniculate nucleus. *J Neurophysiol*. **47**: 869-84.

Symonds, L. L., Rosenquist, A. C. (1984a). Corticocortical connections among visual areas in the cat. *J Comp Neurol*. **229**: 1-38.

Symonds, L. L., Rosenquist, A. C. (1984b). Laminar origins of visual corticocortical connections in the cat. *J Comp Neurol*. **229**: 39-47.

Van Santen, J. P., Sperling, G. (1985). Elaborated Reichardt detectors. *J Opt Soc Am [A]*. **2**: 300-21.

Van Wezel, R. J., Lankheet, M. J., Fredericksen, R. E., Verstraten, F. A., van de Grind, W. A. (1997). Responses of complex cells in cat area 17 to apparent motion of random pixel arrays. *Vision Res*. **37**: 839-52.

Wade, N. J. (1998) A natural history of vision. Cambridge, London: MIT Press.

Watson, A. B., Ahumada, A. J., Jr. (1985). Model of human visual-motion sensing. *J Opt Soc Am A*. **2**: 322-41.

Wertheimer, M. (1912). Experimentelle Studien über das Sehen von Bewegung. *Zeitschrift für Psychologie*. **61**: 161-65.

Zanker, J. (1994a). Modelling human motion perception. I. Classical stimuli. *Naturwissenschaften*. **81**: 156-63.

Zanker, J. (1994b). Modelling human motion perception. II. Beyond Fourier motion stimuli. *Naturwissenschaften*. **81**: 200-9.

Chapter 1

On the velocity tuning of area 18 complex cell responses to moving textures

Co-authors: Martin J.M. Lankheet, Tessa M. van Leeuwen & Wim A. van de Grind

Abstract

Unlike simple cells, complex cells of area 18 give a directionally selective response to motion of random textures, indicating that they may play a special role in motion detection. We therefore investigated how texture motion, and especially its velocity, is represented by area 18 complex cells. Do these cells have separable spatial and temporal tunings or are these non-separable? To answer this question we measured responses to moving random pixel arrays as a function of both pixel size and velocity, for a set of 63 directionally selective complex cells.

Complex cells generally responded to a fairly wide range of pixel sizes and velocities. Variations in pixel size of the random pixel array only caused minor changes in the cells' preferred velocity. For nearly all cells the data much better fitted a model in which pixel size and velocity act separately, than a model in which pixel size and velocity interact so as to keep temporal frequency sensitivity constant. Our conclusion is that the studied population of special complex cells in area 18 are true motion detectors, rather than temporal frequency tuned neurons.

Introduction

Since the first physiological cell classification in areas 17 and 18 of the cat by Hubel and Wiesel (1962), the response properties of these cells and their functional differences have been studied extensively. The major finding concerning area 18 is, that the majority of its neurons is specially sensitive to low spatial and to high temporal frequencies (Movshon et al., 1978a; Orban, 1984). This led to the hypothesis that area 18 plays a major role in motion detection and processing. A psychophysical study combined with lesions in areas 17 and 18 has supported this hypothesis (Pasternak & Maunsell, 1992).

Many simple cells in both area 17 and 18 are selective for the direction of a moving grating. These cells may therefore, play a role in the coding of moving edges and object motion, but they are unable to solve the correspondence problem[1] for moving random textures (Hammond & MacKay, 1975, 1977; Hammond, 1991). Such patterns have frequently been used in both psychophysical and physiological experiments to study the spatio-temporal correlation mechanisms underlying various aspects of motion vision. Unlike simple cells, complex cells respond vigorously to these moving textures, indicating that they easily solve this form of the correspondence problem (Hammond & MacKay, 1975, 1977; Hammond & Reck, 1980; Hammond, 1991). Models for basic motion detectors, like the Reichardt detector as well as motion energy models (Reichardt, 1961; Adelson & Bergen, 1985; Van Santen & Sperling, 1985) suggest an unconfounded representation of velocity. Because of their directional selectivity to moving textures, complex cells are the best candidates for such motion detectors. Yet, so far it remained unclear whether complex

cells are indeed velocity-tuned, irrespective of the spatio-temporal parameters of the moving texture.

Previous studies mostly used sinusoidal gratings to study interactions between spatial and temporal effects in directional selectivity. Velocity tuning for moving sinusoidal gratings requires a co-variation of spatial and temporal frequency, which would yield oriented (tilted) receptive field (RF) profiles in the space-time domain. As noted by Orban (1984), visual neurons may respond independently to either spatial or temporal frequency, without specific tuning for velocity. This is indeed the case for many cortical cells in both cat (Movshon et al., 1978a; McLean & Palmer, 1989) and monkey (Foster et al., 1985; Levitt et al., 1994). Perrone and Thiele (2001) showed that, in monkeys, only in MT neuronal activity represents the speed of a grating. This study aims at characterizing the representation of speed in complex cells in cat area 18 when stimulated by moving random pixel arrays (RPAs).

RPAs consist of contiguous square pixels of which 50% is darker and 50% is lighter than the average luminance. Such patterns are characterized by their speed and pixel size. An RPA is a two-dimensional non-periodic pattern, with a continuous two-dimensional spatial frequency spectrum. An RPA cannot be characterized by a single spatial frequency. However, patterns with different pixel sizes will have different spatial frequency contents, since pixel size characterizes the cut-off spatial frequency of the stimulus. To manipulate the spatial frequency content, we therefore varied the pixel size. Since all spatial frequency components in a moving RPA have the same speed, such a stimulus also contains a broad range of temporal frequencies (white noise). The velocity characterizes the cut-off temporal frequency of the moving stimulus, so varying the velocity of RPAs changes the temporal frequency content of the stimulus.

In terms of spatial and temporal frequencies, RPAs appear more complex than gratings, but for the study of speed tuning of motion detectors, they are more straightforward. Only when corresponding pixels in subsequent frames are matched (correlated), the correspondence problem is solved and motion is detected. Therefore RPAs are ideally suited to study the correlation stage of motion detection. This is essentially the same reason why such patterns are used extensively in the study of stereopsis (Julesz, 1971). Tuning for pixel size and velocity will show directly how speed is represented at this early motion-selective stage in visual processing.

Pixel size and velocity were varied independently for patterns moving in the preferred direction of the cell. As pointed out, velocity-tuned neurons, as measured with sinusoids of different spatial and temporal frequency combinations, will have oriented RF profiles in space-time domain[2]. In our case, varying velocity and pixel size for velocity-tuned neurons, we expect non-oriented RF profiles in velocity-pixel size domain. Such a profile would point to separable velocity tuning and spatial tuning. Oriented profiles in the velocity-pixel size domain, on the other hand, will force us to conclude that velocity tuning in area 18 is confounded by spatial frequency.

Methods

Physiological preparation and recording procedure

Six adult female cats, weighing approximately 3 kg each, were used in this study. The experiments were carried out according to the guidelines of the Law on Animal Research of the Netherlands and of the Utrecht University's Animal Care and Use Committee. Anesthesia for the tracheotomy and craniotomy was induced by intramuscular injection of ketamine (15 mg/kg) and xylazine (0.5 mg/kg) (Aescoket-plus, Aesculaap, BV). During recordings, anesthesia was maintained by ventilating the animal with a mixture of 70% N_2O and 30% O_2, supplemented with 0.3-0.6% halothane (Sanofi Santé, BV, Maassluis). Rectal temperature was monitored and maintained at 38˚ with an electric heating blanket. Local analgesics in the form of Lidocaine or Xylocaine ointments (Astra Pharmaceutica, BV, Zoetermeer) were applied at wounds and pressure points. Heart rate, blood pressure, in- and expired N_2O, O_2, CO_2 and halothane were monitored during the experiment and, when necessary, regulated to correct ranges. Expired CO_2 was kept at 4.5-5.5%. Muscle relaxation was maintained by intravenous infusion of pancuronium bromide (Pavulon, N.V. Organon, Oss) at 0.11 mg/kg/hour together with 1.94% glucose in a ringer solution.

The pupils were dilated with 1% atropine sulfate (Pharmachemie, BV) and the eyelids were retracted with 2% phenylephrine hydrochloride (Veterinary dispensary of Utrecht University). The retinae were projected on a white screen at 57 cm distance from the eyes and the positions of the foveae were estimated from the positions of the optic disks and from the orientation of blood vessels. After completion of a set of measurements for a cell, its RF size and position were marked on the same screen. The eyes were focused at the appropriate viewing distance with gas-permeable, contact lenses (+3.5 to +5.0 diopter, courtesy of NKL, Emmen). Focal correction was assessed by back-projection of the retinal blood vessels onto a white screen. During the experiments clarity of the optics was checked regularly.

The animal was placed in a stereotaxic apparatus (Molenaar & Van de Grind, 1980) with its head fixed by ear bars and tooth clamps. Extracellular single cell recordings from area 18 were obtained with tungsten microelectrodes (impedance 1.0-5.4 MΩ at 500 Hz), insulated with glass or parylene (World Precision Instruments, Inc.). A craniotomy of 0.5 cm diameter was performed above area 18, at Horsley-Clarke co-ordinates P 2-7 and ±(L1.5-L6.5) (Reinoso-Suarez, 1961). The electrode was advanced vertically, through an incision in the dura. Craniotomies were sealed with agar (3% in ringer solution).

Visual stimuli

The RPAs consisting of 50% bright and 50% dark pixels (Julesz, 1971) were generated by a Macintosh G4 computer. The frame rate of the stimulus monitor (Sony,

Multiscan 400 PS) was 100 Hz, corresponding to a frame exposure duration of 10 ms. Delay times were integer multiples of the exposure duration. At the viewing distance of 57 cm and monitor resolution of 1024 x 768 pixels the unit pixel size was 0.03 x 0.03 deg of visual angle. The mean luminance and contrast of the random pixel array were set to 50 cd/m^2 and 0.99. The RPAs had an unlimited pixel lifetime and moved coherently in a window of fixed size. Unless stated otherwise, the stimulus window covered the full screen (34.3 x 25.7 deg). We used RPAs of different pixel sizes and different velocities. RPA pixel sizes were multiples of the elementary monitor pixel size, and will be expressed in deg of visual angle. From now on, 'pixel' refers to the elements of the RPAs, not to monitor pixels, unless explicitly stated. The size of the stimulus window was held constant; a change in pixel size therefore resulted in a change of the number of pixels in the window. Motion of the RPA was achieved by coherently shifting all pixels by n elementary monitor pixels each exposure frame (n could be smaller, larger or equal to the RPA pixel size). Speeds will be expressed in deg of visual angle per second.

Measurement protocol

The search stimulus was a RPA of 0.21 x 0.21 deg pixel size that moved in 0.5 sec intervals in 8 different directions (from 0° till 360° in steps of 45°) at several different velocities. The RF locations were determined manually using a light bar projected onto the screen, and the monitor position was adjusted so as to center the RF on the middle of the screen. Receptive field position and size were determined according to the method of Barlow et al. (1967).

Once a single unit was properly isolated we classified the cell as either simple or complex based on their response to moving sinusoidal gratings (Skottun et al., 1991a,b) and on their direction selectivity to moving texture (Hammond, 1991). Simple cells, with a clearly modulated response, were discarded and the search for a complex cell was continued. Simple cells never showed substantial directionally selective responses to moving RPAs. For complex cells we first determined the optimal velocity for moving RPAs of pixel sizes between 0.12 deg and 0.48 deg, depending on the cell's eccentricity. The optimal velocity was then used to measure direction tuning in both the ipsi- and contra-lateral eye. Subsequent measurements were performed for the dominant eye, with the other eye covered. In the case of a binocular neuron, the ipsi-lateral eye was covered.

Direction tuning was measured quantitatively by presenting moving RPAs in 8 different directions (from 0° till 360° in steps of 45°), in 2 sec trials. Peri-stimulus time histograms (PSTHs) were evaluated online, for at least ten repetitions. Direction selectivity was quantified by the Direction Index (DI), which is defined as follows (Casanova et al., 1992):

$$DI = 1 - \frac{\text{mean response in ND}}{\text{mean response in PD}}$$

where ND stands for non-preferred direction, 180° opposite to the preferred one, and PD for preferred direction. Only neurons with a DI ≥ 0.5, i.e., with a response in the preferred direction at least twice as large as in the non-preferred direction, were included in the final experiments.

To measure the velocity tuning as a function of RPA pixel size, we varied velocity and pixel size in a two-dimensional array of 7 pixel sizes x 7 velocities. Pixel sizes varied from 0.06 deg to 3.48 deg, in equal logarithmic steps. Velocities varied from 3 to 192 deg/s, also in equal logarithmic steps. In a sub-set of the experiments we used a 5x5 matrix, which excluded the largest pixels sizes and highest velocities. Velocity values were chosen to cover the range of velocity tuning for area 18 cells, as reported by Orban et al. (1981). The RPA always moved in the cell's preferred direction. Pixel size-velocity combinations were chosen in such a way that either the pattern moved an integer number of RPA pixels per frame (1-32), or that an integer number of frames was required to move 1 RPA pixel.

Data collection and analysis

Pixel sizes and velocities were randomized within a block. Each trial lasted 2 seconds with an ISI of 130 ms between trials. The spontaneous activity (SA), for a uniform grey stimulus field, was measured at the same mean luminance as the RPA pattern. Each stimulus condition was repeated at least ten times.

Signals were amplified (BAK Electonics, Inc.), filtered and displayed on an oscilloscope (Tektronix) and fed to an audio monitor. Spikes were detected using a window discriminator, and the resulting standardized pulses were recorded at 0.5 ms time resolution by a computer (Macintosh G4). Spike trains, together with all relevant stimulus parameters, were stored on disk for off-line data analysis. Dot displays and PSTHs were analyzed on-line as well, to monitor the data-collection process.

Results

Pixel size and velocity tuning characteristics of area 18 complex neurons

Responses to moving RPAs of different velocities and different pixel sizes were studied in 63 single units in area 18. Complex cells were selected on the basis of their direction selectivity for moving RPAs. On average the DI for the selected cells was 0.78. After determining velocity- and direction tuning, responses were recorded to 49 (7 by 7) different combinations of pixel size and velocity, for motion in the preferred direction. In a minority of the cells a smaller matrix of stimulus parameters was used, mostly 5 by 5. Receptive fields of recorded cells were located in both the left and right visual hemifield, at eccentricities varying from 0.6 to 22 deg. Figure 1 shows an example of results for one cell. The polar plot represents response

amplitudes (mean spike frequencies) for eight different directions. The histograms in Figure 1b show corresponding PSTHs. Typically, the response drops to about 50% in about ± 45 deg relative to the optimum direction.

Initial estimates of direction and velocity tuning were obtained with a pixel size between 0.12 and 0.48 deg. In pilot experiments we verified that the preferred direction did not vary substantially with pixel size. Previously it has been shown that direction tuning varies with velocity in both area 17 (Hammond & Reck, 1980) and 18 (Crook, 1990). These authors have demonstrated that texture sensitive cells have unimodal direction tuning at low, and progressively more bimodal direction tuning at higher velocities. This phenomenon has been explained from linear filtering

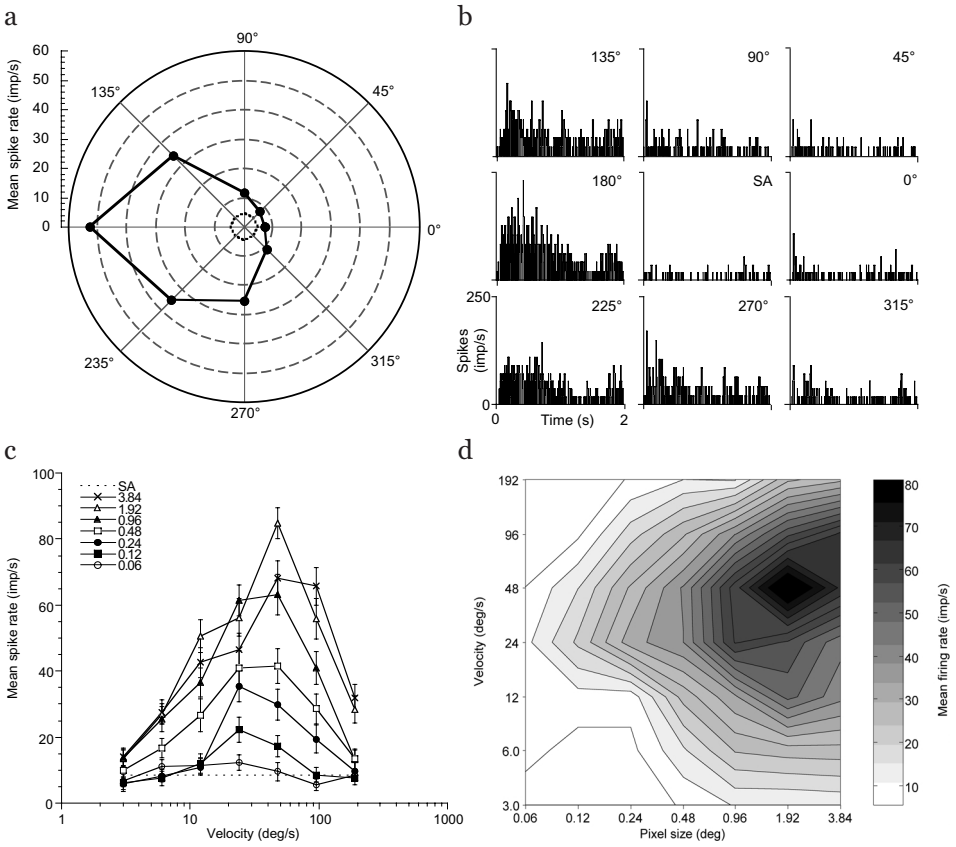

Fig. 1. An example of direction tuning (a,b) and of a pixel size-velocity experiment (c,d). a) The RPAs (pixel size: 0.36 x 0.36 deg) moved in 8 different directions (filled dots), at the cell's preferred velocity (36 deg/s). The SA, measured for a uniform grey field, is represented by the inner dotted circle in the polar plot. Corresponding PSTHs are plotted in b) for each direction of motion and for the SA. The time scale for each PSTH is identical and is indicated on the lowest left insert. c) The mean spike rate as a function of velocity for different pixel sizes. RPAs were moving in the cell's preferred direction. d) The same data as in c, now showing the mean response in a contour plot (inclusive the SA). Responses are coded by shading, the darker the stronger the mean response, as indicated in the legend. Lines indicate constant response magnitudes and are spaced at 20% of the difference between the peak and the minimum response amplitude.

properties by Skottun et al. (1994). In our case this means that contributions from directions deviating from the preferred one may contribute relatively more at higher velocities. These contributions are however evenly distributed around the preferred direction measured at lower speeds, and therefore do not alter the mean preferred direction. We were interested in the representation of speed in the preferred direction, as determined at the preferred velocity and did not study the width of the direction tuning. For this reason, broadening of direction tuning at higher velocities may play a role in our experiments, but in no way compromises our main findings concerning changes of velocity tuning with changes in pixel size. In the final experiment, the direction was fixed at the optimum, and velocity and pixel size were varied systematically. Figure 1c shows the mean responses as a function of velocity, for an RPA moving in the cell's preferred direction. Fig. 1d shows the same data, but now as a contour plot.

Before examining the relationship between tuning for pixel size and velocity, we analyzed separately the preferred velocity and pixel size for our sample of complex cells. At the measured eccentricities (mean: 11 deg; median: 10 deg) most of the cells were tuned to relatively large pixel sizes (0.96 deg or 1.92 deg; few cells to 0.12 deg - 0.48 deg). The larger the RF, the larger the preferred pixel size. In no case was the preferred pixel size the same or larger than the RF size. Best velocities were mostly 12 deg/s and 24 deg/s. In all cases the optimal velocity was below the highest speed we tried (192 deg/s). In addition, we quantified the widths of the velocity and pixel size tuning for each cell, by fitting a third order polynomial to the Pixel size Response Function (PRF), measured at the optimal velocity and to the Velocity Response Function (VRF), measured at the optimal pixel size. The half-width at half-height of each fitted curve was then used as a measure for the tuning width.. The tuning width for pixel size was on average 3.06 octaves, and for velocity on average 2.82 octaves. Thus, complex cells respond well to a broad range of pixel size-velocity combinations.

Interactions between pixel size and velocity tuning

Contour plots, like that in Figure 1d, represent cell responses in a broadband space-time domain. If the tunings for velocity and pixel size are separable, we expect either non-oriented contours, or contours oriented along the principal axes. On the other hand, if cell responses are non-separable, that is if they are tuned to temporal frequency rather than velocity, we expect diagonal orientations in these contour plots. In the latter case, variations in spatial frequency content due to changes in pixel size would have to be compensated for by a similar change in velocity in order to keep the temporal frequency content constant. Perfect compensation would be obtained for velocities equal to a constant ratio relative to the pixel size. For the contour plot on logarithmic scales, this corresponds to a slope of one.

For our population of complex cells we tested which of the two alternative hypotheses (velocity or temporal frequency tuning) gives a better description of the data. We partially adopted the method of Levitt and co-workers (Levitt et al., 1994).

In short, two prediction contour plots are created from the measured data; one for the hypothesis of velocity tuning (separability) and the other for the hypothesis of temporal frequency tuning (non-separability). Hereto, we first determined the PRF for the optimal velocity and the VRF for the optimal pixel size. Optimal pixel size and velocity were estimated by fitting a third-order polynomial to the data points. To calculate the prediction for separable velocity and pixel size tuning, the PRF was replicated at different velocities, scaled (multiplied) by the VRF. For the prediction of velocity tuning varying with pixel size so as to produce invariable temporal frequency tuning, the PRF was again replicated at different velocities, scaled by the VRF, and the whole curve was shifted in position so as to align the peak responses on a diagonal line (slope 1). Figure 2 gives the two prediction contour plots, for the data presented in Figure 1c and d. Figure 2a shows the prediction contour plot for velocity tuning. Figure 2b is the prediction for temporal frequency tuning.

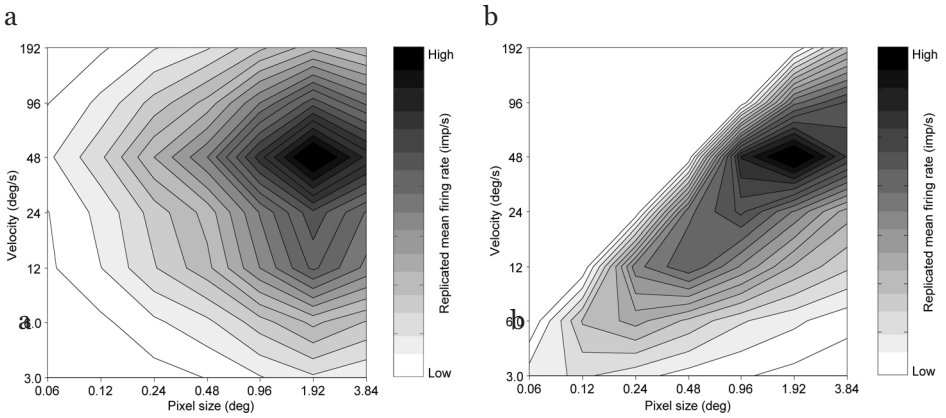

Fig. 2. The two prediction surfaces for the data presented in Figure 1c and d. a) Predicted contour plot for velocity tuning. b) Predicted contour plot for temporal frequency tuning. Both contour plots are coded by shading: the darker, the stronger the response. Since the absolute replicated firing rates are not meaningful, we indicate only the direction of the increase (from low to high). Lines indicate constant response magnitudes and are spaced at 20 % of the difference between the peak and the minimum response amplitude.

Next, we determined the partial correlation between the measured surface and each of the prediction surfaces. For the partial correlation of the data with the velocity tuning prediction (R_v) this takes the form:

$$R_v = \frac{(r_v - r_t \times r_{vt})}{\sqrt{(1 - r_{vt}^2)(1 - r_t^2)}}$$

Here r_v and r_t are the correlations of the data with the velocity tuning prediction and the temporal frequency tuning prediction, r_{vt} is the correlation of the predictions with each other. To calculate the partial correlation of the data with the temporal frequency tuning prediction (R_t) r_v with r_t are interchanged. The cell of Figures 1 and 2 has an R_v of 0.96 and an R_t of -0.16, meaning that the measured contour plot is more in line with the velocity tuning prediction than with the temporal frequency tuning prediction.

In Figure 3, the R_v versus R_t scatter plot is shown for the population of 42 cells, that was tested with a 7x7 parameter matrix. The lines in the graph represent the significance limits for the partial correlation coefficients, based on Fisher's Z-transformation method (Pestman, 1998). In Figure 3, these lines represent correlation values of 0.28, demarcating a significant difference from zero ($p<0.05$). For points within the significance boundaries, the partial correlation coefficients are not significantly different from each other or from zero correlation. The two subsets of cells that were tested with different matrix sizes (7x7 and 5x5), are analysed separately (5x5 not shown), since significance limits differ slightly for different matrix sizes. For cells falling in the region bordered by these limits, both correlation values are low and they will be called *Unclassed*, after Levitt et al. (1994). The region along the diagonal, within the curved significance boundaries, represents cells that showed significant correlations with both predictions ($p<0.05$), but that were not significantly different from each other. These cells are therefore also called *Unclassed*. This group may comprise cases where there is clear dependence, but with a slope deviating from unity (on a logarithmic axis). Cells outside these boundaries correlate significantly better with either one of the predictions, and can be classified as either *Velocity tuned* or *Temporal frequency tuned*.

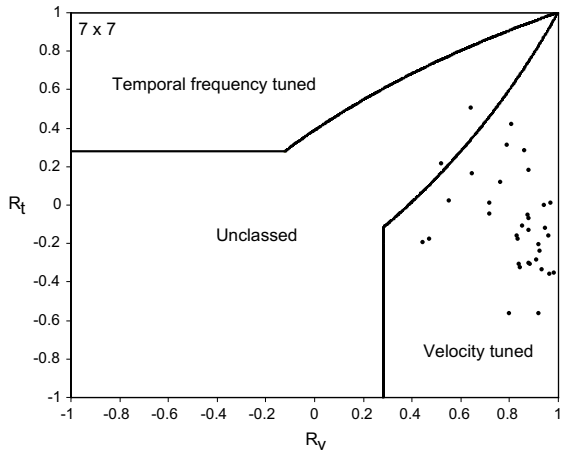

Fig. 3. Scatter plots of the partial correlation coefficients belonging to the velocity tuning (R_v) and to the temporal frequency tuning (R_t) predictions for measurements based on 7x7 matrix of velocity and pixel size combinations.

In 61 out of 63 cases (96%) the responses were classified as *Velocity tuned*. Two cells showed significant correlations to both prediction surfaces and were therefore classified as *Unclassed*. No data point fell in the *Temporal frequency tuned* region. Thus nearly all cells show a high R_v and a low R_t, that is, their pixel size-velocity tuning is better described by the separability prediction and does not show substantial pixel size-velocity co-variation.

It is obvious that a classification as *Velocity tuned* does not exclude some systematic variation of velocity tuning with variations in pixel size. To quantify the shift in velocity tuning with a change in pixel size, we determined linear regression lines through the optimal velocity as a function of pixel size for each cell separately. Figure 4 shows the frequency distribution of slopes for all cells. A slope of 0 corresponds to perfect, separable velocity tuning and pixel size tuning. A slope of unity would correspond to perfect covariation of optimal velocity with pixel size to establish invariant temporal frequency tuning. Figure 4 shows that slopes are close to zero, in agreement with the cells' classifiation as Velocity tuned. The distribution is not symmetrical around zero, but slightly shifted towards positive values, indicating a slight tendency of optimal velocity to increase with increases in pixel size. The majority of the cells (49 of 63, that is 77%) has a slope between -0.1 and 0.4. The median value of the population is 0.2.

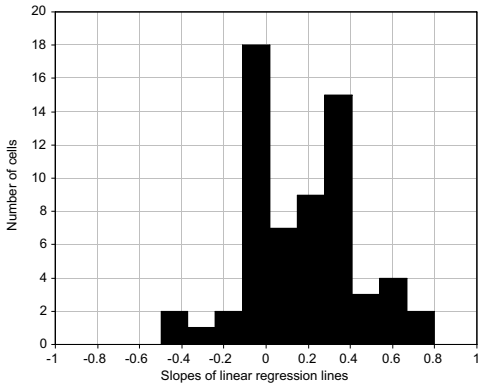

Fig. 4. Distribution of the slopes of linear regression lines through the optimal velocity as a function of pixel size for the entire population of cells. These slopes describe the change of optimal velocity as a function of pixel size.

Discussion

For the vast majority of our sample of area 18 complex cells (96%) velocity tuning is not confounded with spatial tuning. We conclude this from the results after correlating the data with two alternative models. There is some shift in velocity tuning with variations in pixel size (Fig. 4), but for a large proportion of the cells this is not substantial and falls far short of a full compensation for changes in the spatial frequency content of the stimulus that would result in invariable temporal frequency tuning.

Tuning for pixel size for our sample of special complex cells (see section on special complex cells below) does not differ substantially from the spatial frequency characteristics of other subclasses of complex cells and simple cells (Movshon et al., 1978a). The optimal pixel sizes at the mean eccentricity of 11 deg, varied from about 0.12 deg to 1.92 deg. Movshon et al. (1978b) reported optimal spatial frequencies between 0.11 to 0.22 c/deg at a mean eccentricity of 10 deg. Thus, optimal spatial frequencies approximately correspond to the cut-off spatial frequency in RPAs. An extensive study on velocity tuning on both simple and complex cells in areas 17 and 18 was done by Orban et al. (1981). In area 17 and especially in area 18, responses to fast gratings improve with increasing eccentricity. For eccentricities between 5 and 15 deg, in area 18, high velocity limits were between 8 and 100 deg/s (Orban, 1984). Crook measured velocity tuning to moving textures and moving bars for both simple and complex cells in area 17 and 18. He reported that in both areas many of the (complex) cells had higher preferred velocity for a moving texture than for a moving bar. In velocity tuned cells in area 18 at eccentricities up to 12 deg, sometimes up to 18 deg, velocity optima for moving bars range between 16-41 deg/s (Crook, 1990).

Our population of special complex cells at 11 deg mean eccentricity shows similar, but slightly higher preferred velocity (24-48 deg/s) for textures of optimal pixel size. There is a trend of optimal velocities to increase with larger optimal pixel sizes, much as one would expect. This relationship is similar to the covariation of optimal spatial frequency and preferred velocity as reported for area 17 complex cells by Baker (1990) and for area 17 standard and special complex cells by Hammond & Fothergill (1994).

Velocity versus temporal frequency tuning

Our finding, that for many area 18 complex cells velocity tuning does not vary substantially with changes in spatial frequency content of a moving texture, is clearly-different from results found so far. In monkeys, the results on spatio-temporal interactions measured with gratings seem fairly straightforward. V1 and V2 show separable spatial and temporal tunings (Tolhurst & Movshon, 1975; Foster et al., 1985; Levitt et al., 1994). Thus, at these lower levels, velocity is not represented in the activity of individual cells. In the monkey, cells that are velocity tuned rather than temporal frequency tuned, are first encountered in area MT (Newsome et al., 1983; Perrone & Thiele, 2001). In cats, the picture is somewhat more complex than in monkeys. Results for the striate cortex, measured with gratings, are well in line with those for V1 in monkeys: all cells are spatio-temporally separable (Holub & Morton-Gibson, 1981; Bisti et al., 1985). In area 18 however, both separability (McLean & Palmer, 1989; Friend & Baker, 1993), and non-separability (Bisti et al., 1985) has been reported. In PMLS, which is thought to be the homologue of MT, some cells showed spatio-temporal separability and some were non-separable (Morrone et al., 1986). The non-separability in both areas 18 (Bisti et al., 1985) and PMLS (Morrone et al., 1986), however, was such that with increasing temporal

frequency or velocity, the optimal spatial frequency shifted downwards (anti-velocity tuning). Velocity tuning of the type we encountered has only been reported previously for two cells in area 18 (Friend & Baker, 1993).

Our results show that many complex cell responses to moving textures such as RPAs are predominantly velocity tuned and not temporal frequency tuned. Since Friend and Baker (1993) reported temporal frequency-tuned complex cells in area 18 and Bisti et al. (1985) anti-velocity tuned complex cells, we must conclude that area 18 contains various classes of complex cells, that differ in their spatio-temporal characteristics.

Special complex cells

That complex cells do not comprise a homogeneous group was already noticed in the late seventies (Gilbert, 1977; Hammond & MacKay, 1977; Hammond, 1978). They have been divided in three subclasses according to their length summation properties: standard, special and intermediate complex cells (Hammond & Ahmed, 1985). Standard complex cells summate for stimuli whose length matches or exceeds the RF length. Special complex cells respond optimally to contours much shorter than the RF and intermediate complex cells have hybrid characteristics (Hammond & Pomfrett, 1989).

In addition to the standard criterion for distinguishing complex cells from simple cells, we also applied the additional criterion that cells had to respond directionally selectively to moving RPAs of moderate pixel size. This criterion favors selection of special complex cells that prefer contours much shorter than their receptive field (Gilbert, 1977; Hammond & Ahmed, 1985; Hammond & Pomfrett, 1989). These cells are found to be significantly more direction selective than standard complex cells (Hammond & Pomfrett, 1989). Special complex cells often exhibit end-stopping, have the highest spontaneous activity of all striate cortical cells, the highest velocity preference (Gilbert, 1977; Hammond & Ahmed, 1985) and RF sizes that are smaller than those of the standard complex cells (Hammond & Pomfrett, 1989). In addition, Hammond and Pomfrett tested special complex cells on their sensitivity to texture motion. Special complex cells exhibited higher sensitivity to texture motion, especially those that were direction selective and were less sharply tuned for orientation than either standard complex cells or simple cells (Hammond & Pomfrett, 1989, 1990).

Since these response properties very much resemble our observations, we assume that our sample of complex cells in area 18 belong to the class of special complex cells as defined previously. Bisti et al. (1985) and Friend and Baker (1993) classified neurons as complex only by the lack of modulation to sine-wave gratings, and therefore probably measured only standard complex cells, which respond poorly to short contours. It seems likely that the differences in our results and those reported by Bisti et al. (1985) and Friend and Baker (1993) can be accounted for by different sampling criteria of complex cells.

Our findings support the idea of co-existence of functionally different subclasses of complex cells in area 18. Special complex cells in this area may be involved in the direct representation of velocity. These texture sensitive cells might play a role in navigation. On the other hand, standard and intermediate complex cells and simple cells do not appear to represent velocity directly (McLean & Palmer, 1989; Friend & Baker, 1993; Movshon et al., 1978a). They appear to detect the rate of movement of oriented edges. The class of complex cells does not only comprise different subclasses with regard to their RF properties (Gilbert, 1977; Hammond & MacKay, 1977; Hammond, 1978), but also with regard to their most probable functional roles in motion processing.

Footnotes

1. The correspondence problem in (apparent) motion is a problem of matching elements in one frame with corresponding elements in a succeeding frame. Random dot kinematograms are especially well suited to study the correspondence problem (Julesz, 1971).

2. As pointed out, space-time domain in the case of gratings is narrowband, whereas it is broadband in the case of RPAs. When referring to a space-time domain, we will not repeat this fact, but we will always mention the used stimulus.

References

Adelson, E. H., Bergen, J. R. (1985). Spatiotemporal energy models for the perception of motion. *J Opt Soc Am A*. **2**: 284-99.

Baker, C. L., Jr. (1990). Spatial- and temporal-frequency selectivity as a basis for velocity preference in cat striate cortex neurons. *Vis Neurosci*. **4**: 101-13.

Barlow, H. B., Blakemore, C., Pettigrew, J. D. (1967). The neural mechanism of binocular depth discrimination. *J Physiol*. **193**: 327-42.

Bisti, S., Carmignoto, G., Galli, L., Maffei, L. (1985). Spatial-frequency characteristics of neurones of area 18 in the cat: dependence on the velocity of the visual stimulus. *J Physiol*. **359**: 259-68.

Casanova, C., Nordmann, J. P., Ohzawa, I., Freeman, R. D. (1992). Direction selectivity of cells in the cat's striate cortex: differences between bar and grating stimuli. *Vis Neurosci*. **9**: 505-13.

Crook, J. M. (1990). Directional tuning of cells in area 18 of the feline visual cortex for visual noise, bar and spot stimuli: a comparison with area 17. *Exp Brain Res*. **80**: 545-61.

Foster, K. H., Gaska, J. P., Nagler, M., Pollen, D. A. (1985). Spatial and temporal frequency selectivity of neurones in visual cortical areas V1 and V2 of the macaque monkey. *J Physiol*. **365**: 331-63.

Friend, S. M., Baker, C. L., Jr. (1993). Spatio-temporal frequency separability in area 18 neurons of the cat. *Vision Res.* **33**: 1765-71.

Gilbert, C. D. (1977). Laminar differences in receptive field properties of cells in cat primary visual cortex. *J Physiol.* **268**: 391-421.

Hammond, P. (1978). Directional tuning of complex cells in area 17 of the feline visual cortex. *J Physiol.* **285**: 479-91.

Hammond, P. (1991). On the response of simple and complex cells to random dot patterns: a reply to Skottun, Grosof and De Valois. *Vision Res.* **31**: 47-50.

Hammond, P., Ahmed, B. (1985). Length summation of complex cells in cat striate cortex: a reappraisal of the "special/standard" classification. *Neuroscience.* **15**: 639-49.

Hammond, P., Fothergill, L. K. (1994). Cat striate cortex: monocular and interocular comparisons of spatial- frequency selectivity. *An Acad Bras Cienc.* **66**: 95-113.

Hammond, P., MacKay, D. M. (1975). Differential responses of cat visual cortical cells to textured stimuli. *Exp Brain Res.* **22**: 427-30.

Hammond, P., MacKay, D. M. (1977). Differential responsiveness of simple and complex cells in cat striate cortex to visual texture. *Exp Brain Res.* **30**: 275-96.

Hammond, P., Pomfrett, C. J. (1989). Directional and orientational tuning of feline striate cortical neurones: correlation with neuronal class. *Vision Res.* **29**: 653-62.

Hammond, P., Pomfrett, C. J. (1990). Directionality of cat striate cortical neurones: contribution of suppression. *Exp Brain Res.* **81**: 417-25.

Hammond, P., Reck, J. (1980). Influence of velocity on directional tuning of complex cells in cat striate cortex for texture motion. *Neurosci Lett.* **19**: 309-14.

Holub, R. A., Morton-Gibson, M. (1981). Response of Visual Cortical Neurons of the cat to moving sinusoidal gratings: response-contrast functions and spatiotemporal interactions. *J Neurophysiol.* **46**: 1244-59.

Hubel, D. H., Wiesel, T. N. (1962). Receptive fields, binocular interaction and functional architecture in the cat's visual cortex. *J.Physiol.* **160**: 106-54.

Julesz, B. (1971) Foundations of Cyclopean Perception. Chicago: University of Chicago Press.

Levitt, J. B., Kiper, D. C., Movshon, J. A. (1994). Receptive fields and functional architecture of macaque V2. *J Neurophysiol.* **71**: 2517-42.

McLean, J. & Palmer, L.A. (1989). Responses of simple cells in areas 17 and 18 of the cat in the spatiotemporal frequency domain. *Investigative Opthalmology and Visual Science Supplement.* **30**: 111.

Molenaar, J., Van de Grind, W. A. (1980). A stereotaxic method of recording from single neurons in the intact in vivo eye of the cat. *J Neurosci Methods.* **2**: 135-52.

Morrone, M. C., Di Stefano, M., Burr, D. C. (1986). Spatial and temporal properties of neurons of the lateral suprasylvian cortex of the cat. *J Neurophysiol.* **56**: 969-86.

Movshon, J. A., Thompson, I. D., Tolhurst, D. J. (1978a). Spatial and temporal contrast sensitivity of neurones in areas 17 and 18 of the cat's visual cortex. *J Physiol.* **283**: 101-20.

Movshon, J. A., Thompson, I. D., Tolhurst, D. J. (1978b). Receptive field organization of complex cells in the cat's striate cortex. *J Physiol.* **283**: 79-99.

Newsome, W. T., Gizzi, M. S., Movshon, J. A. (1983). Spatial and temporal properties of neurons in macaque MT. *Investigative Opthalmology and Visual Science Supplement.* **24**: 107.

Orban, G. A. (1984) Neuronal operations in the visual cortex: studies of brain function. Berlin: Springer.

Orban, G. A., Kennedy, H., Maes, H. (1981). Response to movement of neurons in areas 17 and 18 of the cat: velocity sensitivity. *J Neurophysiol.* **45**: 1043-58.

Pasternak, T., Maunsell, J. H. (1992). Spatiotemporal sensitivity following lesions of area 18 in the cat. *J Neurosci.* **12**: 4521-9.

Perrone, J. A., Thiele, A. (2001). Speed skills: measuring the visual speed analyzing properties of primate MT neurons. *Nat Neurosci.* **4**: 526-32.

Pestman, W. R. (1998) Mathematical Statistics, an introduction. Berlin, New York: Walter de Gruyter Verlag.

Reichardt, W. (1961) Auto-correlation, a principle for the evaluation of sensory information by the central nervous system. In: Sensory Communication (Rosenblith, W. A., ed.), pp. 303-17. New York: Wiley.

Reinoso-Suarez, F. (1961) Topografischer Hirnatlas der Katze fuer experimental-physiologische Untersuchung. Darmstadt: E. Merck AG.

Skottun, B. C., De Valois, R. L., Grosof, D. H., Movshon, J. A., Albrecht, D. G., Bonds, A. B. (1991b). Classifying simple and complex cells on the basis of response modulation. *Vision Res.* **31**: 1079-86.

Skottun, B. C., Grosof, D. H., De Valois, R. L. (1991a). On the responses of simple and complex cells to random dot patterns. *Vision Res.* **31**: 43-6.

Skottun, B. C., Zhang, J., Grosof, D. H. (1994). On the directional selectivity of cells in the visual cortex to drifting dot patterns. *Vis Neurosci.* **11**: 885-97.

Tolhurst, D. J., Movshon, J. A. (1975). Spatial and temporal contrast sensitivity of striate cortical neurones. *Nature.* **257**: 674-5.

Van Santen, J. P., Sperling, G. (1985). Elaborated Reichardt detectors. *J Opt Soc Am [A].* **2**: 300-21.

Chapter 2

Dynamics of directional selectivity in area 18 and PMLS of the cat

Co-authors: Martin J.M. Lankheet, Bart G. Borghuis & Wim A. van de Grind

Abstract

Visual latencies and temporal dynamics of area 18 and PMLS direction selective complex cells were measured with a reverse correlation method. The method allowed us to specifically analyze the time course of responses to motion steps, without confounding temporal integration effects. Several response latencies and measures of direction tuning dynamics were quantified: Optimal Latency (OL), First and Last Significant Responses (FSR, LSR), the increase and decrease of direction sensitivity in time, and the change of direction tuning in time. FSR, OL and LSR values for PMLS and area 18 largely overlapped. The small differences in mean latencies (3 to 4 ms for FSR and OL and 11.9 ms for the LSR) were not statistically significant. Neither in PMLS nor in area 18 did we find any systematic changes in preferred direction or of direction tuning width during the interval from FSR to LSR. In both areas, development of direction sensitivity was significantly faster than return to the non-direction sensitive state, but no significant difference was found between the two areas. We conclude that the dynamics of primary motion information are highly comparable for area 18 and PMLS and that both areas respond simultaneously. This suggests that motion information is processed in parallel, presumably based on input from the fast conducting thalamocortical Y-pathway.

Introduction

The original view that visual information in the cat is processed hierarchically, from the retinae through area 17, area 18 and 19, up to the higher associational areas (Dreher, 1986) has been largely abandoned by now. Numerous studies have provided evidence for parallel processing rather than a hierarchical processing of visual information (Dinse & Krüger, 1994; Katsuyama et al., 1996; for overview see Stone, 1983 and Matsubara & Boyd, 2002). Important functional insights have come from comparisons of response dynamics in different areas. Dinse and Krüger (1994), for example, measured response latencies to flickering bright stimuli in several visual cortical areas of the cat and analyzed simultaneous activation patterns. They reported a high percentage of simultaneously activated cells in different areas, including areas 17, 18, 19 and some higher cortical areas.

Like in the primate visual system, several cortical areas seem to be involved in motion processing in the cat visual system. Areas 18 and PMLS play an important role in processing of motion (Kiefer et al., 1989; Pasternak et al., 1989; Spear, 1991; Pasternak & Maunsell, 1992). Whereas in primates numerous (modeling) studies discussed the origin of motion sensitive units in area MT (Sereno, 1993; Nowlan & Sejnowski, 1995; Simoncelli & Heeger, 1998; Raiguel et al., 1999), not much research has been directly devoted to the same question in PMLS, which plays a similar role

in the cat visual system (Payne, 1993). In addition to massive inputfrom areas 17 and 18, PMLS also receives substantial input from a variety of thalamic nuclei (Rosenquist, 1985; Rauschecker et al., 1987; for reviews see Dreher, 1986). Areas 18 and PMLS contain direction selective complex cells (Dreher, 1986; Crook, 1990; Merabet et al., 2000) and both areas are strongly (Scannell et al., 1999) and reciprocally (Symonds & Rosenquist, 1984a,b) interconnected. In this paper we study to what extent differences in connectivity and interactions result in different response dynamics. Hereto, we compare complex cell response dynamics for texture motion in areas 18 and PMLS, using optimized texture motion stimuli for each cell.

To quantify the dynamics for directionally selective responses from complex cells in these areas we used a Motion Reverse Correlation (MRC) technique (Borghuis et al., 2003). The stimulus consisted of a Random Pixel Array (RPA) performing a random walk, in which step size and delay were held constant, but (eight) directions were randomized. Spikes were reverse-correlated with the motion steps, yielding the time course of responses to each direction. The method provides a detailed description of the temporal dynamics of direction tuning and allows us to compare latencies, as well as other aspects of the dynamics of directional selectivity, such as tuning width. The motion reverse correlation technique focuses on temporal dynamics of the initial stages in motion processing, and provides a more precise and more straightforward measure of latency to moving stimuli than previously used (Orban et al., 1985; Raiguel et al., 1999). Because in the MRC direction changes after each step, confounding effects of temporal integration are minimized. If directional selectivity in PMLS is (partly) based on motion sensitivity in lower areas, we expect clear differences in either response latencies or in response dynamics.

Methods

Physiological preparation and recording procedure

Nine adult female cats, weighing approximately 3 kg each, were used in this study. The experiments were carried out according to the guidelines of the Law on Animal Research of the Netherlands and of the Utrecht University's Animal Care and Use Committee. Anaesthesia for the tracheotomy and craniotomy was induced by intramuscular injection of ketamine (15 mg/kg) and xylazine (0.5 mg/kg) (Aescoket-plus, Aesculaap, BV). During recordings, anaesthesia was maintained by ventilating the animal with a mixture of 70% N_2O and 30% O_2, supplemented with 0.3-0.6% halothane (Sanofi Santé, BV, Maassluis). Rectal temperature was monitored and maintained at 38° with an electric heating blanket. Local analgesics in the form of Lidocaine or Xylocaine ointments (Astra Pharmaceutica BV, Zoetermeer) were applied at pressure points. Heart rate, blood pressure, in- and expired N_2O, O_2 and halothane were monitored during the experiment and, when necessary, regulated to correct ranges. Expired CO_2 was kept at 4.5-5.5%. Muscle relaxation was

maintained by intravenous infusion of pancuronium bromide (Pavulon, N.V. Organon, Oss) at 0.11 mg/kg/hour together with 1.94% glucose in a ringer solution. Pupils were dilated with 1% atropine sulfate (Pharmachemie, BV) and the eyelids retracted with 2% phenylephrine hydrochloride (Veterinary dispensary of Utrecht University). The retinae were projected on a white screen at 57 cm distance from the eyes and the positions of the foveae were estimated from the positions of the optic disks and from the orientation of blood vessels. The eyes were focused at the appropriate viewing distance with gas-permeable, contact lenses (+3.5 to +5.0 diopter, courtesy of NKL, Emmen). Focal correction was assessed by back-projection of the retinal blood vessels onto a white screen. During the experiments clarity of the optics was checked regularly.

The animal was placed in a stereotaxic apparatus (Molenaar & Van de Grind, 1980) with its head fixed by ear bars and tooth clamps. Extracellular single cell recordings from area 18 and PMLS were obtained with tungsten microelectrodes (impedance 1.0-5.4 MΩ at 500 Hz), insulated with glass or parylene (World Precision Instruments, Inc.). A craniotomy of 0.5 cm diameter was performed above area 18, at Horsley-Clarke coordinates P 2-7 and ±(L1.5-L6.5). For PMLS a craniotomy of 0.8 cm was made at Horsley-Clarke coordinates co-ordinates A4-P4 and ±(L13-L21) (Reinoso-Suarez, 1961). For area 18, the electrode was advanced vertically, for PMLS at an angle of 30 deg, through an incision in the dura. Craniotomies were sealed with agar (3% in ringer solution).

Visual stimuli

Random pixel arrays consisting of 50% bright and 50% dark pixels (Julesz, 1971) were generated by a Macintosh G4 computer. The frame rate of the stimulus monitor (Sony, Multiscan 400 PS) was 100 Hz. The mean luminance and contrast of the random pixel array were set to 50 cd/m^2 and 0.99. At the viewing distance of 57 cm and monitor resolution of 1024 x 768 pixels, the unit pixel size was 0.03x0.03 deg of visual angle. The pixel size of the RPA was always a multiple of the unit pixel size. For area 18 we mostly used a RPA pixel size of 0.24x0.24 deg, and in a few cases 0.12x0.12 deg. No differences were observed in temporal response dynamics for the different pixel sizes. Because direction selective cells in area PMLS were tuned to somewhat larger pixel sizes (see also Merabet et al., 2000), we mostly used a size of 0.48x0.48 deg in PMLS. Unless stated otherwise, the stimulus window measured 24x21 deg, which was large enough to cover the full receptive field.

The reverse correlation method is described in detail elsewhere (Borghuis et al., 2002). A QuickTime demo of the stimulus and some example responses are available on the internet (http://www-vf.bio.uu.nl/lab/NE/people/Ildiko/Demos.html). In short, a RPA, covering the whole RF, moved in eight different directions, changing direction after each step. A pseudo-random sequence containing equal numbers of eight different directions was predefined by randomly shuffling the sequence of steps. The sequence usually contained a few thousands repetitionsfor

each direction. The displacement is defined by the step size (number of unit pixels) and the delay (number of exposure frames between steps).

To obtain the time course of directional selectivity, spikes were reverse correlated with the stimulus sequence. This yielded a probability function for the occurrence of each direction of motion at each point in time preceding a spike. Figure 1a shows an example of the normalized probability for a single complex cell in area 18. A level of 0.125 represents chance level. Correlation between occurrence of spikes (at time 0) and motion direction is highest at about -50 ms in this example. The direction with highest relative probability corresponds to the preferred direction as measured in a classical direction tuning experiment. Figure 1b compares the distribution of relative probabilities at the optimal latency (peak in Figure 1a) to the mean spike rate measured in 1s stimulus intervals in which the RPA moved in the same eight directions. As shown previously (Borghuis et al., 2002), preferred direction as well as tuning width correspond closely for the two methods. The reverse correlation method has the advantage that it allows us to study the dynamics of directional selectivity in great detail.

Both the time of occurrence of spikes and of motion steps were measured at a temporal resolution of 0.5 ms. This resulted in a sparse distribution of motion impulses, and therefore in somewhat noisy cross-correlation functions. Removal of this noise was achieved by smoothing the probability functions using a sliding average with a Gaussian window with a standard deviation of 5 ms (see Figure 2 in Borghuis et al., 2002). The noise level in the recordings (shown as dashed lines in Figure 1a) was determined from a non-correlated part of the sequence (stimuli following spikes).

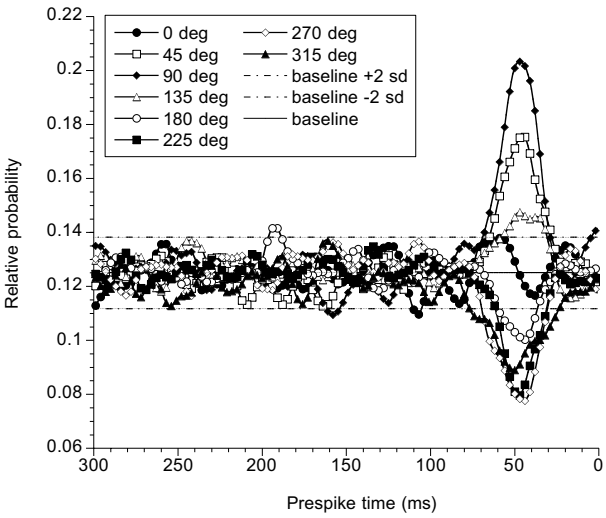

Fig. 1. *Figure continues on facing page.*

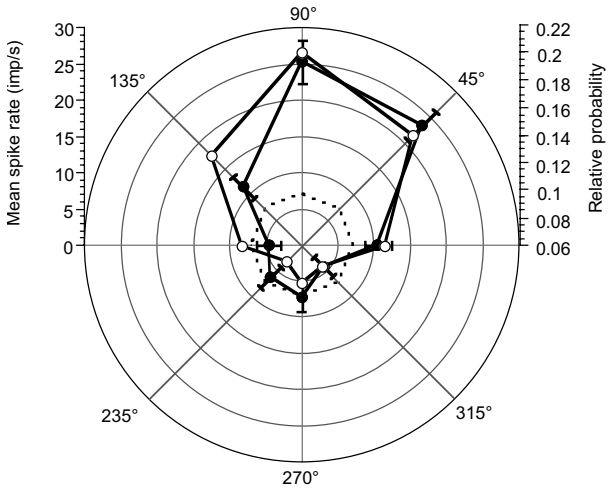

Fig. 1 *continued.* Direction reverse correlogram (temporal resolution 1ms) of an area 18 cell. Prior to the MRC experiment the V_{pref} (48 deg/s) and the optimal step and delay of the cell were determined. In the MRC experiment, the stimulus consisted of 8 different directions and in total 15 000 motion impulses. A new direction was started after every 10 ms, during which the pattern moved coherently one element pixel (0.48 deg). 3122 spikes were fired during the experiment. The stimulus window was 18x18 deg. The ±2 standard deviations (dashed lines) are calculated from a non-correlated part of the probability function. b) Classical direction tuning experiment for the cell in (a) and the relative probabilities of the eight directions at the optimal latency from the experiment in (a). In the classical direction tuning experiment (filled circles), the stimulus (element pixel size: 0.48x0.48 deg) moved in 8 different directions (with 45 deg interval) with the V_{pref}. The dotted line indicates the level of Spontaneous Activity (SA), measured for a uniform grey field. Error bars represent the ±1 standard error of the means. Trial duration: 1s, repetitions: 6.

Measurement protocol

The stimulus used for searching directionally selective units consisted of an RPA of 0.12-0.48 pixel size, moving in 8 different directions in 0.5s intervals, at several different velocities. Once a single unit was isolated, two short experiments were performed to classify the cell as either 'simple' or 'complex'. The first consisted of sinusoidal gratings of different orientation and spatial frequency, moving in 8 different directions. The second experiment consisted of an RPA of 0.12-0.48 pixel size, moving in 8 different directions. Several different velocities were used for both experiments. Simple cells with a modulated response to drifting sinusoids were discarded. Only complex cells responding directionally selective to texture motion were used in subsequent experiments. Directional selectivity was quantified by the direction index (DI), as defined by Casanova et al. (1992):

$$DI = 1 - \frac{\text{mean response in ND}}{\text{mean response in PD}}$$

Only complex cells with a DI of at least 0.5 were used in the present experiments (i.e., a response in the preferred direction which is at least twice as large as in the non-preferred direction). Next, the dominant eye was determined and in the case of

a binocular neuron, the ipsilateral eye was covered. Subsequent experiments were performed for the dominant eye only.

In order to determine the optimal step size and delay, we first performed a standard velocity tuning experiment at the preferred direction. Velocities ranged from 0.2 deg/s to 384 deg/s. Low velocities were achieved by shifting the pattern a single unit pixel every n^{th} exposure frame, high velocities by shifting the pattern n unit pixels each exposure frame. Next, for cells with sufficiently high firing frequency (>30 spikes/s) we determined the optimal step and delay combination at the optimal velocity, by using the so-called Single-Step Pattern Lifetime (SSPL) stimulus. SSPL stimuli contain motion information at a single combination of step size and delay, whereas a continuous, coherently moving pattern contains motion information at many different combinations of step size and delay. This selectivity is achieved by replacing the pattern with a new, random pattern after each coherent step. Responses were obtained for different combinations of step size and delay, all corresponding to the cells' preferred velocity. To minimize the jerkiness of the motion, the pattern was spatially divided in two interleaved sub-patterns that were alternately moved and refreshed. Directional selectivity at each combination of step size and delay was obtained by subtracting responses for the non-preferred direction from those to the preferred direction. Because a SSPL motion stimulus is inherently noisy and contains less motion energy than a coherently moving RPA, only highly active neurons could be driven by such a stimulus. For cells with low firing frequencies, for which an optimal step-delay value could not be determined, we arbitrarily chose a relatively small step size and short delay value, corresponding to the preferred velocity (41 out of 73 cases).

Data collection and analysis

Signals were amplified (BAK Electronics, Inc.), filtered and displayed on an oscilloscope (Tektronix) and fed to an audio monitor. Spikes were detected using a window discriminator and the resulting standardized pulses were recorded at 0.5 ms time resolution by a computer (Macintosh G4). Timing of RPA displacements was stored with the same temporal precision. Responses to direction and velocity tuning and for SSPL experiments were monitored on-line, by updating dot displays and peristimulus time histograms after each trial. During the MRC experiment, probability distributions were visualized in time and updated after every 10^{th} spike. Spike trains and all relevant stimulus parameters were stored on disk for off-line data analysis.

MRC data analysis

The optimal latency and the time instances of the first and last significant responses were quantified according to Mazer et al. (2002). Briefly, the mean variance and its standard deviation (across directions and time) was determined from a piece of the non-correlated part of the probability function (1s after each spike). Next, the variance

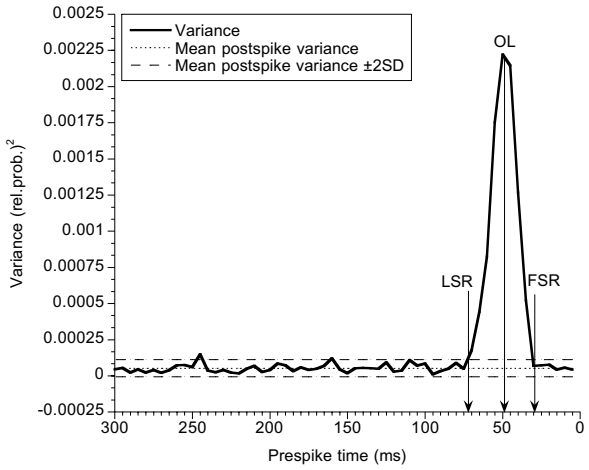

Fig. 2. Overall variance plot of the probability functions for the cell in Fig. 1a. Mean postspike variance and its standard deviation are calculated from a non-correlated portion of the probability functions. Optimal latency (OL), first significant response (FSR) and last significant response (LSR) are marked by arrows.

for the probability functions was calculated for a 300 ms pre-spike interval, at 1 ms resolution. Figure 2 shows an example of the overall variance curve. It expresses the mean, squared deviation of the relative probabilities from chance level. The optimal latency (OL) was defined as the moment the variance curve reached its maximum level. The OL calculated from the variance curve corresponds closely to the time interval between stimulus and spikes at which maximal directional selectivity is obtained. The first and last significant responses (FSR and LSR) were defined as those points in time at which the variance first exceeded, respectively fell below the level of two standard deviations (of the mean variance of the non-correlated part).

In addition to the latencies based on the overall variance curves we used several different measures to characterize and compare the temporal dynamics of directional selectivity in the two areas. To specifically quantify the increase and decline of directional sensitivity, lines were fitted to the rising (points between FSR and OL) and falling (points between OL and LSR) phase of the overall variance curves. The slope-values of these lines represent the speed at which directional sensitivity changes. Since in the variance curve directions are pooled together, the change of directional sensitivity does not necessarily reflect a change in directional selectivity. Moreover, the overall variance curves provide no information on the variability of preferred directions. To quantify the preferred direction during the 300 ms response window, we used the vector sum of probabilities for all directions. The resulting Directional Vector sum (DV) represents the preferred direction and the strength of directional selectivity, taking all eight possible directions into account. The width of direction tuning was determined by fitting Gaussian direction tuning profiles to the probabilities as a function of direction, at each point in time. Because low relative probabilities yielded noise estimates of tuning width, we limited the analysis to a

time window of 10 ms before and after the optimal latency. For a number of cells (9 in area 18 and 3 in PMLS), fits at some time points (mostly at 9 ms and 10 ms before or after the OL) yielded a low correlation coefficient (R<0.8). We discarded these cells from further analysis. For the remaining cells, the width of direction tuning is quantified by the s of the fitted Gaussian.

Results

Population response characteristics

In area 18, experiments were performed on 32 neurons, in PMLS on 41 neurons. The average DI for area 18 cells was 0.80, for PMLS it was 0.76. In area 18, preferred velocities varied from 6 deg/s to 72 deg/s, in PMLS from 3 deg/s to 192 deg/s. The reverse correlogram shown in Figure 1a is exemplary for all area 18 cells and for the vast majority of PMLS cells. Typically, the variance curve showed a single peak. In PMLS however, 5 cells were encountered, that showed a second peak in the variance curve. Figure 3a shows an example of direction tuning for such a 'biphasic' cell. The Figure represents the directional vector sum (DV) plotted on a time axis, showing the change in time of directional selectivity (length of the vector) and of preferred direction. Figure 3b shows a DV plot for the area 18 cell from Figures 1 and 2. Biphasic

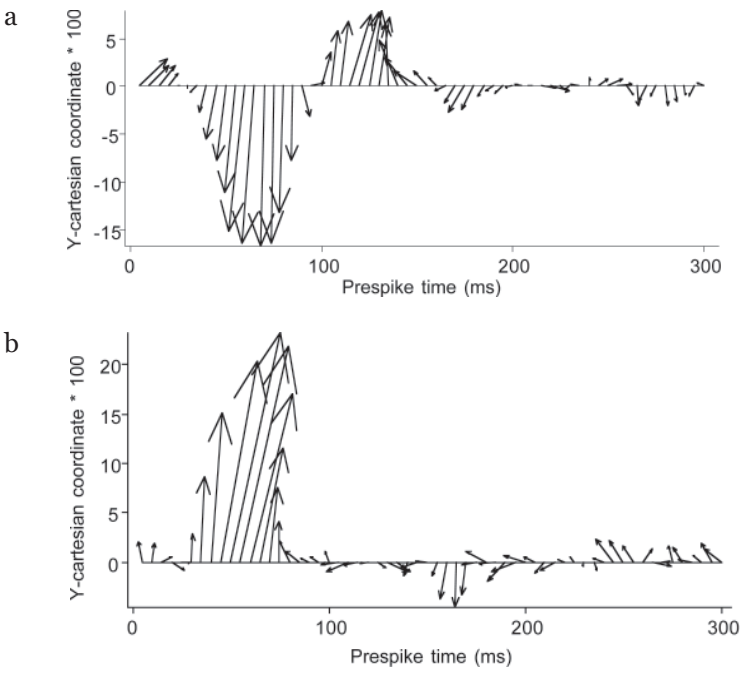

Fig. 3. Directional Vectorsum plots as a function of prespike time of a biphasic PMLS complex cell (a) and of the monophasic area 18 cell from Figs. 1, 2 and 3. At each time instance of the probability function (temporal resolution 1 ms), the direction vectors of the eight different directions were summed. The magnitude and direction of the resulting sum of the vectors is plotted for every 5ms. Therefore the origins of the DVs are equally spaced. The magnitude of a DV is given in Cartesian coordinates and indicated only for the y-coordinate (multiplied by 100 for visibility). An x-coordinate can be found by drawing a perpendicular line.

type of cells have also been found in macaque area MT (Borghuis et al., 2002) where they constitute about 50% of the total population. Because in PMLS biphasic cells form a small, distinctive subgroup, we did not include these cells in the comparison of population characteristics between area 18 and PMLS. In a future study we will specifically address the distinctive response properties of these so-called biphasic cells.

Figure 4 shows the variance curve, averaged for all area 18 cells and for all monophasic cells in area PMLS. Directional selectivity is slightly higher in area 18 than in PMLS, just as it was found by using the classical directional tuning method (see previous paragraph). Mean variance in area 18 reached about 0.003 at its optimum. In PMLS the mean optimal variance was about 27% lower (0.0022). Apart from this clear difference, there were no obvious substantial differences in response profiles between the two areas. In Figures 5 and 6 we quantitatively compare response latencies based on the same data underlying the variance curves in Figure 4.

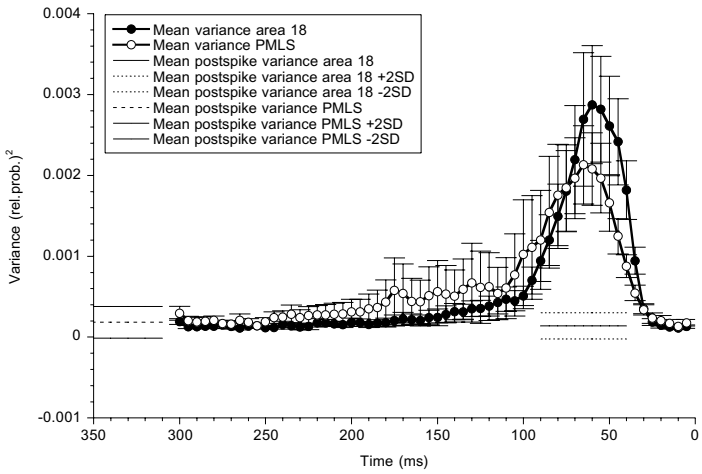

Fig. 4. Mean overall variance curves of 32 area 18 complex cells (solid dots) and 36 PMLS complex cells (open dots). Mean postspike variances are the means of the mean postspike variances of individual cells, which were calculated from the non-correlated portion of the probability functions (see Methods). Error bars represent the ± 1 SEM.

Figure 5a shows the latency of the first significant response (FSR), i.e., the minimal time required for the response to surpass the level of the mean post-spike variance plus two standard deviations. Mean variance and its standard deviations are based on 1s post-spike correlations, reflecting noise in the uncorrelated part of the sequences (see Fig. 2 and 4). The mean FSR in PMLS (34.2 ms) was slightly longer than in area 18 (30.8 ms). Figure 4 shows that this difference partly results from a slightly higher noise level in PMLS, and from a slower increase of the variance. A similar difference between the two areas was found for the optimal latencies. Mean

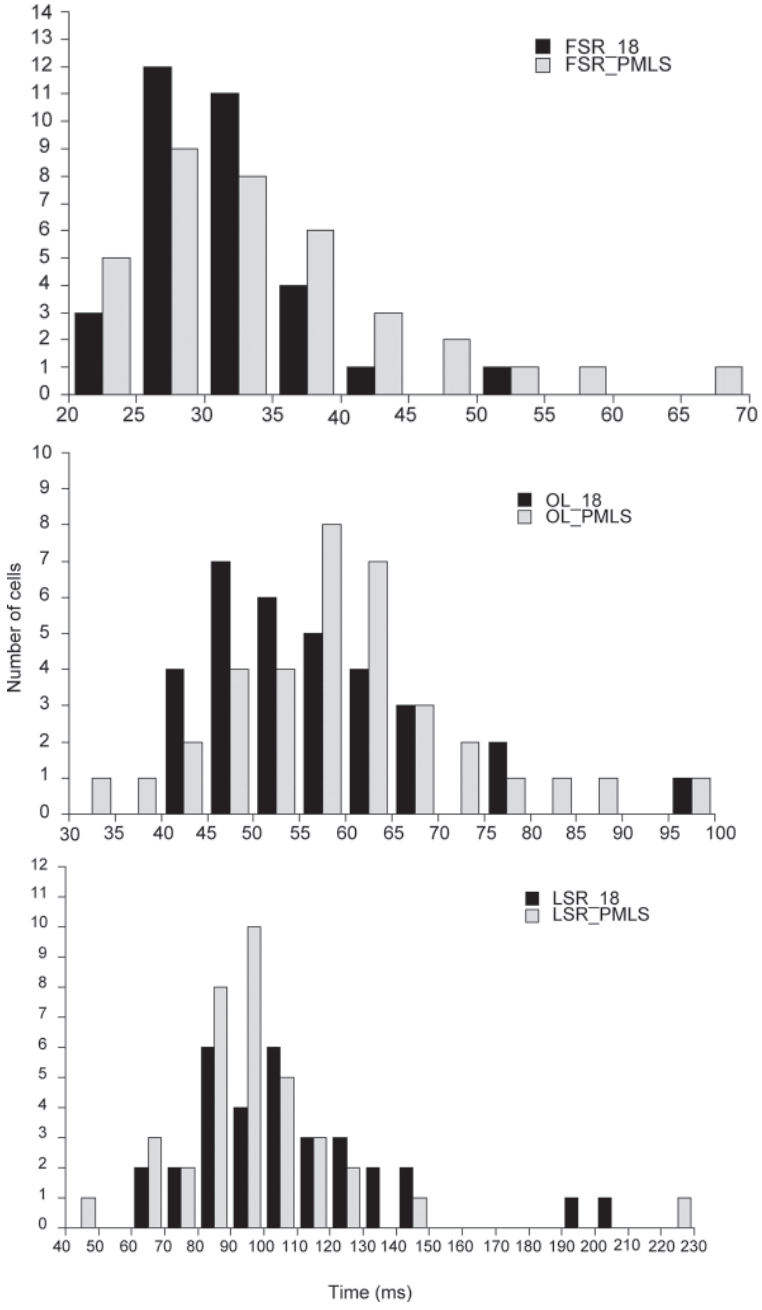

Fig. 5. FSR, OL and LSR distributions of 32 area 18 and 36 PMLS complex cells, following stimulation with MRC, making one step in each direction. Stimulus parameters varied per cell, depending on its preferred velocity and optimal step-delay combination (See Methods for further detail).

optimal latency was 59.1 ms in PMLS and 55.8 ms in area 18. For the LSR the opposite was observed: area 18 had a longer mean LSR (108.6 ms) than PMLS (96.7ms). Figure 5c shows that there was substantial scatter in the LSR latency values. Large scatters are common in latency studies (Ikeda & Wright, 1975; Best et al., 1986; Raiguel et al., 1989; Maunsell & Gibson, 1992; Dinse & Krüger, 1994; Raiguel et al., 1999; Saul & Feidler, 2002) and their range depends partly on the diversity and extensiveness of inputs to an area. None of the observed latency differences between areas, however, turned out to be significant ($p(OL) > 0.2$; $p(FSR) > 0.1$; $p(LSR) > 0.1$).

In our study, part of the scatter might also have been caused by differences in stimulus-delay, which was optimized for about half of the cells (see Methods). In area 18, delay values varied between 10 ms and 80 ms, in PMLS between 10 ms and 160 ms. For short delays motion steps follow each other rapidly, creating an opportunity for temporal interactions. Cells mostly fired single spikes in response to individual steps in a fast sequence. For long delays the opportunity for temporal interactions were less, which resulted in slightly longer responses to steps in the preferred direction. The resulting increase in latency values with stimulus delay was however very modest and turned out to be non-significant within an area. Only area 18 OL values measured with 10 ms and 40 ms and with 10 ms and 20 ms and PMLS LSR values measured with 10 ms and 20 ms yielded a small but significant difference.

Direction tuning dynamics

Analysis of the directional vector sum (DV) as a function of pre-spike interval showed no systematic variation in preferred direction. Apart from 5 biphasic cells (Figure 3) that reverse their preferred direction for longer prespike intervals, cells in area 18 and in monophasic PMLS neurons showed no systematic change of preferred directions. In both areas, the majority of the cells showed little or no variation in the angle. Few cells showed small, but non-systematic changes. No differences were observed between the change of directions for monophasic cells in area 18 and in PMLS.

To compare the velocity of increase and decrease of directional sensitivity we determined the slopes of the lines fitted to the points between the FSR and OL and OL and LSR of the variance curves. Mean correlation coefficient (R) for fits to the rising part was 0.95 (SD: 0.07) in area 18 and 0.93 (SD: 0.11) in PMLS. Mean correlation coefficients for the interval from OL to LSR were 0.89 (SD: 0.08) for Area 18 and 0.92 (SD: 0.07) for PMLS. Figure 6 compares the distribution of slopes for the two areas. Slopes were normalized to the maximum variance level at the optimal latency.

Within each area, the mean slope of the increasing part was significantly steeper than the mean slope for the decreasing part ($p < 0.0001$ for area 18; $p < 0.002$ for PMLS). No significant differences were found in the increasing and decreasing mean slope values between the areas ($p > 0.2$ for increasing and $p > 0.4$ for decreasing part). These results show that both in area 18 and in PMLS directional sensitivity increases faster than it decreases.

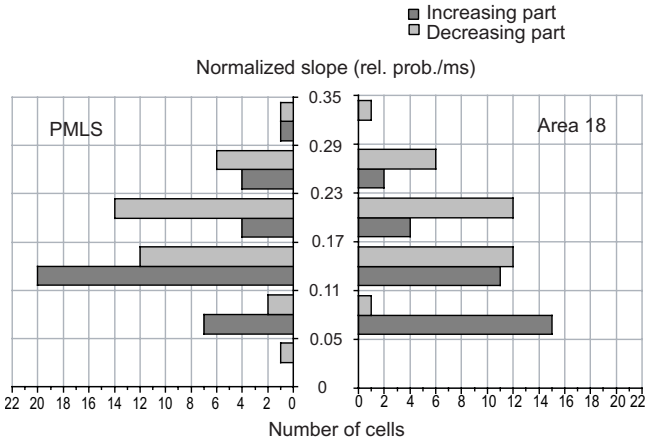

Fig. 6. Frequency distributions of the slopes of lines, fitted to the overall variance curves in both areas. Slope values were normalised by dividing them by the variance at the time of OL.

Finally, we analyzed to what extent the sharpness of the direction tuning changes during the course of the response profile. Does the tuning width change in time, and if so, is this different for areas 18 and PMLS? We determined the change in width as a function of time, for a 10 ms interval before and after the optimal latency. To this end, we determined the s of the fitted Gaussian to the relative probability points (see Methods). In Figure 7 the mean s and its standard deviation is shown for a population of 23 area 18 and 31 PMLS cells.

No substantial changes in the mean s values were found in the 10 ms period before and after the OL within or between the areas. For individual cells, no systematic change in s values was seen in the 10 ms period around the OL: some cells showed a slight sharpening of their tuning at the OL, some continued to sharpen their tuning beyond the time of the OL. The majority of the cells, however, did not change their tuning width in the whole period.

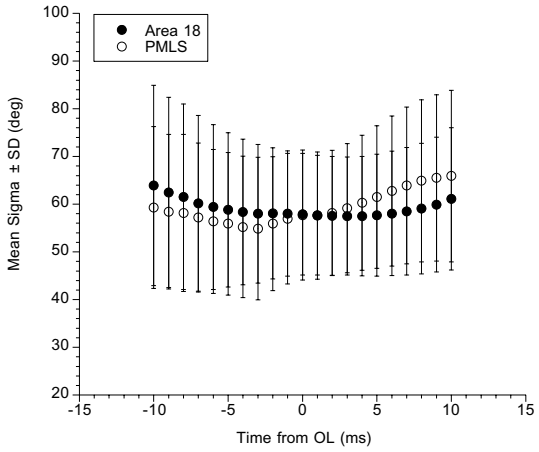

Fig. 7. Mean sigma values plotted as a function of time 10 ms before and 10 ms after the optimal latency. Filled circles represent area 18, open circles represent PMLS data. Error bars represent the ±1 standard error of the means.

Discussion

We have found slight differences in the mean latency values (FSR, OL, LSR) between area 18 and PMLS complex cells, PMLS cells having on average longer FSR and OL, but shorter LSR values than area 18 neurons. The differences were between 3.3 ms and 11.92 ms and were statistically not significant. For non-moving, flickering bright stimuli however, Dinse and Krüger (1994) did find a significant ($p < 0.00001$) difference in mean response latencies between area 18 (mean: 40.4 ms ; SD: 9.4 ms) and PMLS (mean: 66.7 ms; SD: 23.2 ms). They have found lengthening in the mean latency along the measured pathway in the following order: LGN (37.9 ms; SD: 7.1 ms), area 18, area 17 (52.7 ms; SD: 19.6 ms), PMLS, area 7 (83.5 ms; SD: 31.8 ms), area 19 (93.6 ms; SD: 29.6 ms), which is more in agreement with the theory of serial rather than parallel processing pathways. However, they also calculated the percentage of cells that were activated following visual stimulation in different areas, and found a high percentage of cells which were activated simultaneously. In addition, because of the large overlap in the latency distributions (see their Figure 1), they concluded that most of the neurons within different stages of the pathway are simultaneously active when stimulated with bright flickering stimuli. For our moving stimuli, the difference in the mean OL between area 18 and PMLS was only 3.3 ms, which is considerably less than the 26.3 ms found for flickering stimuli by Dinse and Krüger (1994). What do these different results mean in terms of serial or parallel processing and in terms of stimulus specific responses? Let us first consider the question of stimulus specificity. The disadvantage of using the same visual stimulus for each cortical area in the study of Dinse and Krüger is that different neurons

within andbetween cortical areas are tuned to different visual attributes. Furthermore, it has been shown that subcortical latency measurements depend on stimulus parameters such as spatial frequency and contrast (Bolz et al., 1982; Sestokas & Lehmkuhle, 1986), location of the stimulus within the RF (Boltz et al., 1982; Orban et al., 1985), the size of the stimulus and the background illumination (Boltz et al., 1982). Though not yet shown for cortical cells, it might be that sub-optimal stimuli may even reverse the order of response latencies in different types of neurons, like in the case of retinal X and Y-cells (Boltz et al., 1982). In contrast to the study of Dinse and Krüger (1994), we optimized the stimuli for each cell and stimulated the entire RF, which makes us confident about the reliability and comparability of our latency measurements and excludes the above mentioned possibility of latency-order-reversal.

The second issue is the question whether a significant latency difference between two areas implies serial information processing or not. Dinse and Krüger (1994) argued that assuming a signal propagation time of 5-15 ms between different processing stages, the differences they have found between subsequent stages (which were between 2.5 ms and 16.8 ms; see order of activation in previous paragraph) do not imply sequential processing of visual information. The question remains however, whether the substantial and significant mean latency difference of 26.3 ms between the strongly interconnected area 18 and PMLS,(Scannel et al., 1999) does still support their view. The small latency differences between area 18 and PMLS in the present study (between 3.3 and 11.92 ms) argue for simultaneous processing of directional information in these areas. This implies that information about motion direction is processed at the same time in these areas.

The simultaneous activation of directional selective complex cells in area 18 and PMLS suggests that PMLS complex cell direction selectivity does not (entirely) depend on area 18 complex cell activity as one might expect, and the reverse relation does not hold either. Because of the design of our study, the present results cannot confirm these hypotheses. However, studies which argue for the importance of pathways bypassing area 18 (and area 17) in the activation of PMLS direction selective neurons, make this possibility more likely. For example, there is evidence that direction selective PMLS neurons receive fast conducting Y-type input from the lateral posterior nucleus (LP) (Rauschecker et al., 1987). However, the same study also gave some evidence for the theory that directional selectivity of LS neurons is probably jointly determined by the LP input and interactions with the striate cortex or with intra-areal circuitry. Also, when LP was deactivated, direction selectivity in PMLS was not altered (Minville & Casanova, 1998), suggesting that LP is not necessary to generate direction selectivity in PMLS. On the other hand, lesioning area 17 and area 18 did not result in reduction of direction selective cells in PMLS (Guedes et al., 1983; but see Spear & Baumann, 1979, Guido et al., 1990). Our latency results support the hypothesis that DS in PMLS does not exclusively result from cortical DS at lower cortical levels. It seems that the largest part of directionally

selective complex cells in PMLS derive their directional selectivity from non-directionally selective input form the thalamus. For example, it might be the case that DS in area 18 (but perhaps in PMLS too) is generated by the different timing information of the lagged and non-lagged Y-cells (Saul & Humphrey, 1990; Mastronarde et al., 1991). For area 17 simple cells, such thalamic DS generation by lagged and non-lagged X-cells has been indicated already (Saul & Humprhrey, 1990; Jagadeesh et al., 1997; Saul & Feidler, 2002).

Numerous studies have described the thalamocortical projections to area 18 and PMLS. We will not discuss the anatomy in detail, but two important findings need to be mentioned. First, it has been shown, that PMLS neurons are predominantly driven by the Y-cell pathway (Wang et al., 1997), either directly through the LP-pulvinar complex (Rauschecker et al., 1987) or by direct Y-cell input from the LGN (Berson, 1985). Similarly, area 18 neurons are driven by the Y-cell pathway mainly through the LGN (Sherman, 1985), some of them monosynaptically (Harvey, 1980). Similarly to PMLS, area 18 also receives direct Y-pathway input from extrageniculate subcortical areas like the LP-pulvinar complex (Rackowski & Rosenquist, 1983). We suggest that the similarity of FSR and OLs in area 18 and PMLS, and their relatively small scatter in our study, probably reflect input from the fast conducting Y-pathway to both areas. Whether our population of complex cells in these areas reflect direct or indirect afferent input through the Y-pathway remains to be explored. The fact that the response offset (LSR) shows a larger difference between both areas, might reflect the different effects of local circuitry.

More support for similarity of area 18 and PMLS direction selective complex cells is given by our results on the temporal dynamics of directional selectivity. The speed of the increase and decrease in overall direction sensitivity differed significantly within both areas, the development taking place faster than the decrease to base level. This might point to a need of a single cell to remain directionally sensitive for a longer time period in order to integrate information with other incoming inputs. There was no substantial difference between the areas in the development or decrease of overall direction sensitivity. This finding is quite intriguing, since it shows that the temporal dynamics of direction sensitivity shows more variation within area 18 and within PMLS, than between these areas. This in turn suggests that similar local circuitry is involved in developing and phasing out direction sensitivity of complex cells in both areas. The idea of similar local circuitry is also supported by the similar results on the sharpness of directional tuning dynamics in both areas. In none of the areas were the cells changing the sharpness of their directional tuning substantially in a 10 ms period around the OL. It thus seems that the time point of best directional sensitivity (OL) does not correspond with a single time point at which a cell is most sharply tuned, but that there is a broader time period (at least 20 ms) in which the width of the tuning remains fairly constant. Such a margin is desirable if one thinks of proper further convergence and integration of directional information from many complex cells.

In this study we showed that area 18 and PMLS do not differ from each other in terms of timing and temporal dynamics of basic motion direction representation of simple translational texture motion. In this respect, these areas seem to be more similar than expected on the basis of anatomical and previous electrophysiological data. In comparison with area 18 and other cat visual areas, more sophisticated RFs in PMLS have been reported (Von Grünau & Frost, 1983,1987; Toyama et al., 1985, 1991; Niida et al., 1997), though until now, only in the spatial domain. The group of PMLS cells in this study, showing biphasic directional responses in time, shows that elaborate RFs in PMLS exist also in the temporal domain.

References

Berson, D. M. (1985). Cat lateral suprasylvian cortex: Y-cell inputs and corticotectal projection. *J Neurophysiol.* **53**: 544-56.

Best, J., Reuss, S., Dinse, H. R. (1986). Lamina-specific differences of visual latencies following photic stimulation in the cat striate cortex. *Brain Res.* **385**: 356-60.

Bolz, J., Rosner, G., Wassle, H. (1982). Response latency of brisk-sustained (X) and brisk-transient (Y) cells in the cat retina. *J Physiol.* **328**: 171-90.

Borghuis, B. G., Perge, J. A., Vajda, I., van Wezel, R. J., van de Grind, W. A., Lankheet, M. J. (2003). The motion reverse correlation (MRC) method: A linear systems approach in the motion domain. *J Neurosci Methods.* **123**: 153-66.

Casanova, C., Nordmann, J. P., Ohzawa, I., Freeman, R. D. (1992). Direction selectivity of cells in the cat's striate cortex: Differences between bar and grating stimuli. *Vis Neurosci.* **9**: 505-13.

Crook, J. M. (1990). Directional tuning of cells in area 18 of the feline visual cortex for visual noise, bar and spot stimuli: a comparison with area 17. *Exp. Brain Res.* **80**: 545-61.

Dinse, H. R., Krüger, K. (1994). The timing of processing along the visual pathway in the cat. *Neuroreport.* **5**: 893-7.

Dreher, B. (1986) Thalamocortical and corticocortical interconnections in the cat visual system: relation to the mechanisms of information processing. In: Visual Neuroscience (Pettigrew, J. D., Sanderson, K. J. and Levick, W. R., ed.), pp. 290-314. Cambridge: Cambridge University Press.

Guedes, R., Watanabe, S., Creutzfeldt, O. D. (1983). Functional role of association fibres for a visual association area: the posterior suprasylvian sulcus of the cat. *Exp Brain Res.* **49**: 13-27.

Guido, W., Tong, L., Spear, P. D. (1990). Afferent bases of spatial- and temporal-frequency processing by neurons in the cat's posteromedial lateral suprasylvian cortex: effects of removing areas 17, 18, and 19. *J Neurophysiol.* **64**: 1636-51.

Harvey, A. R. (1980). The afferent connexions and laminar distribution of cells in area 18 of the cat. *J Physiol.* **302**: 483-505.

Ikeda, I., Wright, M. J. (1975). Retinotopic distribution, visual latency and orientation tuning of 'sustained' and 'transient' cortical neurons in area 17 of the cat. *Exp Brain Res.* **22**: 385-98.

Jagadeesh, B., Wheat, H. S., Kontsevich, L. L., Tyler, C. W., Ferster, D. (1997). Direction selectivity of synaptic potentials in simple cells of the cat visual cortex. *J Neurophysiol.* **78**: 2772-89.

Julesz, B. (1971) Foundations of Cyclopean Perception. Chicago: University of Chicago Press.

Katsuyama, N., Tsumoto, T., Sato, H., Fukuda, M., Hata, Y. (1996). Lateral suprasylvian visual cortex is activated earlier than or synchronously with primary visual cortex in the cat. *Neurosci Res.* **24**: 431-5.

Kiefer, W., Kruger, K., Strauss, G., Berlucchi, G. (1989). Considerable deficits in the detection performance of the cat after lesion of the suprasylvian visual cortex. *Exp Brain Res.* **75**: 208-12.

Mastronarde, D. N., Humphrey, A. L., Saul, A. B. (1991). Lagged Y cells in the cat lateral geniculate nucleus. *Vis Neurosci.* **7**: 191-200.

Matsubara, J. A., Boyd, J. D. (2002) Relationship of LGN afferents and cortical efferents to cytochrome oxidase blobs. In: The cat primary visual cortex (Payne, B. R. and Peters, A., ed.), pp. 221-58. San Diego, London: Academic Press.

Maunsell, J. H., Gibson, J. R. (1992). Visual response latencies in striate cortex of the macaque monkey. *J Neurophysiol.* **68**: 1332-44.

Mazer, J. A., Vinje, W. E., McDermott, J., Schiller, P. H., Gallant, J. L. (2002). Spatial frequency and orientation tuning dynamics in area V1. *PNAS.* **99**: 1645-50.

Merabet, L., Minville, K., Ptito, M., Casanova, C. (2000). Responses of neurons in the cat posteromedial lateral suprasylvian cortex to moving texture patterns. *Neuroscience.* **97**: 611-23.

Minville, K., Casanova, C. (1998). Spatial frequency processing in posteromedial lateral suprasylvian cortex does not depend on the projections from the striate-recipient zone of the cat's lateral posterior-pulvinar complex. *Neuroscience.* **84**: 699-711.

Molenaar, J., Van de Grind, W. A. (1980). A stereotaxic method of recording from single neurons in the intact in vivo eye of the cat. *J Neurosci Methods.* **2**: 135-52.

Niida, T., Stein, B. E., McHaffie, J. G. (1997). Response properties of corticotectal and corticostriatal neurons in the posterior lateral suprasylvian cortex of the cat. *J Neurosci.* **17**: 8550-65.

Nowlan, S. J., Sejnowski, T. J. (1995). A selection model for motion processing in area MT of primates. *J Neurosci.* **15**: 1195-214.

Orban, G. A., Hoffmann, K. P., Duysens, J. (1985). Velocity selectivity in the cat visual system. I. Responses of LGN cells to moving bar stimuli: a comparison with cortical areas 17 and 18. *J Neurophysiol.* **54**: 1026-49.

Pasternak, T., Horn, K. M., Maunsell, J. H. (1989). Deficits in speed discrimination following lesions of the lateral suprasylvian cortex in the cat. *Vis Neurosci.* **3**: 365-75.

Pasternak, T., Maunsell, J. H. (1992). Spatiotemporal sensitivity following lesions of area 18 in the cat. *J Neurosci.* **12**: 4521-9.

Payne, B. R. (1993). Evidence for visual cortical area homologs in cat and macaque monkey. *Cereb Cortex.* **3**: 1-25.

Raiguel, S. E., Lagae, L., Gulyas, B., Orban, G. A. (1989). Response latencies of visual cells in macaque areas V1, V2 and V5. *Brain Res.* **493**: 155-9.

Raiguel, S. E., Xiao, D. K., Marcar, V. L., Orban, G. A. (1999). Response latency of macaque area MT/V5 neurons and its relationship to stimulus parameters. *J Neurophysiol.* **82**: 1944-56.

Rauschecker, J. P., von Grünau, M. W., Poulin, C. (1987). Thalamo-cortical connections and their correlation with receptive field properties in the cat's lateral suprasylvian visual cortex. *Exp Brain Res.* **67**: 100-12.

Reinoso-Suarez, F. (1961) Topografischer Hirnatlas der Katze fuer experimental-physiologische Untersuchung. Darmstadt: E. Merck AG.

Rosenquist, A. C. (1985) Connections of visual cortical areas in the cat. In: Cerebral Cortex (Peters, A. & Jones, E. G., ed.), pp. 81-117. New York: Plenum Press.

Saul, A. B., Feidler, J. C. (2002). Development of response timing and direction selectivity in cat visual thalamus and cortex. *J Neurosci.* **22**: 2945-55.

Saul, A. B., Humphrey, A. L. (1990). Spatial and temporal response properties of lagged and nonlagged cells in cat lateral geniculate nucleus. *J Neurophysiol.* **64**: 206-24.

Scannell, J. W., Burns, G. A., Hilgetag, C. C., O'Neil, M. A., Young, M. P. (1999). The connectional organization of the cortico-thalamic system of the cat. *Cereb Cortex.* **9**: 277-99.

Sereno, M. E. (1993). Neuronal computation of pattern motion: modeling stages of motion analysis in the primate visual cortex. Cambridge, MA: MIT Press.

Sestokas, A. K., Lehmkuhle, S. (1986). Visual response latency of X- and Y-cells in the dorsal lateral geniculate nucleus of the cat. *Vision Res.* **26**: 1041-54.

Sherman, S. M. (1985) functional organization of the W-, X- and Y-cell pathways in the cat, a review and hypothesis. In: Progress in Psychobiology and physiological pshycology (Sprague, J. M. and Epstein, A. N., ed.), pp. 233-314: New York: Academic Press.

Simoncelli, E. P., Heeger, D. J. (1998). A model of neuronal responses in visual area MT. *Vision Res.* **38**: 743-61.

Spear, P. D. (1991). Functions of extrastruate visual cortex in non-primate species. In: The Neural Basis of Visual Dysfunction (Leventhal, A. G., ed.), pp. 339-70: Macmillan Press.

Spear, P. D., Baumann, T. P. (1979). Effects of visual cortex removal on receptive-field properties of neurons in lateral suprasylvian visual area of the cat. *J Neurophysiol.* **42**: 31-56.

Stone, J. (1983) Parallel processing in the visual system. New York, London: Plenum Press.

Symonds, L. L., Rosenquist, A. C. (1984). Corticocortical connections among visual areas in the cat. *J Comp Neurol.* **229**: 1-38.

Symonds, L. L., Rosenquist, A. C. (1984). Laminar origins of visual corticocortical connections in the cat. *J Comp Neurol.* **229**: 39-47.

Toyama, K., Kitaoji, H., Umetani, K. (1991). Binocular neuronal responsiveness in Clare-Bishop cortex of Siamese cats. *Exp Brain Res.* **86**: 471-82.

Toyama, K., Komatsu, Y., Kasai, H., Fujii, K., Umetani, K. (1985). Responsiveness of Clare-Bishop neurons to visual cues associated with motion of a visual stimulus in three-dimensional space. *Vision Res.* **25**: 407-14.

Von Grünau, M., Frost, B. J. (1983). Double-opponent-process mechanism underlying RF-structure of directionally specific cells of cat lateral suprasylvian visual area. *Exp Brain Res.* **49**: 84-92.

Von Grünau, M., Zumbroich, T. J., Poulin, C. (1987). Visual receptive field properties in the posterior suprasylvian cortex of the cat: a comparison between areas PMLS and PLLS. *Vision Res.* **27**: 343-56.

Wang, C., Dreher, B., Huxlin, K. R., Burke, W. (1997). Excitatory convergence of Y and non-Y information channels on single neurons in the PMLS area, a motion area of the cat visual cortex. *Eur J Neurosci.* **9**: 921-33.

Zumbroich, T. J., von Grunau, M., Poulin, C., Blakemore, C. (1986). Differences of visual field representation in the medial and lateral banks of the suprasylvian cortex (PMLS/PLLS) of the cat. *Exp Brain Res.* **64**: 77-93.

Chapter 3

SPATIO-TEMPORAL REQUIREMENTS FOR DIRECTION SELECTIVITY IN AREA 18 AND PMLS COMPLEX CELLS

Co-authors: Martin J.M. Lankheet & Wim A. van de Grind

Abstract

The spatiotemporal requirements for direction selectivity were studied in two extrastriate motion processing areas in the cat, area 18 and PMLS. The stimulus was a Random Pixel Array (RPA), moving with a single-step pattern lifetime. Stimulus parameters were optimized for each neuron and responses to different step and delay combinations were measured at the preferred velocity. A subset of direction selective complex cells in area 18 was tuned to a medium spatial displacement and temporal delay, indicating a preference for non-smooth motion. Other area 18 complex cells responded best to the smallest step-delay combination. Whether or not a cell showed a band-pass characteristic for step-delay tuning depended on the grain size of the RPA. Smaller grain sizes favored a preference for non-smooth motion. Area 18 cells tuned to larger grain sizes showed larger optimal and maximal step sizes. This corresponded to a higher preferred velocity and larger receptive field size, but was independent of the precise eccentricity of the cell. In PMLS, all recorded complex cells preferred the smoothest motion, irrespective of grain size. In area 18, additional experiments were done for extensive step-delay combinations, covering multiple velocities, to study possible interactions between tuning for step size and delay. Results showed that the optimal spatial displacement was independent of temporal delay. The results are discussed in terms of basic local motion detectors.

Introduction

Perceptually, apparent motion is indistinguishable from continuous, real motion if the temporal sampling rate of the moving pattern is sufficiently high (Morgan, 1980). In fact, the limit of coherent motion perception is at a sampling rate[1] (Van Doorn & Koenderink, 1982b) which is well below the flicker fusion limit of 30-60 Hz (Kelly, 1972), indicating that real motion is also discontinuously sampled by the motion system. In cats and primates directional selectivity in the geniculate-cortical pathway first arises at the level of the primary visual cortex, and a great deal of effort has been put in determining the spatiotemporal requirements for directional selectivity at the first cortical stages (e.g. Cremieux et al., 1984; Duysens et al., 1987 for the cat, and Mikami et al., 1986; Newsome et al., 1986 for the monkey). In the cat, directionally selective simple and complex cells have been studied most extensively in area 17. Although not all of these area 17 studies made a distinction between simple and complex cells (Cremieux et al., 1984; Duysens et al., 1987; Baker, 1988), there is now agreement that simple (Ganz & Felder, 1984; Goodwin et al., 1975; Emerson & Gerstein, 1977; Baker & Cynader, 1986) and complex cells in area 17 (Van Wezel et al., 1997; Baker & Cynader, 1986) are tuned to a specific combination of spatial displacement and temporal delay of a moving stimulus. They loose direction

selectivity not only for steps and delays that are too large, but also for values that are too small.

Spatiotemporal requirements for directional selectivity in higher order motion processing areas have hardly been studied. In cats, areas 18 and PMLS are unequivocally involved in motion processing (Pasternak & Maunsell, 1992; Kiefer et al., 1989; Pasternak et al., 1989; Spear, 1991). Yet, it is unknown whether the spatiotemporal limitations in these areas are similar to those found in area 17. Results for area 18 neurons were only discussed in combination with those for area 17 neurons (Duysens et al., 1987) and only one study (Grüsser & Grüsser-Cornehls, 1973) touched on the spatial and temporal limits of directional selectivity in cat suprasylvian cortex, which includes PMLS. The spatiotemporal requirements for (apparent) motion processing are specially interesting in these areas, because results may reveal to what extent findings in primary visual cortex differ from other parallel (area 18) and subsequent (PMLS) motion processing stages. In the present study we describe the tuning characteristics of directionally selective complex cell responses in area 18 and PMLS, for step size and delay to textures in apparent motion.

We used random pixel arrays in apparent motion. Step size and delay were manipulated to study spatial and temporal tuning. Only complex cells solve the motion correspondence problem inherent in these stimuli, showing both directional and velocity tuning. Simple cells on the other hand, even those responding directionally selective to sine gratings, show no selectivity for the direction of motion. Our stimulus was specifically designed to measure tuning for step size and delay in complex cells: we used a RPA moving with a Single Step Pattern Lifetime (SSPL) similar to that used in human psychophysical experiments (Fredericksen et al., 1993; Lankheet et al., 2002) and for area 17 complex cells by Van Wezel et al. (1997). Whereas a moving pattern of Unlimited Pixel Lifetime (ULPL) contains motion energy at multiple combinations of step and delay ($V=n S/nT$), a SSPL stimulus contains motion energy at a single step size/delay combination and is therefore a suitable stimulus for studying the step and delay tuning characteristics of visual neurons.

In the majority of studies on the spatiotemporal requirements of direction selectivity, the optimal or maximal spatial displacement (D_{opt}, D_{max}) and temporal delay ($T_{opt,}$ T_{max}) values were determined. Physiological studies have shown that eccentricity and velocity influence $D_{opt,}$ D_{max} and $T_{opt,}$ T_{max} (Orban, 1984; Duysens et al., 1987; Baker, 1988). Human psychophysical studies presented evidence that stimulus size influences D_{max} (Eagle & Rogers, 1996; Morgan et al., 1997; Morgan, 1992; Sato, 1990). The various physiological studies exploring spatio-temporal requirements for (apparent) motion differed in both stimulus and measurement paradigms. Stimuli were either jumping (gratings), two-flashed or continuously moving bars (or texture), having different sizes and moving with different velocities to stimulate neurons at different eccentricities. Nevertheless, the absolute values of $D_{opt,}$ D_{max} and $T_{opt,}$ T_{max} were being compared among these studies. To bypass this

problem of response dependency on stimulus parameters and to be able to compare $D_{opt,}$ D_{max} and $T_{opt,}$ T_{max} for a cell population even within a cortical area, we equalized the relative response magnitudes by optimizing the stimulus parameters for each measured cell. First, we determined the smallest pixel size from the used range, that elicited a directionally selective response and determined the preferred speed for the preferred direction at that particular pixel size. Then we constructed a SSPL stimulus of a same pixel size, moving in the preferred and anti-preferred direction of the cell, and with the preferred velocity, by changing the step and delay in appropriate proportions. In this way we obtained spatiotemporal tuning curves appropriate for a cell's preferred velocity and at a relatively small pixel size that elicited directionally selective responses.

Studying the spatiotemporal requirements for directional selectivity at the preferred velocity is the first step in characterizing the cell's response properties. Area 18 complex cells, however, show fairly broad tuning for texture velocity (Vajda et al., 2002). Such broad velocity tuning might result from variations in either step or delay (or both). To determine the contributions from variations in preferred step and delay values to the width of velocity tuning, we performed additional SSPL experiments for a subset of area 18 complex cells, at a wide range of step and delay combinations.

Methods

Physiological preparation and recording procedure

Six adult female cats, weighing approximately 3 kg each, were used in this study. The experiments were carried out according to the guidelines of the Law on Animal Research of the Netherlands and of the Utrecht University's Animal Care and Use Committee. Anaesthesia for the tracheotomy and craniotomy was induced by intramuscular injection of ketamine (15 mg/kg) and xylazine (0.5 mg/kg) (Aescoket-plus, Aesculaap, BV). During recordings, anesthesia was maintained by ventilating the animal with a mixture of 70% N_2O and 30% O_2, supplemented with 0.3-0.6% halothane (Sanofi Santé, BV, Maassluis). Rectal temperature was monitored and maintained at 38˚ with an electric heating blanket. Local analgesics in the form of Lidocaine or Xylocaine ointments (Astra Pharmaceutica, BV, Zoetermeer) were applied at wounds and pressure points. Heart rate, blood pressure, inhaled and expired N_2O, O_2, CO_2 and halothane were monitored during the experiment and, when necessary, regulated to correct ranges. Expired CO_2 was kept at 4.5-5.5%. Muscle relaxation was maintained by intravenous infusion of pancuronium bromide (Pavulon, N.V. Organon, Oss) at 0.11 mg/kg/hour together with 1.94% glucose in a ringer solution.

Pupils were dilated with 1% atropine sulphate (Pharmachemie, BV) and the eyelids were retracted with 2% phenylephrine hydrochloride (Veterinary dispensary

of Utrecht University). The retinae were projected on a white screen at 57 cm distance from the eyes and the positions of the foveae were estimated from the positions of the optic disks and from the orientation of blood vessels. After completion of a set of measurements for a cell, its position was marked on the same screen. The eyes were focused at the appropriate viewing distance with gas-permeable contact lenses (+3.5 to +5.0 diopter, courtesy of NKL, Emmen). Focal correction was assessed by back-projection of the retinal blood vessels onto a white screen. During the experiments clarity of the optics was checked regularly.

The animal was placed in a stereotaxic apparatus (Molenaar & Van de Grind, 1980) with its head fixed by ear bars and tooth clamps. Extracellular single cell recordings from area 18 were obtained with tungsten microelectrodes (impedance 1.0-5.4 MΩ at 500 Hz), insulated with glass or parylene (World Precision Instruments, Inc.). A craniotomy of 0.5 cm diameter was performed above area 18, at Horsley-Clarke co-ordinates P 2-7 and ±(L1.5-L6.5). For PMLS a craniotomy of 0.8 cm was made at Horsley-Clarke co-ordinates A4-P4 and L13-L21 (Reinoso-Suarez, 1961). For area 18, the electrode was advanced vertically, for PMLS at an angle of 30 deg, through an incision in the dura. Craniotomies were sealed with agar (3% in ringer solution).

Visual stimuli

RPAs consisting of 50% black and 50% white pixels (Julesz, 1971) were generated by a Macintosh G4 computer. The frame rate of the stimulus monitor (Sony, Multiscan 400 PS) was 100 Hz, corresponding to a frame exposure duration of 10 ms. Delay times were integer multiples of the frame duration. At the viewing distance of 57 cm and monitor resolution of 1024 x 768 pixels the unit pixel size was 0.03 x 0.03 deg of visual angle. The size of RPA pixels was always a multiple of the unit pixel size. Unless stated otherwise, the stimulus window covered the full screen (34.3 x 25.7 deg). Mean luminance and contrast of the RPAs were set to 50 cd/m^2 and 0.99.

RPAs with both unlimited pattern lifetime (ULPL) and with single step pattern lifetime (SSPL) were used. In the case of ULPL stimuli, coherent motion was generated by shifting the pattern n unit pixels each exposure frame (with n independent of RPA pixel size). In the case of motion with SSPL, the pattern was randomly refreshed after each coherent motion step. For SSPL motion stimuli, steps were integer multiples of the pattern pixel size. While in the case of the ULPL stimulus, lower velocities could be achieved by stepping a smaller distance than the pattern pixel size, in the case of the SSPL stimulus, this was achieved by shifting the pixels each i^{th} exposure frame. Thus, in the SSPL stimuli, motion could not be detected based on a displacement of pixel boundaries or other local information, but required solving the global motion correspondence problem. For SSPL stimuli, the pattern was refreshed after each coherent step, thus the stimuli consisted of an alternation of coherent and incoherent steps. Refreshing the pattern after each coherent motion step assures that no coherent motion information is present at multiples of the

intended step size delay combination. A schematic drawing of this type of motion is shown as a space-time plot in Figure 1. For more stimulus detail see Fredericksen et al. (1993).

Fig. 1. Schematic representation of the Single Step Pattern Lifetime (SSPL) stimulus. The upper horizontal row represents a finite number of dark and light pixels. Motion is represented in a space-time domain. One row of pixels is moving to the left. At every odd step, the pixels are moving coherently and at every even step, they are randomly refreshed (50% chance that a pixel will change luminance). This alternation lasts until the end of the last motion step.

Measurement protocol

The search stimulus was a RPA of ULPL moving in 0.5 sec intervals in 8 different directions (from 0 deg to 315 deg in steps of 45 deg). Pixel size and velocity were both varied, pixel sizes ranging from 0.06 deg to 0.48 deg. RF size and orientation were determined using a hand-held light bar, according to the method of Barlow et al. (1967). For some cells however the procedure failed due to masking by a relatively high spontaneous activity.

Once a single unit was properly isolated, the cell was classified as either simple or complex based on responses to moving sinusoidal gratings (Skottun et al., 1991a,b) and on direction selectivity to moving textures (Hammond, 1991). Simple cells, with a clearly modulated response to sine wave gratings, were discarded and the search for a complex cell was continued. Simple cells never showed significant directionally selective responses to moving RPAs.

Area 18 cells in this study had an eccentricity within 10 deg of the area centralis. Most cells responded directionally selective to a pixel size of 0.24 deg or larger. A minority of the cells, however, showed directional selectivity to a pixel size of 0.12 deg or less. For area 18 we mostly used a pixel size of 0.24 deg, both for the measurements at the preferred velocity and for the extended step and delay combinations including other velocities.

PMLS cells were recorded within 25-30 deg of the area centralis and most of these cells required a pixel size of at least 0.48 deg for directional selectivity. Few cells were directionally selective for patterns of smaller pixel sizes.

For complex cells in both areas, we first determined the optimal velocity for moving RPAs of ULPL with a small pixel size that still gave directionally selective response. The optimal velocity was then used to measure direction tuning in both the ipsi- and contralateral eye. Subsequent measurements were performed for the dominant eye only, with the other eye covered. In the case of a binocular neuron, the ipsilateral eye was covered.

Direction tuning was measured quantitatively by presenting moving RPAs with ULPL in 8 different directions (from 0 - 315 deg in steps of 45 deg), at the cell's $V_{pref.}$ Peri-Stimulus Time Histograms (PSTHs) were evaluated online, for at least ten repetitions of 2 s trials. Direction selectivity was quantified by the Direction Index (DI), which was defined as follows (Casanova et al., 1992):

$$DI = 1 - \frac{\text{mean response in ND}}{\text{mean response in PD}}$$

where non-PD stands for Non-preferred Direction, opposite to the Preferred Direction (PD). Only neurons with a DI ≥ 0.5, that is, with a response in the preferred direction at least twice as large as in the non-preferred direction, were included in subsequent SSPL experiments.

SSPL experiments

Once the PD at the V_{pref} was determined, the SSPL experiment was started. The RPA with SSPL moved in the PD and non-PD of the cell at the $V_{pref.}$ Because SSPL motion contains less motion energy than ULPL motion, response levels and directional selectivity were generally lower. If necessary, we increased the pixel size of the pattern and performed SSPL experiments with one or two larger pixel sizes as well. In this case velocity tuning and direction tuning were re-measured at larger pixel sizes.

Mostly 10 different combinations of step and delay were used, each corresponding to the cell's $V_{pref.}$ Step and delay values were linearly spaced, e.g. for a V_{pref} of 48 deg/s and a pixel size of 0.48 deg, the step value ranged from 0.48 deg to 4.8 deg and the corresponding delay values ranged from 10 ms to 100 ms. Each stimulus condition was repeated ten times. Spontaneous activity was measured in randomly interleaved trials for a uniform gray field with the same mean luminance as the RPA pattern. Trials with different stimulus conditions were randomized within a block. Trial duration was 1.5-2 s, and the time between trails was 0.5 s. The stimulus window always covered the whole RF.

For a subset of area 18 neurons (n=11), extensive measurements were made for a wide range of step-delay combinations. In these experiments patterns with a pixel size of 0.24 x 0.24 deg moved in the PD and non-PD of the cell, in at least 7x7 different combinations of step and delay (representing a wide range of velocities). We refer to these experiments as SSPL matrix experiments.

General data analysis

Signals were amplified (BAK Electronics, Inc.), filtered and displayed on an oscilloscope (Tektronix) and fed to an audio monitor. Spikes were detected using a window discriminator, and the resulting standardized pulses were recorded by a computer (Macintosh G4) at 0.5 ms time resolution. Spike trains, together with all relevant stimulus parameters were stored on disk for off-line data analysis. Dot displays and PSTHs were analyzed on-line as well, to monitor and adjust the data-collection process.

SSPL data analysis

In order to quantify directional selectivity for SSPL motion, the responses in the non-PD were subtracted from those in the PD for the same step-delay combination. One of the questions we were interested in was the presence of a clear optimum step-delay combination. If directional selectivity as a function of step-delay is band-pass, the cell prefers apparent motion rather than smooth motion. On the other hand, if the step-delay tuning curve is low-pass, it means that the smallest value of step and delay, corresponding to the smoothest motion, yielded highest directional selectivity. To test whether a step-size tuning curve was band-pass or low-pass, we determined whether the response significantly declined or increased in the direction of the smallest step size and delay. To this end, we performed pair-wise left and right sided T-tests on combinations of the smallest step size and all larger step sizes. Cells that did not show significant differences had either unreliable responses or were velocity-tuned. Because our experiments did not allow us to differentiate between these two situations, we excluded these cells from further analysis.

For cells with band-pass tuning curves, we determined the optimal step and delay value (D_{opt}-T_{opt}) by simply taking the step-delay combination at which directional selectivity peaked. Obviously, for low-pass cells, no optimal step and delay combination could be determined. To compare our results for the band-pass and low-pass tuned cells, and to related measures in the literature, we also quantified the maximum step size (D_{max}) and delay (T_{max}). The maximum was quantified as the point on the step-delay tuning curve where directional selectivity crossed the level of 1.75 times the cell's standard deviation on the spontaneous activity. For the band-pass tuned cells in area 18 this level of 1.75*SD corresponded to a level 50% below the maximum on average (with a SD of 0.64, n=10). D_{max} and T_{max} values were interpolated between data points with the help of a 4^{th} order polynomial fit to the declining part of the step size-delay tuning curve. We chose a 4^{th} order polynomial because it appeared to have the optimal number of degrees of freedom to interpolate between data points. Since there were no band-pass cells in PMLS we could not estimate D_{max}-T_{max} combinations.

Results

Step-delay measurements in area 18 and PMLS

Preferred direction was determined at the preferred speed and subsequent SSPL experiments were performed on 24 complex cells in area 18 and 27 PMLS complex cells. Pixel sizes varied from 0.06 to 0.48 deg. An example of measurements on an area 18 complex cell is shown in Figure 2. Figure 2a shows that this cell is directionally selective to RPAs of ULPL of 0.24 deg pixel size. Directional tuning was measured at the preferred speed as determined from a velocity tuning experiment (Fig. 2b). In the SSPL experiment, a RPA moved in the PD and non-PD of the cell. Step and delay values all corresponded to the cell's preferred velocity at this pixel size.

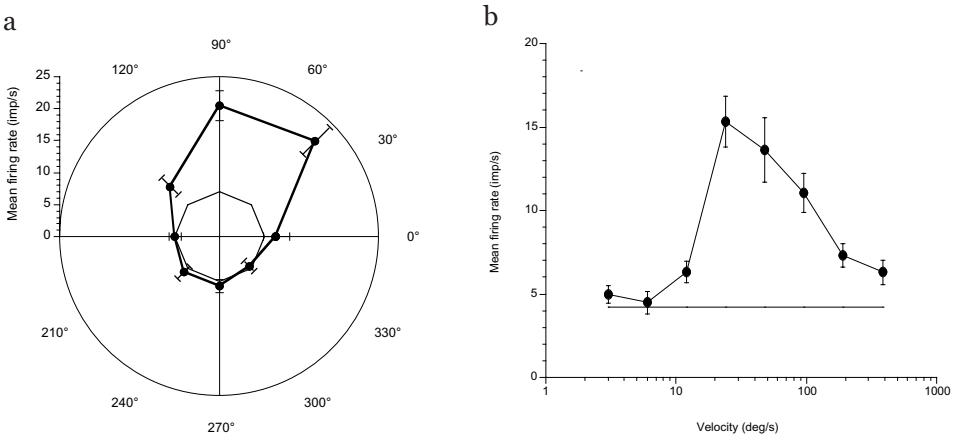

Fig. 2. *Figure continues on facing page.*

The peristimulus time histograms (PSTH) in Figure 2c illustrate the firing characteristics of this cell. For a step size of 0.48 deg and delay of 20 ms, responses to individual steps can be seen. At larger steps, however, the cell did not give a directionally selective response. Figure 2d shows the mean response rates for motion in the PD and non-PD, as well as their difference. This example clearly shows band-pass characteristics. Directional selectivity peaked at a step-delay combination of 0.72 deg (D_{opt}) and 30 ms (T_{opt}). The decline of directional selectivity for decreasing step-delay values was highly significant.

In area 18, for 10 cells out of 24, directional selectivity significantly declined for decreasing step size (band-pass cells). For 12 cells in area 18, directional selectivity was significantly higher at the smallest step-delay combination (low-pass cells). In PMLS, none of the cells was band-pass and 20 cells (74%) showed low-pass response.

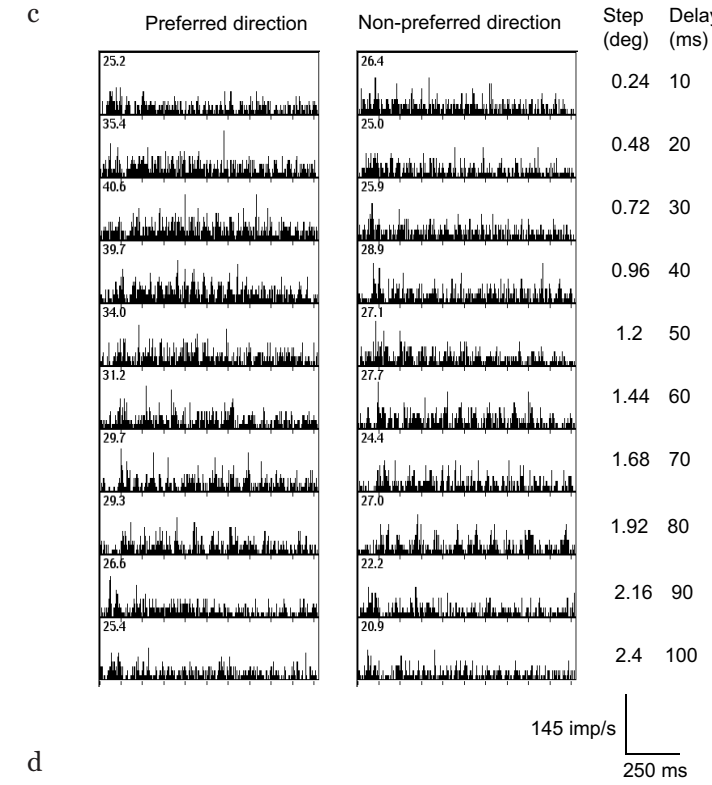

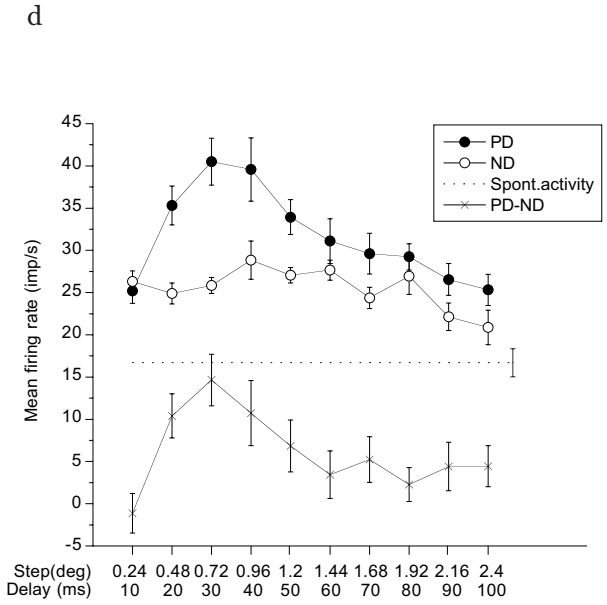

Fig. 2 *continued*. Direction tuning experiment (a) and velocity tuning experiment (b) for an area 18 complex cell with an RPA with ULPL of 0.24 deg pixel size. In both graphs (a and b), solid dots represent responses to the moving stimuli, while the solid lines without markers denote the level of spontaneous activity. Error bars represent the ±1 standard error of the means. c) Peristimulus Time Histograms (PSTHs) of the area 18 complex cell (from a and b) responses to RPAs of 0.24 deg pixel size moving with SSPL. The left column shows responses to stimuli moving in the cell's preferred direction (PD). On the right, responses to the non-preferred (non-PD) are shown (180 deg opposite to the PD). In the upper left corner of each histogram, the mean spike rate is given in impulses per second. At the right, values of the different step and delay combinations are given, all pair-wise combinations representing the Vpref of the cell (24 deg/s). Bin width: 4 ms. d) Average response of the area 18 complex cell from (c), belonging to the same experiment. Filled dots represent responses to the PD, open dots to the non-PD, crosses represent differences between PD and ND. Error bars represent the ±1 standard error of the means.

If SSPL experiments required larger pixel sizes than used in the initial ULPL direction tuning experiments (6 cells in area 18 and 5 cells in PMLS), we first re-measured the velocity tuning at these larger pixel sizes and determined $V_{pref,}$ before starting the SSPL experiment. In both areas we obtained different D_{opt} and / or D_{max} values for different pixel sizes. This is not surprising, because for most cells V_{pref} differed slightly for different pixel sizes. For one area 18 cell, V_{pref} was exactly the same at two different pixel sizes and the SSPL experiments could have yielded the same absolute D_{opt} value. In this cell however, the smaller pixel size elicited low-pass and the larger pixel size a band-pass response curve. In Figure 3, the distribution of all band-pass and low-pass measurements is shown as a function of the pixel size, both for area 18 and PMLS.

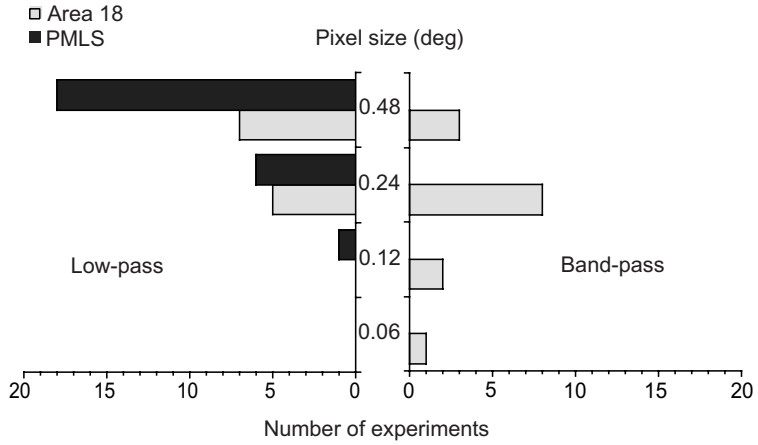

Fig. 3. Frequency distribution of band-pass and low-pass tuned cells in area 18 and PMLS. The graph shows results obtained from 18 area 18 and 20 PMLS cells. Note the absence of band-pass tuned cells in PMLS.

Figure 3 shows that the tuning in area 18 depends partly on the pixel size. It shows that for a pixel size of 0.24 more experiments yielded band-pass than low-pass response curves, while for a pixel size of 0.48 deg the opposite is true. It seems likely, that a pixel size of 0.24 deg was 'too large' for some cells to get a band-pass tuning, while for other cells a pixel size of 0.48 deg was 'small enough' to get a band-pass tuning. None of the cells measured in PMLS showed band-pass tuning. Even for a pixel size of 0.12 deg, the smallest step-delay combination evoked the strongest response in PMLS cells.

The fact that the shape of the step size tuning curve depends partly on pixel size, at least in area 18, makes it impossible to unequivocally categorize a cell as band-pass or low-pass. We can only do so if we subdivide our cell population according to the pixel size used. In Figure 4, we present frequency histograms of the calculated D_{opt} and D_{max} and in Figure 5 for $T_{opt,}$ T_{max} as functions of the pixel size for

the population of area 18 cells. In PMLS, we could not calculate D_{max} and $T_{max,}$ because of the lack of band-pass tuned cells (see Methods).

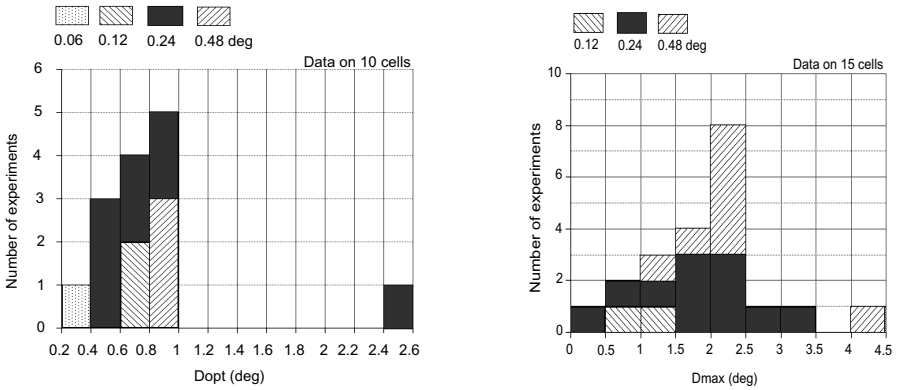

Fig. 4. Distribution of the D_{opt} values of the area 18 band-pass cells (top) and distribution of the D_{max} values of band-pass and low-pass area 18 cells (bottom). For 3 cells (1 band-pass and 2 low-pass) the directional response curve did not cross the value of 1.75 * the SD of the SA, therefore only 15 cells are represented in the bottom graph. In both graphs, the distribution is categorized according to the pixel size that was used in the experiment.

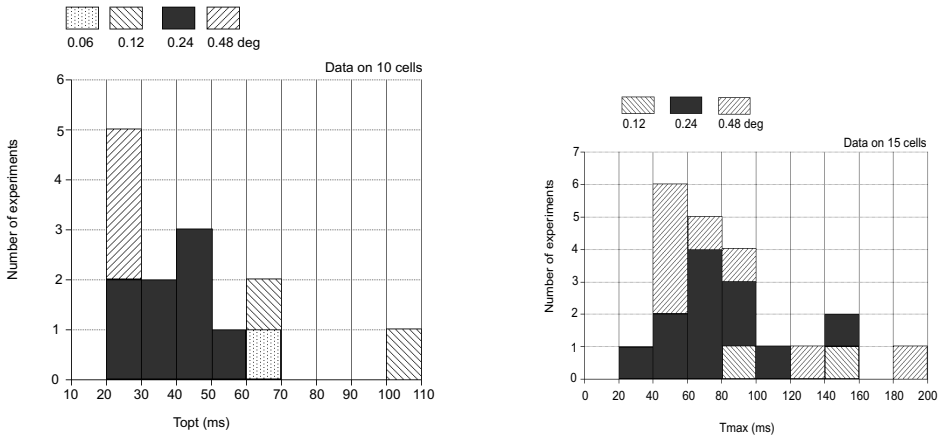

Fig. 5. Distribution of the T_{opt} values of the area 18 band-pass cells (top) and distribution of the T_{max} values of band-pass and low-pass area 18 cells (bottom). For 3 cells (1 band-pass and 2 low-pass) the directional response curve did not cross the value of 1.75 * the SD of the SA, therefore only 15 cells are represented in the bottom graph. In both graphs, the distribution is categorized according to the pixel size that was used in the experiment.

For all the pixel sizes D_{opt} values for the band-pass cells of area 18 ranged from 0.36 deg to 2.4 deg and the T_{opt} values ranged from 20 ms to 100 ms. D_{max} values ranged from 0.24 deg to 4.22 deg and T_{max} values ranged from 20 ms to 188 ms. There is a tendency of getting larger D_{opt} or D_{max} with larger pixel sizes. This is most obvious for the D_{max} distribution (lower graph in Fig. 4). Fig. 5 shows that measurements with larger pixel sizes resulted in both a shorter T_{opt} and $T_{max.}$ We have also looked at the D_{opt} and D_{max} dependence on $V_{pref.}$ A slight increase in D_{opt} and D_{max} was seen with increasing velocity, a relationship that has also been reported for area 17 complex cells (Van Wezel et al., 1997). The ratios of D_{max} to D_{opt} ranged from 1.45 to 4.39, with an average of 2.77 (SD: 1.07).

Step tuning versus delay tuning in area 18

For a subset of area 18 cells (n=11) extensive, multiple velocity step-delay experiments were performed with RPAs of 0.24 x 0.24 deg pixel size. In these experiments the pattern was moving in the cell's PD and non-PD. In Figure 6, two examples are shown of responses to different combinations of step and delay values. Both cells' V_{pref} was 48 deg/s, which is represented by the step-delay combinations along the diagonal. No clear orientation of the directional responses is visible along equal speed lines in Figure 6, but rather along the line of optimal spatial displacement.

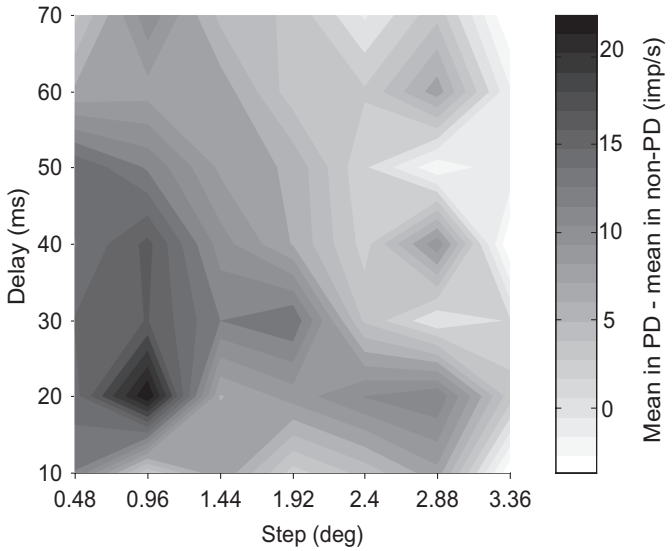

Fig. 6. *Figure continues on facing page.*

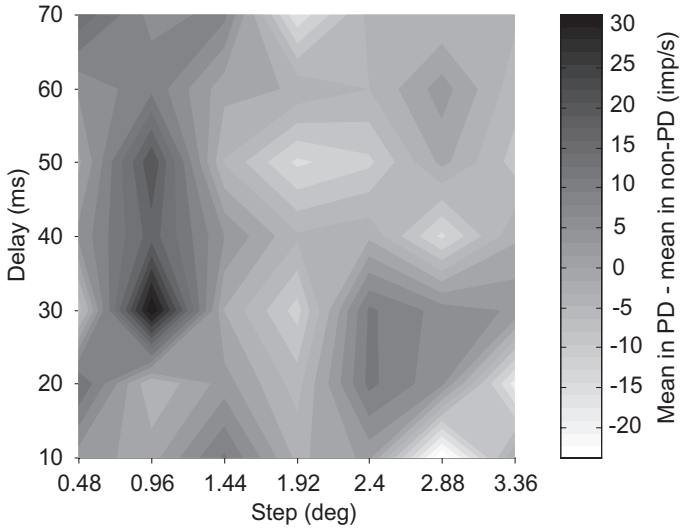

Fig. 6 *continued.* Average firing rates of two area 18 complex cells to different combinations of step and delay values, measured with RPAs of SSPL. Mean firing rate is indicated by shading: the darker, the higher the response.

Separability and dependence of step and delay of these 11 cells were tested with a method, adapted from Levitt and co-workers (Levitt et al., 1994), which was also applied in our previous study on the velocity tuning of area 18 complex cells (Vajda et al., 2002). In short, cell responses were fitted to two models: one representing perfect independence and the other one representing perfect dependency of step and delay. Significant independence was found in the case of 5 cells, the rest giving nonsignificant correlations with both models. None of the cells exhibited dependence on the step and delay of the moving pattern.

Discussion

We report that area 18 contains direction selective complex cells that are tuned for spatial displacement and temporal delay of a moving RPA. However, tuning for step size and delay in this area is not independent of the spatial grain (pixel size) of the patterns. Cells with relatively low spatial resolution, that were therefore measured with large pixel sizes, generally did not show an optimum step-delay combination. Smaller pixel sizes, on the other hand, more often tended to give clear tuning to specific step and delay values at the preferred velocity (Fig. 3).

In PMLS, complex cells did not show an optimum step-delay combination: the smallest step size was always the most effective. This indicates a difference in motion processing between the two areas and is probably partly related to the larger pixel sizes required to drive PMLS complex cells. However, cells with direction selectivity for smaller pixel sizes did not show band-pass tunings either (Fig. 3).

Although the number of cells we recorded is fairly limited and the eccentricities were only partially overlapping in the two areas, the results are difficult to reconcile with hierarchical processing from area 18 to PMLS. Complex cells in the former area show clear band-pass tuning, whereas PMLS cells do not.

In area 18, within the group of the band-pass cells, we have looked at the D_{opt} value distribution as a function of pixel size. The same was done for both band-pass and low-pass cells for the calculated $D_{max.}$ In general, cells had a higher D_{opt} and D_{max} when the pattern pixel size was large and a smaller D_{opt} and D_{max} when it was small (Fig. 4). This shows that pixel size did not only influence the shape of the response curve, but also the values of the optimum and maximum spatial displacement.

The question arises whether the effect of pixel size on optimal and maximal step and delay values is based on a common factor: the velocity preference of the cell. To answer this question, we look at the relation of pixel size and velocity. In Figure 7, this is illustrated for the population of area 18 cells.

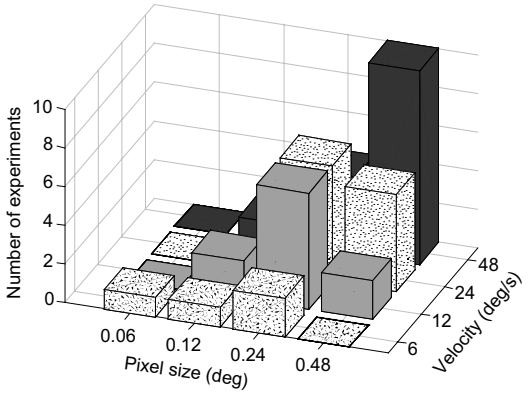

Fig. 7. The distribution of the area 18 cells as function of the pixel size that elicited directional selective response and as a function of the preferred velocity at that particular pixel size. Data of in total 18 cells are presented.

Figure 7 shows that cells that responded directionally selective to smaller pixel sizes had in general lower preferred velocities, while those that responded to larger pixel sizes had higher preferred velocities. This relationship explains why using larger pixel sizes generally resulted in a shorter T_{opt} (and T_{max}) (Fig. 5): high velocities required stepping relatively large distances in short time periods (delays). Lower velocities on the other hand corresponded to smaller steps with longer delays (see Methods). It also explains why D_{opt} and D_{max} increase slightly as a function of velocity.

For sinusoidal gratings, it has been found that cat cortical neurons have lower optimal spatial frequencies, larger RFs and are usually tuned to higher velocities at

higher eccentricities (Maffei & Fiorentini, 1977; Duysens et al., 1982; Orban & Kennedy, 1981; Wilson & Sherman, 1976). Orban et al. (1981), however, found that the correlation between optimal velocity and RF width can only be partially related to the common factor of eccentricity: even within a given eccentricity class of area 17 and 18 cells, there is a correlation between RF width and velocity sensitivity. In our experiments, area 18 cells were within 10 deg of the area centralis, while PMLS cells were within 25-30 deg. For 8 cells in area 18 we mapped the receptive fields quite precisely. These cells responded directionally selective to various pixel sizes. We have determined their total RF area, the RF width along the PD as well as their eccentricity and compared these data with their D_{opt} and V_{pref} values at the smallest pixel sizes that elicited directionally selective responses. Positive correlations were found between V_{pref} and eccentricity, V_{pref} and total RF area, while there was only a slight tendency for the total RF area to increase with eccentricity. Cells having larger RF lengths in the PD direction also showed a slightly higher velocity preference than cells with shorter lengths. A positive correlation was found between the total RF area and the smallest pixel size that elicited a directionally selective response. There was no correlation between eccentricity and pixel size. In a previous study, we reported the same correlation between RF size and pixel size (Vajda et al., 2002). These results agree with the above mentioned finding of Orban et al. (1981) and suggest that irrespective of the precise eccentricity of the RF of an area 18 complex cell (though within an eccentricity class, in our case within 10 deg of the fovea), its total size (and width), V_{pref} and smallest pixel size to which it responds directionally selective are all positively correlated. Accordingly, D_{opt} depends jointly on the V_{pref} and pixel size, all having larger values in cells with larger RF areas.

Our findings indicate, that a comparison of values of D_{opt} or D_{max} from different studies, should not only consider the RF size of the cells, but their V_{pref} for a certain stimulus size as well. The question remains how stimulus size affects the tuning and D_{opt} value(s) in a single cell. We found only one cell that had exactly the same optimal velocity for two different pixel sizes, but this cell had a band-pass tuning to a large pixel size and was low-pass for a smaller pixel size. In the present study we adjusted the velocity for each pixel size. In order to quantify the effect of pixel size on step size tuning irrespective of velocity differences, one would have to follow a different procedure. Data obtained in the present study however, argue against a simple relationship between pixel size tuning and step size tuning. Based on the present results, we suggest that at least in area 18, cells that respond directionally selective to patterns consisting of larger pixel sizes and are generally tuned to higher velocities are underlied by local motion detectors, which units, like for example Adelson & Bergen's oriented linear spatial filters (Adelson & Bergen, 1985), have a larger spatial separation than those cells, that respond directionally selective to smaller pixel sizes, have lower preferred velocities and are 'built up' of units having a smaller spatial separation.

Results from human psychophysical experiments on the spatiotemporal properties of motion detection were interpreted in terms of the span and delay between two inputs of elementary correlators (Van Doorn & Koenderink, 1982a,b; Van de Grind et al., 1986). Van de Grind et al. (1986) have found that subfield sizes increase with the detectors' tuning velocity and that the average span is approximately 2-4 times the average subfield diameter. Our results are in line with these findings.

Results from the SSPL matrix experiments did not show clear orientation along equal speed lines, but rather along the line of temporal delay. This suggests that the optimal displacement for these neurons is independent of the temporal delay. This is in agreement with the findings of Van Wezel et al. (1997) on area 17 complex cells measured with the same stimulus paradigm. It also corresponds with results of Baker and Cynader (1988) on area 17 neurons (both simple and complex), tested by two-flashed bar stimuli, and with the results of Baker et al. (1991) on area 17 and 18 neurons (simple and complex) by jumping gratings. Our results suggest that tuning for velocity of area 18 complex cells does not depend on inseparable tuning of spatial displacement and temporal delay, but rather on a broad tuning for temporal delay.

FOOTNOTE

1. The sampling rate or its equivalent presentation period at which humans perceive coherent motion decreases with increasing velocity and can be estimated by the formula $T=89 * v^{-0.4}$, where T is the critical period in ms and v is the velocity in deg/s.

REFERENCES

Adelson, E. H., Bergen, J. R. (1985). Spatiotemporal energy models for the perception of motion. *J Opt Soc Am A.* **2**: 284-99.

Baker, C. L., Jr. (1988). Spatial and temporal determinants of directionally selective velocity preference in cat striate cortex neurons. *J Neurophysiol.* **59**: 1557-74.

Baker, C. L., Jr., Cynader, M. S. (1986). Spatial receptive-field properties of direction-selective neurons in cat striate cortex. *J Neurophysiol.* **55**: 1136-52.

Baker, C. L., Jr., Cynader, M. S. (1988). Space-time separability of direction selectivity in cat striate cortex neurons. *Vision Res.* **28**: 239-46.

Baker, C. L., Jr., Friend, S. M., Boulton, J. C. (1991). Optimal spatial displacement for direction selectivity in cat visual cortex neurons. *Vision Res.* **31**: 1659-68.

Barlow, H. B., Blakemore, C., Pettigrew, J. D. (1967). The neural mechanism of binocular depth discrimination. *J Physiol.* **193**: 327-42.

Casanova, C., Nordmann, J. P., Ohzawa, I., Freeman, R. D. (1992). Direction selectivity of cells in the cat's striate cortex: differences between bar and grating stimuli. *Vis Neurosci.* **9**: 505-13.

Cremieux, J., Orban, G. A., Duysens, J. (1984). Responses of cat visual cortical cells to continuously and stroboscopically illuminated moving light slits compared. *Vision Res.* **24**: 449-57.

Duysens, J., Maes, H., Orban, G. A. (1987). The velocity dependence of direction selectivity of visual cortical neurones in the cat. *J Physiol.* **387**: 95-113.

Duysens, J., Orban, G. A., van der Glas, H. W., Maes, H. (1982). Receptive field structure of area 19 as compared to area 17 of the cat. *Brain Res.* **231**: 293-308.

Eagle, R. A., Rogers, B. J. (1996). Motion detection is limited by element density not spatial frequency. *Vision Res.* **36**: 545-58.

Emerson, R. C., Gerstein, G. L. (1977). Simple striate neurons in the cat. II. Mechanisms underlying directional asymmetry and directional selectivity. *J Neurophysiol.* **40**: 136-55.

Fredericksen, R. E., Verstraten, F. A., van de Grind, W. A. (1993). Spatio-temporal characteristics of human motion perception. *Vision Res.* **33**: 1193-205.

Ganz, L., Felder, R. (1984). Mechanism of directional selectivity in simple neurons of the cat's visual cortex analyzed with stationary flash sequences. *J Neurophysiol.* **51**: 294-324.

Goodwin, A. W., Henry, G. H., Bishop, P. O. (1975). Direction selectivity of simple striate cells: properties and mechanism. *J Neurophysiol.* **38**: 1500-23.

Grüsser, O. J., Grüsser-Cornehls, U. (1973) Neuronal mechanisms of visual movement perception and some psychophysical and behavioural correlations. In: *Handbook of Sensory Physiology* (Jung, R., ed.), pp. 333-429. Berlin, New York, Heidelberg: Springer.

Hammond, P. (1991). On the response of simple and complex cells to random dot patterns: a reply to Skottun, Grosof and De Valois. *Vision Res.* **31**: 47-50.

Julesz, B. (1971) Foundations of Cyclopean Perception. Chicago: University of Chicago Press.

Kelly, D. H. (1972) Flicker. In: *Handbook of Sensory Physiology* (Jameson, D. & Hurvich, L. M., ed.), pp. 273-302. New York: Springer.

Kiefer, W., Kruger, K., Strauss, G., Berlucchi, G. (1989). Considerable deficits in the detection performance of the cat after lesion of the suprasylvian visual cortex. *Exp Brain Res.* **75**: 208-12.

Lankheet, M. J., van Doorn, A. J., van de Grind, W. A. (2002). Spatio-temporal tuning of motion coherence detection at different luminance levels. *Vision Res.* **42**: 65-73.

Levitt, J.B., Kiper, D.C. & Movshon, J.A. (1994). Receptive fields and functional architecture of macaque V2. *J Neurophysiol.* **71**: 2517-42.

Maffei, L., Fiorentini, A. (1977). Spatial frequency rows in the straite visual cortex. *Vision Res.* **17**: 257-64.

Mikami, A., Newsome, W. T., Wurtz, R. H. (1986). Motion selectivity in macaque visual cortex. II. Spatiotemporal range of directional interactions in MT and V1. *J Neurophysiol*. **55**: 1328-39.

Molenaar, J., van de Grind, W. A. (1980). A stereotaxic method of recording from single neurons in the intact in vivo eye of the cat. *J Neurosci Methods*. **2**: 135-52.

Morgan, M. J. (1980). Analogue models of motion perception. *Philos Trans R Soc Lond B Biol Sci*. **290**: 117-35.

Morgan, M. J. (1992). Spatial filtering precedes motion detection. *Nature*. **355**: 344-6.

Morgan, M. J., Perry, R., Fahle, M. (1997). The spatial limit for motion detection in noise depends on element size, not on spatial frequency. *Vision Res*. **37**: 729-36.

Newsome, W. T., Mikami, A., Wurtz, R. H. (1986). Motion selectivity in macaque visual cortex. III. Psychophysics and physiology of apparent motion. *J Neurophysiol*. **55**: 1340-51.

Orban, G. A. (1984) *Neuronal operations in the visual cortex: studies of brain function*. Berlin: Springer.

Orban, G. A., Kennedy, H. (1981). The influence of eccentricity on receptive field types and orientation selectivity in areas 17 and 18 of the cat. *Brain Res*. **208**: 203-8.

Orban, G. A., Kennedy, H., Maes, H. (1981). Response to movement of neurons in areas 17 and 18 of the cat: velocity sensitivity. *J Neurophysiol*. **45**: 1043-58.

Pasternak, T., Horn, K. M., Maunsell, J. H. (1989). Deficits in speed discrimination following lesions of the lateral suprasylvian cortex in the cat. *Vis Neurosci*. **3**: 365-75.

Pasternak, T., Maunsell, J. H. (1992). Spatiotemporal sensitivity following lesions of area 18 in the cat. *J Neurosci*. **12**: 4521-9.

Reinoso-Suarez, F. (1961) *Topografischer Hirnatlas der Katze fuer experimental-physiologische Untersuchung*. Darmstadt: E. Merck AG.

Sato, T. (1990). Effects of dot size and dot density on motion perception with random dot kinematograms. *Perception Supplement*. **19**: 329.

Skottun, B. C., De Valois, R. L., Grosof, D. H., Movshon, J. A., Albrecht, D. G., Bonds, A. B. (1991b). Classifying simple and complex cells on the basis of response modulation. *Vision Res*. **31**: 1079-86.

Skottun, B. C., Grosof, D. H., De Valois, R. L. (1991a). On the responses of simple and complex cells to random dot patterns. *Vision Res*. **31**: 43-6.

Spear, P. D. (1991) *Functions of extrastruate visual cortex in non-primate species.* (Leventhal, A. G., ed.), pp. 339-70. MacMillian Press Scientific & Medical.

Vajda, I., Lankheet, M. J., van Leeuwen, T. M., van de Grind, W. A. (2002). On the velocity tuning of area 18 complex cell responses to moving textures. *Vis Neurosci*. **19**: 651-9.

Van de Grind, W. A., Koenderink, J. J., van Doorn, A. J. (1986). The distribution of human motion detector properties in the monocular visual field. *Vision Res.* **26**: 797-810.

Van Doorn, A. J., Koenderink, J. J. (1982a). Spatial properties of the visual detectability of moving spatial white noise. *Exp Brain Res.* **45**: 189-95.

Van Doorn, A. J., Koenderink, J. J. (1982b). Temporal properties of the visual detectability of moving spatial white noise. *Exp Brain Res.* **45**: 179-88.

Van Wezel, R. J., Lankheet, M. J., Fredericksen, R. E., Verstraten, F. A., van de Grind, W. A. (1997). Responses of complex cells in cat area 17 to apparent motion of random pixel arrays. *Vision Res.* **37**: 839-52.

Wilson, J. R., Sherman, S. M. (1976). Receptive-field characteristics of neurons in cat striate cortex: Changes with visual field eccentricity. *J Neurophysiol.* **39**: 512-33.

Chapter 4

Temporal interactions in direction selective complex cells of area 18 and PMLS of the cat

Co-authors: Martin J.M. Lankheet, Bart G. Borghuis & Wim A. van de Grind

Abstract

Temporal interactions in direction sensitive complex cells in area 18 and PMLS were studied using a reverse correlation method. Reverse correlograms to combinations of two temporally separated motion directions were examined and compared in the two areas. A comparison to the first order reverse correlograms allowed us to identify nonlinear suppression or facilitation due to pair-wise combinations of motion directions. Area 18 and PMLS differed very much from each other. Area 18 showed a single type of nonlinear behavior: similar directions facilitated and opposite directions suppressed spike probability. This effect was most pronounced for motion steps that followed each other immediately and decreased with increasing delay between steps. In PMLS, the picture was much more diverse. Some cells exhibited nonlinear interactions that were opposite to those in area 18 (facilitation for opposite directions and suppression for similar ones), while the majority did not show a systematic interaction profile. We conclude that nonlinear second-order reverse correlation characteristics reveal different functional properties, despite similarities in the first order reverse correlation profiles. Directional interactions in time revealed optimal integration of similar directions in area 18, but motion opponency - at least in some cells - in PMLS.

Introduction

Complex cells that are sensitive to the direction of texture motion have been found in several visual areas in the cat cortex, including area 17, area 18 and PMLS (Hammond & MacKay, 1975, 1977; Hamada, 1987; Crook, 1990; Merabet et al., 2000). In area 17 and 18, these cells were classified as special complex cells. They prefer contour lengths that are much shorter than their Receptive Field (RF) diameter, exhibit higher sensitivity to texture motion than other types of complex cells, and are direction sensitive to such motion (Hammond & Ahmed, 1985; Hammond & Pomfrett, 1989, 1990). In PMLS, complex cells that are sensitive to the direction of texture motion were not assigned to any specific class as a consequence of their more diverse spatial RF structures (Von Grünau & Frost, 1983, 1987; Toyama et al., 1985, 1991; Krüger et al., 1993a,b; Niida et al., 1997; Akase et al., 1998; Li et al., 2000, 2001; Brosseau-Lachaine et al., 2001). All of these complex cells share the ability to solve the motion correspondence problem and are therefore thought to play a direct role in motion coherence detection.

Recently, we compared the temporal properties for direction tuning of such complex cells in area 18 and PMLS (Vajda et al., 2003a) by using a Motion Reverse Correlation (MRC) method (Borghuis et al., 2003). Both area 18 and PMLS play a role in motion perception (Kiefer et al, 1989; Pasternak et al., 1989; Spear, 1991; Pasternak & Maunsell, 1992). Suprisingly however, the majority of PMLS cells showed

response dynamics similar to complex cells in area 18. The similarity in response dynamics would suggest similar RF properties in the two areas, but PMLS receptive fields are known to be considerably more complex than in area 18. Spatial motion opponency was for example reported for complex cells in PMLS (Von Grünau & Frost, 1983) but not in areas 17 or 18. Based on the spatial RF differences in the two areas, we expect that directional interactions in time are more prominent in PMLS than in area 18.

In the present study we therefore specifically examined temporal interactions between different motion directions in both areas. To do so, we adapted the MRC technique (Borghuis et al., 2003) and examined reverse correlation profiles to combinations of two temporally separated motion directions. In our previous study (Vajda et al., 2003a) we applied a first-order analysis, in which spikes were reverse correlated with individual motion impulses of RPAs moving in one of eight different directions. In the present study we used a second order analysis in which spikes were correlated with all combinations of stimulus directions that preceded it and then averaging these preceding stimulus waveforms. In this way we could determine the contribution of specific combinations of directions to the first order reverse correlogram, which was the average of all possible combinations.

If temporal interactions do not play a role, the second order profile for different directions should be predictable from the first order profiles. Comparing the predictions to the measured profiles for different combinations allows one to pinpoint nonlinear suppression or facilitation due to previous motion directions. We have made predictions of the second order reverse correlation profiles and compared them to the measured second order profiles for our area 18 and PMLS complex cells, that exhibited direction sensitivity for moving RPAs. Similarity in this second order temporal domain would point to a common or comparable temporal mechanism of motion direction processing in both areas. Differences in reverse correlation profiles on the other hand, would suggest that the temporal mechanisms underlying motion direction processing are different in the two areas, as holds for the spatial RF structure.

Besides revealing expected general differences between area 18 and PMLS, the second order analysis might also shed light on the origin of the so-called biphasic reverse correlation profiles in PMLS. Although the majority of PMLS cells showed similar, monophasic temporal properties as found in area 18, some cells showed a biphasic reverse correlogram, corresponding to a change of preferred direction over time (Vajda et al., 2003a). Similar profiles were also found in about 50 percent of the cells in macaque area MT (Borghuis et al., 2003). The biphasic profile could either be due to intrinsic response properties such as adaptation, or it might result from temporal interactions between opponent motion directions. The second order analysis will quantify the role of specific combinations of directions.

Methods

The physiological preparation, recording procedure, visual stimuli, measurement protocol and general data collection were described more extensively in our previous paper (Vajda et al., 2003a). In brief, nine adult cats were used in this study. The experiments were carried out according to the guidelines of the Law on Animal Research of the Netherlands and of the Utrecht University's Animal Care and Use Committee. Anesthesia for the tracheotomy and craniotomy was induced by intramuscular injection of ketamine (15 mg/kg) and xylazine (0.5 mg/kg) (Aescoket-plus, Aesculaap, BV). During recordings, anesthesia was maintained by ventilating the animal with a mixture of 70% N_2O and 30% O_2, supplemented with 0.3-0.6% halothane (Sanofi Santé, BV, Maassluis). Rectal temperature was monitored and maintained at 38˚. Analgesics (Lidocaine or Xylocaine ointments) were applied at pressure points. Heart rate, blood pressure, in- and expired N_2O, O_2 and halothane were monitored during the experiment. Muscle relaxation was maintained by intravenous infusion of pancuronium bromide (Pavulon, N.V. Organon, Oss) at 0.11 mg/kg/hour together with 1.94% glucose in a ringer solution.

Pupils were dilated with 1% atropine sulphate (Pharmachemie, BV) and the eyelids retracted with 2% phenylephrine hydrochloride (Veterinary dispensary of Utrecht University). The retinae were projected on a white screen at 57 cm distance from the eyes and the positions of the foveae were estimated from the positions of the optic disks and from the orientation of blood vessels. The eyes were focused at the appropriate viewing distance with gas-permeable, contact lenses. Focal correction was assessed by back-projection of the retinal blood vessels onto a white screen. The animal was placed in a stereotaxic apparatus (Molenaar & Van de Grind, 1980) with its head fixed by ear bars and tooth clamps. Extracellular single cell recordings were obtained with tungsten microelectrodes (impedance 1.0-5.4 MΩ at 500 Hz), insulated with glass or parylene (World Precision Instruments, Inc.). A craniotomy of 0.5 cm diameter was performed above area 18, at Horsley-Clarke coordinates P 2-7 and ±(L1.5-L6.5). For PMLS a craniotomy of 0.8 cm was made at Horsley-Clarke coordinates co-ordinates A4-P4 and ±(L13-L21) (Reinoso-Suarez, 1961). For area 18, the electrode was advanced vertically, for PMLS at an angle of 30 deg, through an incision in the dura. Craniotomies were sealed with agar (3% in ringer solution). We will briefly summarize the measurement procedures and basic first order analysis before we focus on the description of the second order analysis, the main topic of the present paper.

Random pixel arrays consisting of 50% bright and 50% dark pixels (Julesz, 1971) were generated by a Macintosh G4 computer. The frame rate of the stimulus monitor (Sony, Multiscan 400 PS) was 100 Hz. The mean luminance and contrast of the RPAs were set to 50 cd/m^2 and 0.99 respectively. At the viewing distance of 57 cm and monitor resolution of 1024 x 768 pixels, the unit pixel size was 0.03 deg x 0.03 deg of visual angle. The pixel size of the RPA was either 0.48 deg x 0.48 deg or

0.24 deg x 0.24 deg. Unless stated otherwise, the stimulus window measured 24 deg x 21 deg, which was large enough to cover the full receptive field.

A detailed measurement protocol is given in the Methods section of our previous paper (Vajda et al., 2003a). In short, complex cells, sensitive to the direction of moving RPAs, were selected and their preferred velocity was determined for motion in the preferred direction. For a subset of cells in both areas (56%), the preferred step and delay values at the preferred velocity were determined and used in the MRC experiments. For the remaining cells, the smallest step and delay values, that corresponded to the preferred velocity were used. In PMLS, the smallest step and delay value was always the preferred combination, while in area 18 this was not always the case. In area 18 we found cells with clear optima at some intermediate step size and delay combination (Vajda et al., 2003b). Eight cells, included in the MRC data set, showed a preference for such an intermediate combination. For these cells, however, neither the first order, nor the second order reverse correlation results deviated from what was found for neurons, which had their optimum at the smallest spatial displacement and temporal delay or for which the arbitrarily chosen smallest step and delay value was used.

In the MRC method (Borghuis et al., 2003) as we used it, an RPA makes a random walk, in eight different directions (from 0 deg to 315 deg in steps of 45 deg) consisting of a random sequence of single steps. To obtain a balanced sequence in which all directions were presented equally often (several thousands of repetitions), a predefined array that contained equal numbers of all directions, was randomly shuffled. The 'speed' of the pattern was defined by the step size (number of unit pixels) and delay (number of exposure frames between steps). At each step a new motion impulse (direction) was presented.

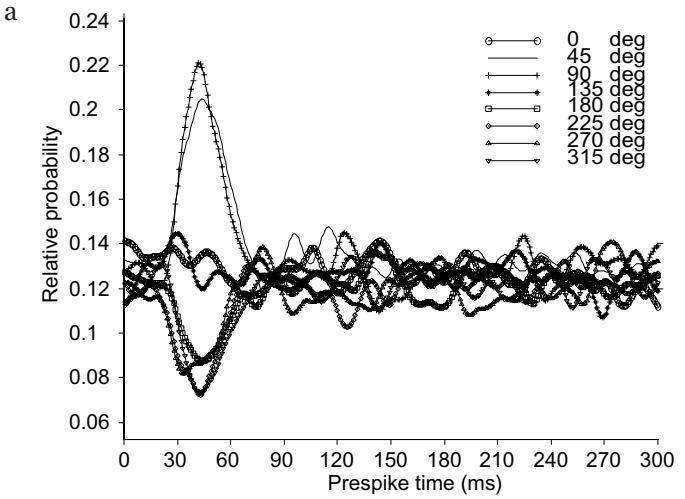

Fig. 1. *Figure continues on facing page.*

b

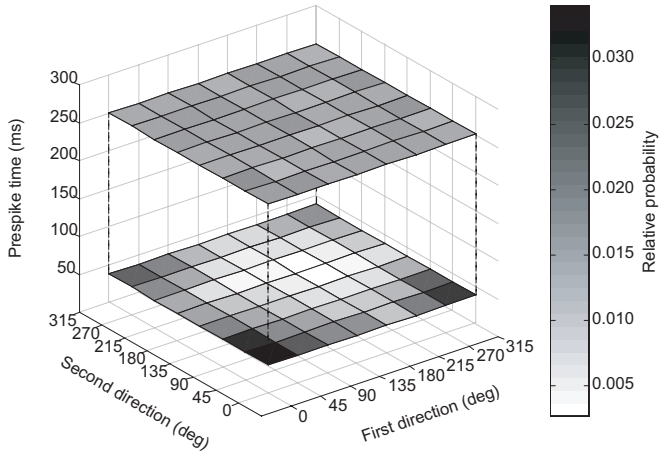

Fig. 1 *continued*. a) First order direction reverse correlation data for an area 18 complex cell. The stimulus consisted of 8 different directions and in total 30000 motion impulses. A new direction was started every 10 ms. b) Part of a second order reverse correlogram of a monophasic PMLS cell. Stimulus parameters were the same as for the cell in (a). Direction-combinations are represented on the x-y plane, time preceding the spikes on the z-axis. Shading denotes the magnitude of the relative probability (chance level at 0.015). For clarity, only two time-slices are shown from the data: at prespike times 38 ms and at 250 ms. See text for further explanation.

First order and second order reverse correlation analysis

In the first order analysis, spikes were reverse correlated with the 8 individual stimulus directions. This yielded a relative probability function for the occurrence of each motion direction at each point in time preceding a spike, a value of 1/8 representing chance level (Fig. 1a). From now on, relative probability of a stimulus or a stimulus-combination preceding a spike will be interchangeably used with the term reverse correlation (RC)-amplitude. In the second order analysis, spikes were reverse correlated with all 64 possible combinations of stimulus direction pairs (64). The time interval between the members of each pair (*dt*[ms]) was always a multiple of the delay value between steps, (*dt*=n*T, where n=1,2,3,4 and T is the delay value in ms).

This analysis yielded relative probability functions for the occurrences of specific pairs of directions with various time intervals (*dt's*), at each point in time preceding a spike. From now on, the time interval will be simply denoted by its delay value, *dt*, expressed as number of delay units, which equals the number of steps. A *dt* value of *i* therefore means an interval of *i* steps. From now on, we use the word 'successive' to denote a *dt* value of 1. In Figure 1b, a piece of a second order reverse correlogram is illustrated for a single *dt* value. In this case, a value of 1/64 represents chance level. Both the time of occurrence of spikes and of motion steps were measured with a temporal resolution of 0.5 ms. This resulted in a sparse distribution of motion impulses, and therefore in somewhat noisy cross-correlation

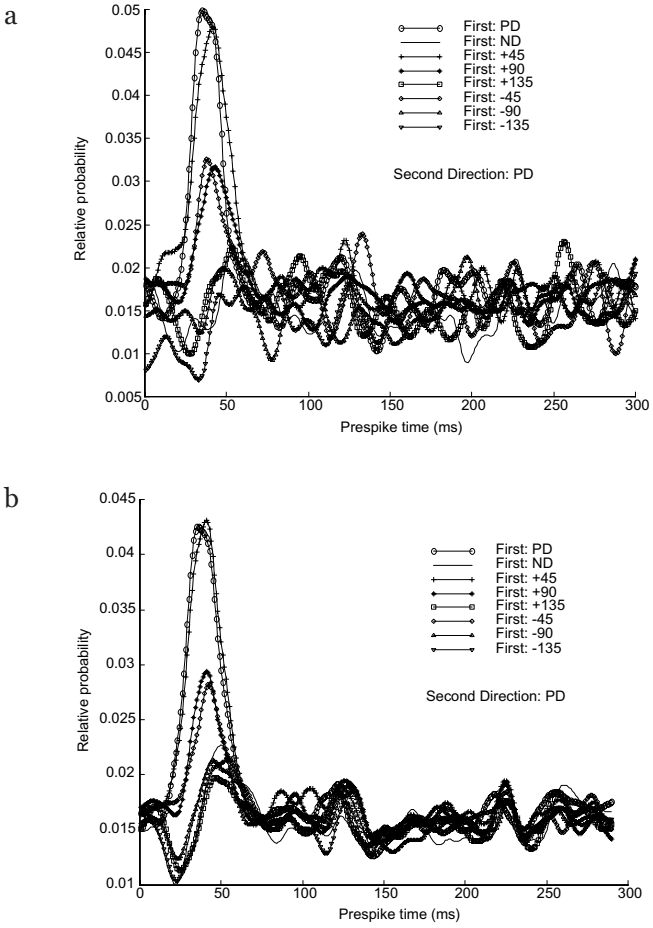

Fig. 2. a) Second order reverse correlation curves for 8 direction combinations, where the second direction was always in the PD. Results are for the area 18 cell shown in Fig. 1a. Panel b) gives the predicted second order reverse correlation curves for the same cell and for the same direction combinations. See text for further explanation.

functions. The noise level was reduced by smoothing the probability functions using a sliding average with a Gaussian window with a standard deviation of 5 ms (see Fig. 2 in Borghuis et al., 2003).

Second order MRC analysis

To develop a baseline for the quantification of temporal interactions between different motion directions, we used the first order results to predict results for linear combinations of motion steps. The rationale is that some directional combinations might be special and might therefore be more highly correlated with spikes. This should become visible as a deviation from the first order prediction, which treats responses as independent. To obtain a prediction based on independence of

responses at each prespike time point, the relative probability of the occurrence of a specific direction was multiplied by the relative probabilities of each direction occurring *n* motion steps earlier in time (n={1,2,3,4}). In this way, we obtained arrays of 64 time functions, expressing the relative probability of each possible direction-combination to precede (cause) a spike. If the cell sums individual motion step probabilities linearly and individual directions act independently, then the linear combination of separate probabilities with an appropriate time delay should accurately predict the relation between combinations and spikes. Figure 2a illustrates 8 out of 64 components of a second order reverse correlation for successive motion pairs. These are results for the area 18 neuron from Figure 1a. The 8 combinations in Figure 2a are the cases in which the second direction was in the cell's PD. Each curve in the graph represents one of the 8 different first directions that preceded the PD. In Figure 2b, the predicted relative probabilities are shown for the same combination of directions as in panel a.

Figure 2a shows that different direction-combinations occur with different probabilities at different points in time preceding a spike. For example, the highest probability of firing occurred at around 40 ms after the second motion step, if a PD was preceded by a PD (curve with open circles in Fig. 2a). Such a result is not suprising, since the first order probability curve for the PD (but for all other directions too) has a certain width in time (Fig. 1a). Thus the RC-amplitude to the PD-PD stimulus combination partly results from temporal integration of overlapping RC-amplitudes to the PD at two subsequent time-steps. Such summation occurs for all combinations of directions and determines the time course of relative probabilities for combinations. The elevation of the relative probability for the PD-PD combination in Figure 2a, however, cannot be entirely accounted for by integration of RC-amplitudes to the PD-PD at two subsequent time-steps. This can easily be verified by comparing the measured RC-amplitudes of Figure 2a to the linear prediction in Figure 2b. Figure 2b shows that the predicted value for the PD-PD stimulus combination is less than what we measured. A similar effect was seen when the first direction differed 45 deg, and to a lesser extent for 90 deg difference relative to the PD. Suppressing effects were seen for successive stimuli at angles of 180 deg or ±135 deg relative to each other.

Figure 2 shows clear differences between predicted and actually measured temporal interactions. To present similar results for all 64 combinations, rather than just the 8 examples in Figure 2, we plotted the full data set in a different format in Figure 3. Different combinations are orderly arranged along the abscissa, whereas the time preceding spikes is presented on the ordinate. Darker shades correspond to high relative probabilities. Figure 3a shows measured data and Figure 3b predicted values, based on a first order analysis.

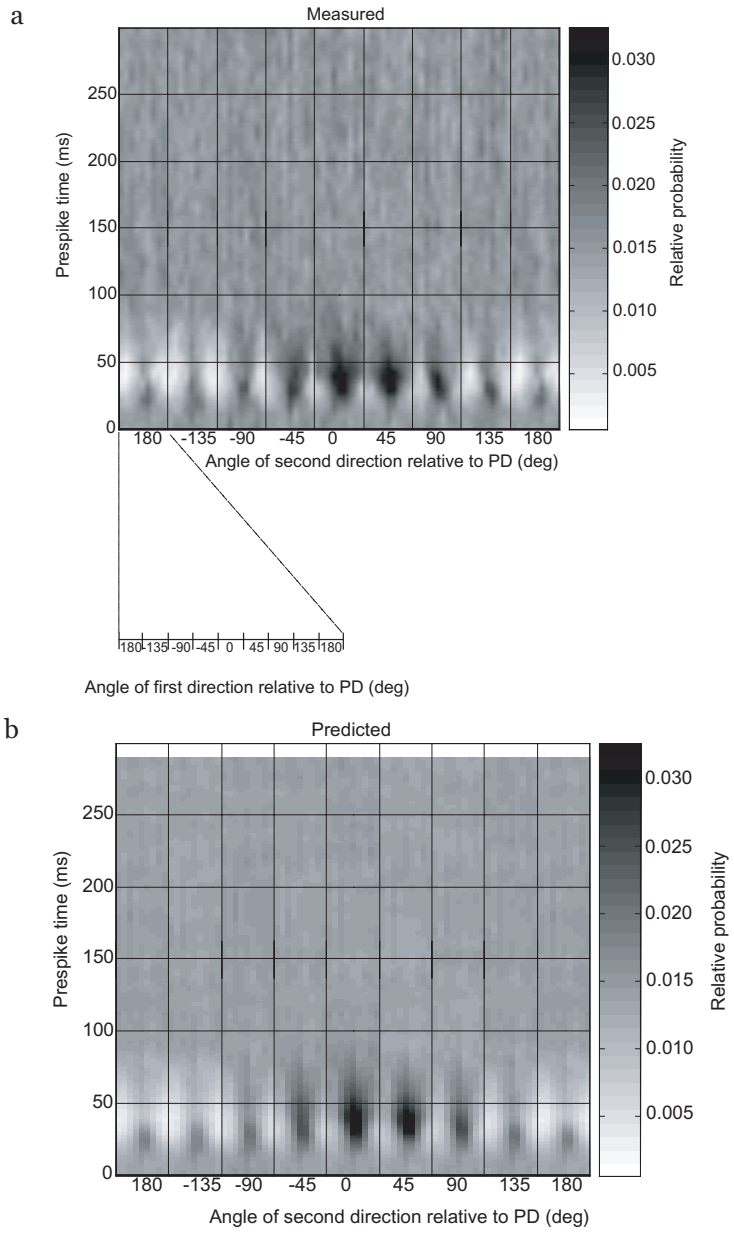

Fig. 3. a) Second order reverse correlogram for the same cell as in Fig. 1a and 2. All 64 combinations of two successive directions are plotted as a function of time, up to -300 ms. The major x-axis represents the angle of the second direction relative to the PD. Within each second direction category, the angles of the first directions are given, relative to the PD (enlarged piece of one subaxis). Shading denotes the magnitude of the relative probability of observing a particular combination of direction. b) Predicted second order RC-amplitudes for the cell in (a). Ordering of the first and second directions are the same as in (a).

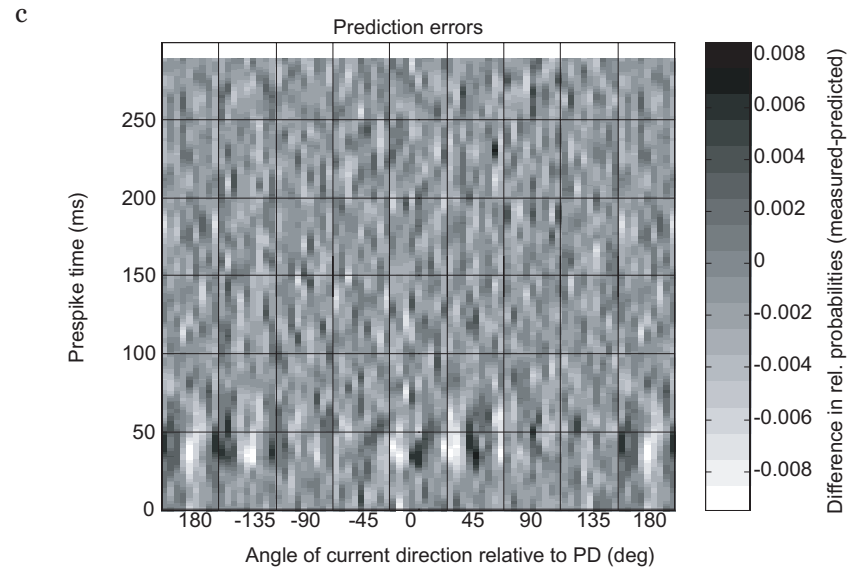

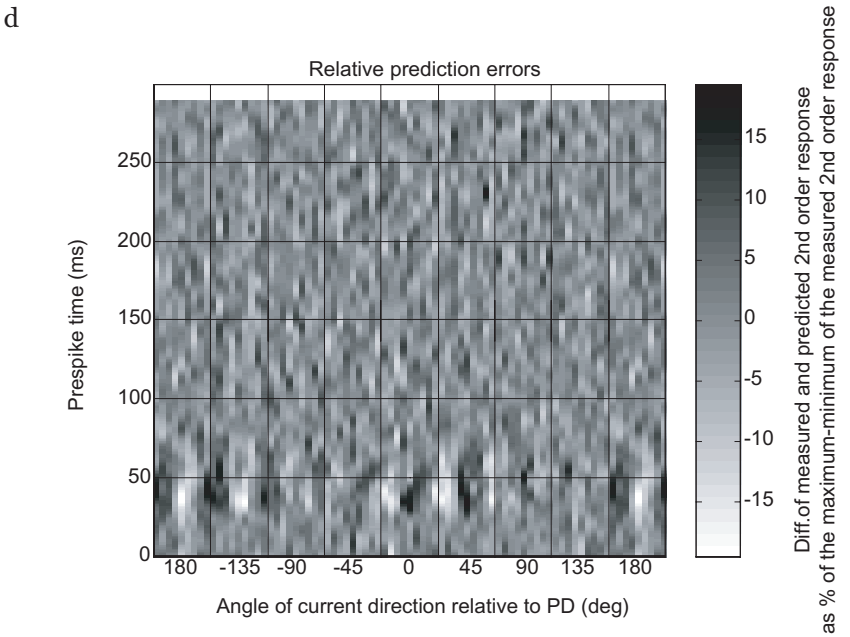

Fig. 3 *continued*. c) Differences between the measured second order RC-amplitudes and the predicted ones, with the same arrangement of second and first directions as in (a) and (b). d) Differences between the measured second order RC-amplitudes and predicted ones shown as percentages of the difference between maximum and minimum of the measured RC-amplitudes. Stimulus categorization as in the previous subfigures. In (b), (c) and (d), values for the last 10 ms are left open, because the predicted array is 300-dt ms long. See text for further explanation.

Figure 3a shows a regular pattern of facilitation (black spots) and suppression (white spots) and Figure 3b illustrates that this pattern follows the prediction based on linear temporal integration reasonably well, at least qualitatively. To quantify the differences, predicted RC-amplitudes were subtracted from the measured ones with results as illustrated for one cell in Figure 3c. The resulting differences were expressed as a percentage of the total RC-amplitude range for a cell (maximum - minimum of the measured probability values). Figure 3c shows, that the prediction errors vary between about ±15 percent. The errors suggest a regular pattern of directionally selective interactions. In the results, we will describe and quantify these interactions for complex cells in area 18 and in PMLS.

Results

Area 18

Data for 32 complex cells in area 18 were qualitatively highly similar. In all cases the first order analyses revealed a similar, monophasic reverse correlogram with a mean peak latency of about -56 ms. The pattern of nonlinear, directional interactions was also highly similar across the whole population of cells. Therefore, we summarized the results by averaging the relative prediction errors for all cells. Hereto, directions were expressed relative to the preferred direction. Figure 4a shows the results for different pairs of successive stimulus directions. The pattern of nonlinearities (errors in the linear predictions due to interactions between members of a pair) is similar to that for the cell in Figure 3. Enhancing effects were seen for successive stimuli at

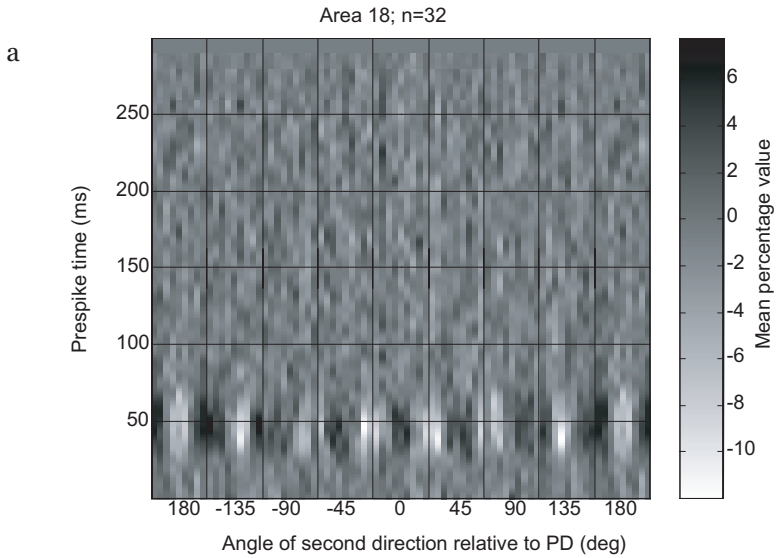

Fig. 4. *Figure continues on facing page.*

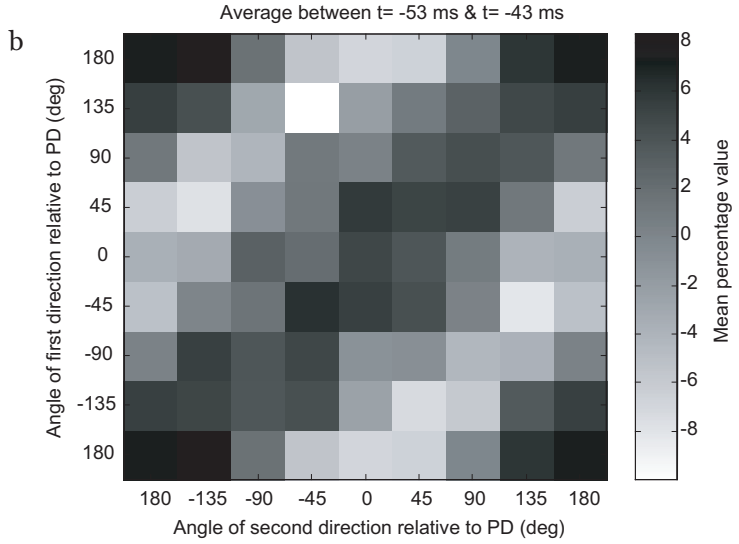

Fig. 4. a) Array of the mean temporal interactions for *dt*=1 of the area 18 cell population (see Fig. 3d and text for further explanation). Stimulus categorization as in Fig. 3a. b) Average slice plot of 11 slices of (a) taken at prespike times between -43 ms and -53 ms.

angles between 0 deg, ±45 deg, and to a lesser extent also at ±90 deg. Suppressing effects were present when this angle was larger, either ±135 deg or 180 deg.

Mean prediction errors were between +8 and -12 percent. In order to capture the pattern of directional interactions, we plotted the important segment of Figure 4a in another format in Figure 4b. Figure 4b shows a matrix of 8x8 directions, averaged over a time period of 11 ms, centered around the maximum deviations (-47 ms) in Figure 4a.

As a next step in the analysis, a mean relative prediction error array was obtained for each *dt*. For each of these arrays, at each prespike time, the variance of the percentage values was calculated in order to quantify the magnitude of nonlinear temporal interactions in time. The resulting variance curves are shown in Figure 5. For the successive stimulus combinations, the largest variance occurred at about -50 ms. The longer the time between stimuli, the lower the peak of the variance curves, corresponding to a reduction of nonlinear temporal interactions. The peak shifted towards shorter times with increasing *dt*. This was however partly determined by the analysis method. Predictions based on multiplying the first-order probability functions for larger *dt*'s, shifted the resulting peak(s) away from the reference spike-time. Subtracting these curves from the measured, non-shifted ones, thus resulted in a shift of the peak towards the reference spike-time.

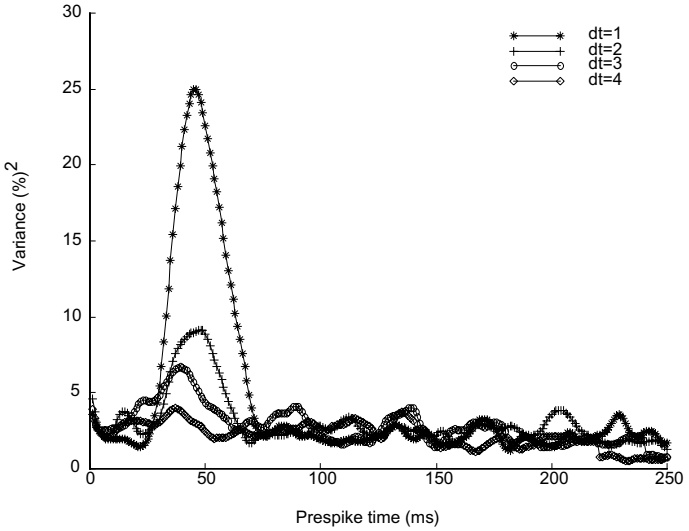

Fig. 5. Variance curves of area 18 mean relative prediction errors for different time intervals of stimulus combinations (*dt*'s). Intervals were multiples of motion step durations, as indicated in the inset. For each relative prediction error, at each prespike time, the variance across the stimulus combinations was calculated and plotted up to -250 ms. See text for further details.

PMLS

Our previous first order analysis revealed two basic types of reverse correlograms in PMLS: monophasic and biphasic ones (Vajda et al., 2003a). Monophasic reverse correlograms, like in area 18, exhibited preferences for a single or a small number of neighboring directions (mean peak latency about -60 ms). Biphasic cells on the other hand, showed increased sensitivity for their non-preferred (non-PD) direction at longer prespike times than for their preferred direction, that is, these cell's preferred direction changed over time. The majority of the PMLS cells (88%) showed monophasic response behavior. Five PMLS cells exhibited to various degrees biphasic behavior. Because of their distinct first order reverse correlation characteristics, we will first present results of the second order analysis on monophasic PMLS cells and thereafter consider the biphasic cells.

Monophasic PMLS cells

An example of a monophasic cell's first order reverse correlogram is shown in Figure 6a. For the same cell, the relative prediction errors for *dt*=1 are shown in Figure 6b. In Figure 6b, the majority of nonlinear interactions is visible between -30 ms and -60 ms. Positive effects were seen for the combination of first ND, second PD, but first PD, second ND and first -135, second +45 were also more effective than predicted. For all of these stimulus combinations, the first and second directions

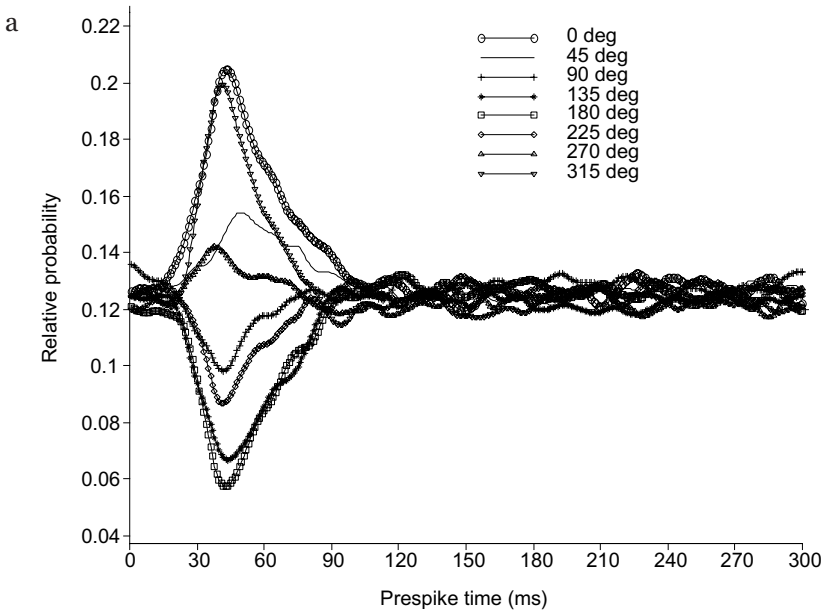

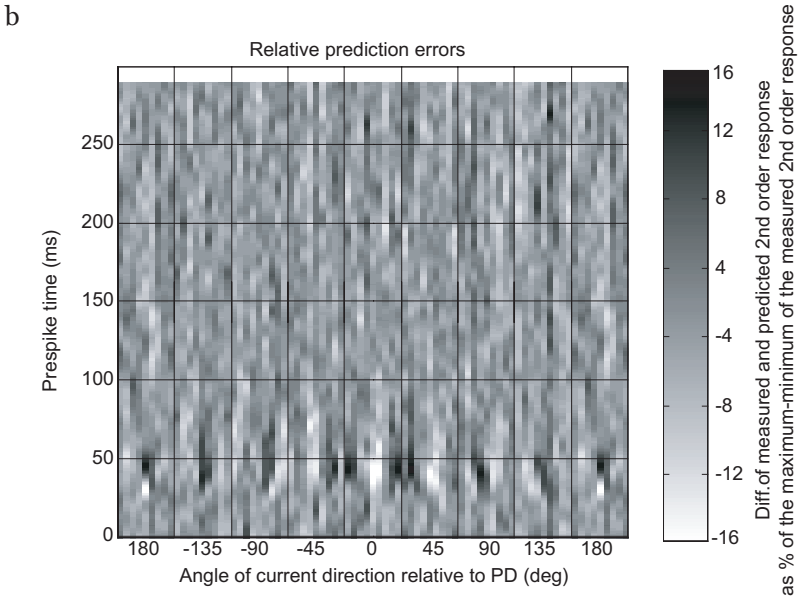

Fig. 6. a) First order reverse correlograms of a monophasic PMLS cell. The stimulus sequence consisted of 30000 motion impulses, presented with a time delay of 10 ms. b) Differences between the measured second order responses and the predicted ones for the cell from (a) for dt=1, shown as percentages of the maximum minus minimum of the measured responses. Stimulus categorization as in Fig. 3a.

were opposite to each other. Suppressive effects were seen predominantly at combinations of first PD, second PD, and to a lesser extent at combinations, where the first and second directions were either 0 deg or 45 deg apart. The directional interactions for this monophasic PMLS cell were opposite to those found for area 18. Five cells from the entire monophasic population in PMLS (n=36) showed similar nonlinear temporal interactions. The majority of cells in PMLS, however, showed no obvious, systematic directional interactions. Figure 7 shows the relative prediction errors averaged for all monophasic PMLS cells for successive motion steps.

Unlike our finding for the area 18 cell population, the mean relative prediction error plot did not show a systematic pattern of nonlinear interactions (Fig. 7). Although the range of relative prediction errors was similar to that in area 18 (compare shading values in Fig. 4a and Fig. 7), the nonlinear interactions were randomly spread throughout the different stimulus combinations and prespike times. These interactions therefore represent a higher noise level in the PMLS recordings, rather than systematic directional interactions. This is also reflected in the variances over time, as shown in Figure 8 for four *dt* values. The variance curves in Figure 8 do not show a systematic increase or decrease, except that the curves for *dt*=3 and *dt*=4 peak at t=0. We think this is an artifact and will come back to it in the Discussion.

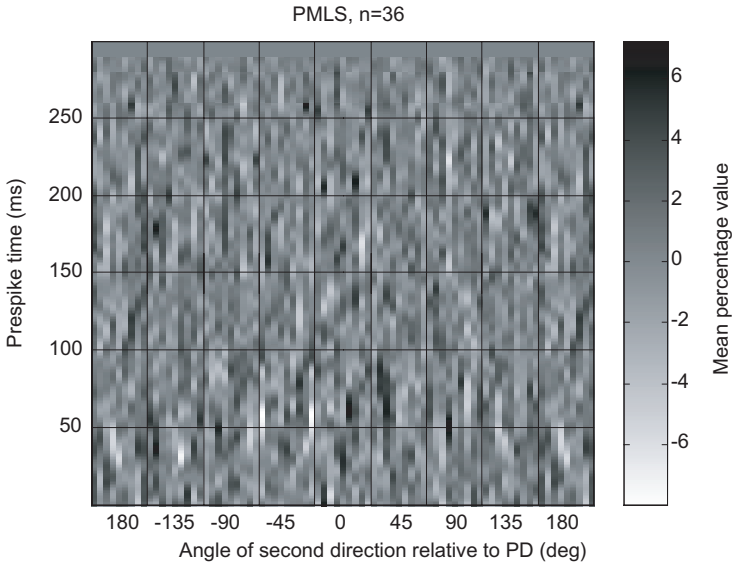

Fig. 7. Array of mean temporal interactions for *dt*=1 of the PMLS cell population (see Fig. 3d and text for further explanation). Stimulus categorization as in Fig. 3a.

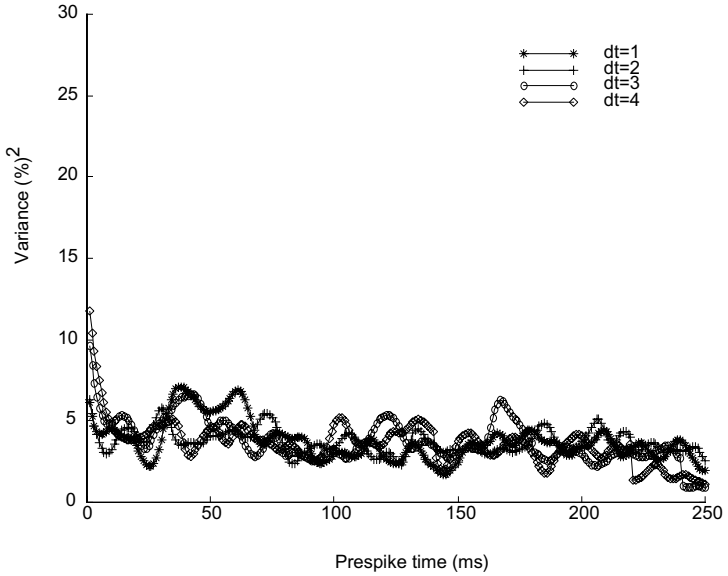

Fig. 8. Variance curves of monophasic PMLS mean relative predicted errors for different time intervals between members of stimulus pairs. Intervals were multiples of motion step durations, as indicated in the inset. For each mean percentage array, at each prespike time, the variance across the stimulus combinations was calculated and plotted up to -250 ms.

Biphasic neurons

First order reverse correlograms for a biphasic PMLS complex cell are depicted in Figure 9a. The first peak in the first order correlogram had a latency of about 60 ms. The cell had a preferred delay of 80 ms, the value used in MRC measurements. The time difference between the two peaks was 105 ms. The observed reversal of preferred direction in biphasic cells could be due to several different phenomena. It could result from cell-specific, intrinsic response properties, such as an automatic gain control (adaptation), or it could result from delayed negative feedback from similarly tuned cells. Our data do not allow us to distinguish between these possible mechanisms. However, we can determine to what extent the second peak is due to nonlinear directional interactions. If the second peak is due to a specific combination of directions, say non-PD-PD, then we should expect large prediction errors around the time of the second peak, i.e. at a delay of 160 ms.

Only for a single biphasic cell, the one shown in Figure 9, did we find an increased prediction error at the expected time. Figure 9b shows a positive prediction error for a combination of PD followed by the non-PD, i.e. an RC-amplitude increase larger than expected on the basis of first order correlograms. Clearly, this effect is opposite to what causes the biphasic profile. To establish the noise level in interaction plots, we extended the nonlinear analysis to a time period of 1s rather than the 300

ms used up to now. Figure 10 presents variance curves for several *dt* values, for all five biphasic cells. The bottom panel in Figure 10a shows data for the cell in Figure 9.

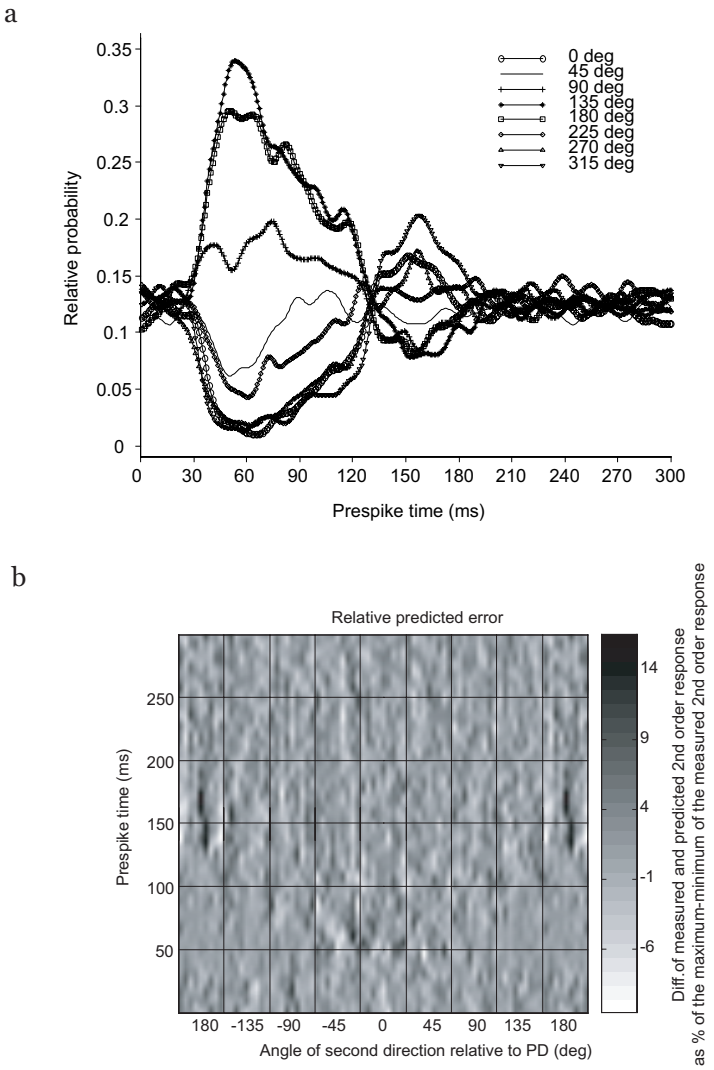

Fig. 9. a) First order reverse correlograms of a biphasic PMLS cell. b) Differences between the measured second order profiles and the predicted ones for the cell from (a) for *dt*=1, shown as percentages of the maximum minus minimum of the measured responses. Stimulus categorization as in Fig. 4a. This cell had a preferred delay of 80 ms.

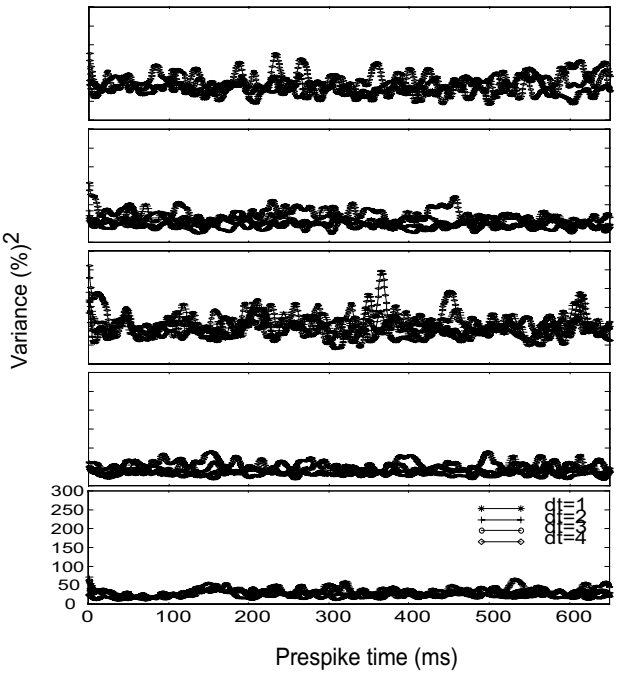

Fig. 10. Variance curves of the biphasic PMLS cells for different time intervals (dt) of stimulus combinations. Each panel represents one cell. Scaling and the symbols of the inset hold for all panels. The bottom panel gives the results for the cell in Fig. 9.

There is a consistent increase around 160 ms in the bottom panel, but the increase does not surpass the noise level in the variance data. The other cells showed no consistent effects (upper four panels in Fig. 10). The analysis thus excludes that nonlinear interactions due to specific combinations of directions play a major role in causing a biphasic reverse correlation profile.

Summary of the main results

The main finding of the present study is, that area 18 special complex cells show considerable nonlinear interactions between the members of a pair of temporally separated motion directions (Fig. 4, 5) and that most of the PMLS complex cells with 'special complex' -like behavior do not show such nonlinear effects (Fig. 7, 8). Reverse correlograms for area 18 neurons exhibited facilitatory nonlinear second order temporal interactions for motion directions less than 90 deg apart (Fig. 4a, b). Suppressive effects were observed for directions separated by at least 135 deg (Fig. 4a, b). Successive motion directions caused the strongest nonlinear behavior. The nonlinear interaction effects decreased with increasing temporal separation of the members of a direction pair (Fig. 5).

Results for 'special complex'-like PMLS cells were heterogeneous. Few monophasic neurons exhibited nonlinear behavior, and only one nonlinear biphasic cell was encountered (Fig. 9 and bottom panel in Fig. 10). The type of nonlinear interaction found in PMLS was quite opposite to that found in area 18. Opposite motion directions caused facilitatory and similar directions inhibitory temporal interactions (Fig. 6). The entire cell population, however, did not show a systematic increase or decrease in magnitude of interactions (Fig. 7, 8).

Discussion

Our main finding is that area 18 and PMLS complex cells that are sensitive to the direction of texture motion, differ in their second order temporal behavior: area 18 neurons form a homogenous group, exhibiting facilitatory nonlinear temporal interactions for similar motion directions, and suppressive interactions for opposite directions. These effects were strongest for directions that had small temporal offsets (dt=1, dt=2). PMLS on the other hand, included a variety of cells. From the monophasic cell population, some cells exhibited a nonlinear second order interaction effect that was opposite to that found in area 18. For these cells, opposite directions were facilitatory and similar directions were inhibitory. From the cells with a biphasic first order reverse correlation profile only one showed some nonlinear temporal interaction, while the rest of the biphasic cells had linear second order temporal characteristics.

Studies that have analyzed higher order temporal and/or spatial interactions mostly used (ternary) white noise stimuli of optimally oriented, multiple or single bars (Baker, 2001; Citron & Emerson, 1983; Emerson et al., 1987; Jacobson et al., 1993; Gaska et al., 1994). Studies on complex cells were focused on the nonlinearities in processing of image luminance and possible direction selectivity that might arise from extra nonlinear behavior of primarily linear (space-time oriented) luminance filters (Emerson et al., 1992; Baker, 2001; Touryan et al., 2002). Nonlinear direction selective subunits in complex cells have been found (Emerson et al., 1987) and evidence is accumulating that their nonlinear behavior is a squaring operation (Emerson et al., 1992; Touryan et al., 2002) that might underlie the computation of motion energy (Adelson & Bergen, 1985). These studies concerned the generation of complex cell direction selectivity. In the present study, however, direction selectivity of complex cells was a prerequisite, a starting point. We did not study the emergence of direction selectivity. Taking the complex cells' first order directional selective behavior (Vajda et al., 2003a) for granted, we wanted to find out whether there are nonlinear temporal interactions in the directionally selective responses of these neurons. To our knowledge, no other study has addressed this or a similar question yet.

The reverse correlation profiles of both the monophasic and biphasic PMLS cells require some additional attention. For larger time separations between motion directions (*dt*=3 & *dt*=4) variance magnitudes indicating nonlinear interactions were quite large between t=0 and about t=-10 ms (Fig. 8 and 10). This was not seen for the monophasic area 18 cells at corresponding times and *dt* values. In the case of monophasic PMLS cells, we explain this effect by the assumption that neurons were not strictly monophasic, but that some of them might have had a slightly biphasic character, which was difficult to exclude or ascertain from the first order reverse correlogram. Namely, in the case of biphasic cells this effect can be explained by the greater variation in the predictions than in the monophasic cells. In biphasic cells, the exact shape and timing of both peaks of the first order reverse correlogram influence the predictions. This influence is stronger at higher *dt* values, when the predicted RC-amplitude at short *t* values is a direct consequence of a multiplication of first order reverse correlation data at the times around the two peaks. Subtracting the predictions from the measured RC-amplitudes at short *t* values often results in high residual values, as reflected by a rise of the variance curves for *dt*=3 and *dt*=4. A detailed discussion of such estimation-errors of higher order responses to white-noise stimuli can be found in the book by Marmarelis and Marmarelis (1978).

Area 18 neurons

In area 18, an RPA making multiple steps in the preferred or similar directions was more effective in eliciting spikes than would be predicted from the first order reverse correlograms. This effect was largest for successive stimuli. Motion steps in opposite directions were less effective than predicted. These results clearly showed that the cell's response to a motion pulse depended strongly on the recent history of stimulus directions. Reverse correlograms to stimulus pairs differed from the linear sum of the separate RC-amplitudes. For complex cells in area 18 the effects increase responsiveness to stimulus pairs of similar directions, and thus ameliorate coherence detection. Temporal integration of briefly presented motion stimuli is therefore highly effective in these cells.

Figure 5 showed that the nonlinear effects rapidly vanished as the time between members of pairs of motion steps increased. The question arises to what extent the observed nonlinear effect directly correlates with the cells' response level. Do the effects depend on temporal overlap of first order RC-amplitudes, or do they remain, even after the overlap has completely disappeared? To answer this question, we first calculated the population variance curve for the first order RC-amplitudes of all area 18 complex cells. Such a curve gives an estimate of the overall amplitude and width of the first order RC-amplitudes. Next we determined the temporal overlap in the variance curve, and the same curve shifted by the mean time interval for the different *dt* values. On average, a *dt* value of 4 corresponded to a time delay of 80 ms (a single step delay was on average 20 ms). We found that the decline in nonlinear effects corresponded nicely with the decline in temporal overlap: for a time shift of

80 ms the variance curves still showed a small overlap. The nonlinear integration can therefore be explained quite well by an accelerating stimulus-response curve. The idea is that a single motion step is relatively ineffective due to the initial, shallow slope of the response curve, whereas a second stimulus can push the response into the steeper part.

For monophasic PMLS neurons that showed nonlinear second order behavior, the opposite of the area 18 directional interactions was observed: opposite stimulus directions (or nearly opposite) caused a decrease of responsiveness, while similar directions enhanced spike probability. Such a behavior makes a cell more sensitive to sudden changes in directions (temporal motion contrast). Biphasic reverse correlation profiles, found in 5 PMLS cells out of 41, were found not to result from specific combinations of stimulus directions. The first order profile shows a preference for non-PD followed by the PD. The nonlinear interaction analysis, however, did not reveal any such preferences. For the one cell showing an effect it was in fact reversed. The biphasic profile in these PMLS cells therefore results from another mechanism, which might either be intrinsic to the cell's responsivity to single directions, or result from linear summation of interactions between cells. Our analysis cannot differentiate between such possible mechanisms.

Based on the present results, we suggest that special complex cells in area 18 and PMLS are optimized for different tasks. Area 18 neurons form a homogenous population in terms of nonlinear second order behavior in the temporal domain. This area seems to play a straightforward role in local motion coherence detection where optimal integration is required. PMLS cells on the other hand form a heterogeneous population, where motion opponency rather than optimal integration seems to play a more important role. A minority of the cells, those with a biphasic profile, seem to be tuned to reversals of direction. The wide variety of interactions in PMLS is well in line with its presumed versatile role in visual processing. As examples we mention three-dimensional motion (Akase et al., 1998; Rauschecker et al., 1987; Brenner & Rauschecker, 1990; Li et al., 2000; Brosseau-Lachaine et al., 2001), depth perception (Krüger et al., 1993b; Bacon et al., 2001) or other motion related tasks such as ocular near response (Bando et al., 1992; Takagi et al., 1992; Takada et al., 2000; Toda et al., 2001), saccade-related responses (Yin & Greenwood, 1992), ocular following reflex (Zernicki et al., 1994) or visual attention (Lomber, 2001).

The biphasic profile that we found in a minority of the PMLS cells remains somewhat of a puzzle. It seems unlikely that the time difference between the first and second peak arises from lateral interactions within PMLS. The time difference was on average 60 ms, much longer than would be expected for local interactions, and also much longer than the delayed cortical response in macaque V1 and MT areas for a change of non-preferred to preferred motion directions (Bair et al., 2002). The most likely explanation at present seems to be an intrinsic gain control mechanism. If this hypothesis is correct, then our data suggest that motion adaptation first starts to play a role at the level of PMLS in cat extrastriate visual cortex.

References

Adelson, E. H., Bergen, J. R. (1985). Spatiotemporal energy models for the perception of motion. *J Opt Soc Am A*. **2**: 284-99.

Akase, E., Inokawa, H., Toyama, K. (1998). Neuronal responsiveness to three-dimensional motion in cat posteromedial lateral suprasylvian cortex. *Exp Brain Res*. **122**: 214-26.

Bacon, B. A., Mimeault, D., Lepore, F., Guillemot, J. P. (2001). Spatial disparity sensitivity in area PMLS of the Siamese cat. *Brain Res*. **906**: 149-56.

Bair, W., Cavanaugh, J. R., Smith, M. A., Movshon, J. A. (2002). The timing of response onset and offset in macaque visual neurons. *J Neurosci*. **22**: 3189-205.

Baker, C. L., Jr. (2001). Linear filtering and nonlinear interactions in direction-selective visual cortex neurons: a noise correlation analysis. *Vis Neurosci*. **18**: 465-85.

Bando, T., Takagi, M., Toda, H., Yoshizawa, T. (1992). Functional roles of the lateral suprasylvian cortex in ocular near response in the cat. *Neurosci Res*. **15**: 162-78.

Borghuis, B. G., Perge, J. A., Vajda, I., van Wezel, R. J., van de Grind, W. A., Lankheet, M. J. (2003). The motion reverse correlation (MRC) method: A linear systems approach in the motion domain. *J Neurosci Methods*. **123**: 153-66.

Brenner, E., Rauschecker, J. P. (1990). Centrifugal motion bias in the cat's lateral suprasylvian visual cortex is independent of early flow field exposure. *J Physiol*. **423**: 641-60.

Brosseau-Lachaine, O., Faubert, J., Casanova, C. (2001). Functional sub-regions for optic flow processing in the posteromedial lateral suprasylvian cortex of the cat. *Cereb Cortex*. **11**: 989-1001.

Citron, M. C., Emerson, R. C. (1983). White noise analysis of cortical directional selectivity in cat. *Brain Res*. **279**: 271-7.

Crook, J. M. (1990). Directional tuning of cells in area 18 of the feline visual cortex for visual noise, bar and spot stimuli: a comparison with area 17. *Exp Brain Res*. **80**: 545-61.

Emerson, R. C., Citron, M. C., Vaughn, W. J., Klein, S. A. (1987). Nonlinear directionally selective subunits in complex cells of cat striate cortex. *J Neurophysiol*. **58**: 33-65.

Emerson, R. C., Korenberg, M. J., Citron, M. C. (1992). Identification of complex-cell intensive nonlinearities in a cascade model of cat visual cortex. *Biol Cybern*. **66**: 291-300.

Gaska, J. P., Jacobson, L. D., Chen, H. W., Pollen, D. A. (1994). Space-time spectra of complex cell filters in the macaque monkey: a comparison of results obtained with pseudowhite noise and grating stimuli. *Vis Neurosci.* **11**: 805-21.

Hamada, T. (1987). Neural response to the motion of textures in the lateral suprasylvian area of cats. *Behav Brain Res.* **25**: 175-85.

Hammond, P., Ahmed, B. (1985). Length summation of complex cells in cat striate cortex: a reappraisal of the "special/standard" classification. *Neuroscience.* **15**: 639-49.

Hammond, P., MacKay, D. M. (1975). Differential responses of cat visual cortical cells to textured stimuli. *Exp Brain Res.* **22**: 427-30.

Hammond, P., MacKay, D. M. (1977). Differential responsiveness of simple and complex cells in cat striate cortex to visual texture. *Exp Brain Res.* **30**: 275-96.

Hammond, P., Pomfrett, C. J. (1989). Directional and orientational tuning of feline striate cortical neurones: correlation with neuronal class. *Vision Res.* **29**: 653-62.

Hammond, P., Pomfrett, C. J. (1990). Directionality of cat striate cortical neurones: contribution of suppression. *Exp Brain Res.* **81**: 417-25.

Jacobson, L. D., Gaska, J. P., Chen, H. W., Pollen, D. A. (1993). Structural testing of multi-input linear-nonlinear cascade models for cells in macaque striate cortex. *Vision Res.* **33**: 609-26.

Julesz, B. (1971) Foundations of Cyclopean Perception. Chicago: University of Chicago Press.

Kiefer, W., Kruger, K., Strauss, G., Berlucchi, G. (1989). Considerable deficits in the detection performance of the cat after lesion of the suprasylvian visual cortex. *Exp Brain Res.* **75**: 208-12.

Krüger, K., Kiefer, W., Groh, A. (1993b). Lesion of the suprasylvian cortex impairs depth perception of cats. *Neuroreport.* **4**: 883-6.

Krüger, K., Kiefer, W., Groh, A., Dinse, H. R., von Seelen, W. (1993a). The role of the lateral suprasylvian visual cortex of the cat in object-background interactions: permanent deficits following lesions. *Exp Brain Res.* **97**: 40-60.

Li, B., Chen, Y., Li, B. W., Wang, L. H., Diao, Y. C. (2001). Pattern and component motion selectivity in cortical area PMLS of the cat. *Eur J Neurosci.* **14**: 690-700.

Li, B., Li, B. W., Chen, Y., Wang, L. H., Diao, Y. C. (2000). Response properties of PMLS and PLLS neurons to simulated optic flow patterns. *Eur J Neurosci.* **12**: 1534-44.

Lomber, S. G. (2001). Behavioral cartography of visual functions in cat parietal cortex: areal and laminar dissociations. *Prog Brain Res.* **134**: 265-84.

Marmarelis, P. Z., Marmarelis, V. Z. (1978) Analysis of Physiological Systems. The White-Noise Approach. New York: Plenum Press.

Merabet, L., Minville, K., Ptito, M., Casanova, C. (2000). Responses of neurons in the cat posteromedial lateral suprasylvian cortex to moving texture patterns. *Neuroscience*. **97**: 611-23.

Molenaar, J., Van de Grind, W. A. (1980). A stereotaxic method of recording from single neurons in the intact in vivo eye of the cat. *J Neurosci Methods*. **2**: 135-52.

Niida, T., Stein, B. E., McHaffie, J. G. (1997). Response properties of corticotectal and corticostriatal neurons in the posterior lateral suprasylvian cortex of the cat. *J Neurosci*. **17**: 8550-65.

Pasternak, T., Horn, K. M., Maunsell, J. H. (1989). Deficits in speed discrimination following lesions of the lateral suprasylvian cortex in the cat. *Vis Neurosci*. **3**: 365-75.

Pasternak, T., Maunsell, J. H. (1992). Spatiotemporal sensitivity following lesions of area 18 in the cat. *J Neurosci*. **12**: 4521-9.

Rauschecker, J. P., von Grünau, M. W., Poulin, C. (1987). Centrifugal organization of direction preferences in the cat's lateral suprasylvian visual cortex and its relation to flow field processing. *J Neurosci*. **7**: 943-58.

Reinoso-Suarez, F. (1961) Topografischer Hirnatlas der Katze fuer experimental-physiologische Untersuchung. Darmstadt: E. Merck AG.

Spear, P. D. (1991) Functions of extrastruate visual cortex in non-primate species. In: The Neural Basis of Visual Dysfunction (Leventhal, A. G., ed.), pp. 339-70: Macmillan Press.

Takada, R., Hara, N., Yamamoto, K., Toda, H., Ando, T., Hasebe, H., Abe, H., Bando, T. (2000). Effects of localized lesions in the lateral suprasylvian cortex on convergence eye movement in cats. *Neurosci Res*. **36**: 275-83.

Takagi, M., Toda, H., Yoshizawa, T., Hara, N., Ando, T., Abe, H., Bando, T. (1992). Ocular convergence-related neuronal responses in the lateral suprasylvian area of alert cats. *Neurosci Res*. **15**: 229-34.

Toda, H., Yoshizawa, T., Takagi, M., Bando, T. (2001). The properties of convergence eye movements evoked from the rostral and caudal lateral suprasylvian cortex in the cat. *Neurosci Res*. **39**: 359-67.

Touryan, J., Lau, B., Dan, Y. (2002). Isolation of relevant visual features from random stimuli for cortical complex cells. *J Neurosci*. **22**: 10811-8.

Toyama, K., Kitaoji, H., Umetani, K. (1991). Binocular neuronal responsiveness in Clare-Bishop cortex of Siamese cats. *Exp Brain Res*. **86**: 471-82.

Toyama, K., Komatsu, Y., Kasai, H., Fujii, K., Umetani, K. (1985). Responsiveness of Clare-Bishop neurons to visual cues associated with motion of a visual stimulus in three-dimensional space. *Vision Res*. **25**: 407-14.

Vajda, I., Lankheet, M.J.M., Borghuis, B.G., Van de Grind, W.A. (2003a). Dynamics of directional selectivity in area 18 and PMLS of the cat. Submitted to Cerebral Cortex.

Vajda, I., Lankheet, M.J.M., Van de Grind, W.A. (2003b). Spatio-temporal requirements for direction selectivity in area 18 and PMLS complex cells. Submitted to Vision Research

Von Grünau, M., Frost, B. J. (1983). Double-opponent-process mechanism underlying RF-structure of directionally specific cells of cat lateral suprasylvian visual area. *Exp Brain Res*. **49**: 84-92.

Von Grünau, M. W., Zumbroich, T. J., Poulin, C. (1987). Visual receptive field properties in the posterior suprasylvian cortex of the cat: a comparison between the areas PMLS and PLLS. *Vision Res*. **27**: 343-56.

Yin, T. C., Greenwood, M. (1992). Visuomotor interactions in responses of neurons in the middle and lateral suprasylvian cortices of the behaving cat. *Exp Brain Res*. **88**: 15-32.

Zernicki, B., Stasiak, M. (1994). The contralateral impairment of the orienting ocular-following reflex after lesions of the lateral suprasylvian cortex in cats. *Acta Neurobiol Exp (Warsz)*. **54**: 405-9.

Nederlandse samenvatting

Nederlandse samenvatting

Het verwerken van visuele bewegingsinformatie is van levensbelang voor alle dieren die een visueel systeem bezitten. Alle visuele informatie, dus ook beweging, wordt als tweedimensionaal beeld op het netvlies (de retina) van het oog geprojecteerd. Het netvlies is een zeer complex en gevoelig weefsel dat licht omzet in elektrische signalen, de actiepotentialen. Dit zijn elektrische ontladingen door celmembranen van zenuwcellen (neuronen), die met speciale micro-electrodes kunnen worden gedetecteerd. Door middel van actiepotentialen kunnen neuronen heel snel informatie met elkaar uitwisselen.

Niet alle soorten cellen produceren actiepotentialen. In het netvlies van de kat doen alleen de zogenaamde ganglioncellen dat. Zoals elke visuele zenuwcel heeft ook elke ganglioncel zijn eigen Receptieve Veld (RV). Het RV wordt gedefinieerd als dat gebied in het visuele veld, waarvan het vuurpatroon verandert wanneer het wordt gestimuleerd met bepaalde visuele prikkels. De receptieve velden van ganglioncellen hebben een circulair-symmetrische opbouw: de cel wordt in het midden van het RV gestimuleerd door licht óf donker, terwijl de omgeving het tegengestelde gedrag vertoont. We spreken van 'On-centrum/Off-omgeving'- of 'Off-centrum/On-omgeving'-cellen, waarbij 'On' verwijst naar stimulatie door licht en 'Off' naar stimulatie door donker.

Er zijn drie hoofdtypen retinale ganglioncellen (X, Y en W), die onder andere van elkaar verschillen in de grootte van hun receptieve velden, in de morfologie van hun cellichamen, en in de geleidingssnelheid van hun uitlopers. Door middel van hun lange uitlopers (axonen) die in de optische zenuw zijn samengebundeld, geven ganglioncellen visuele informatie door naar het corpus geniculatum laterale in de thalamus, dat in het Engels 'lateral geniculate nucleus' (LGN) heet en voortaan met deze afkorting wordt aangeduid. In de LGN vindt het volgende stadium van verwerking plaats.

De axonen van verschillende soorten retinale ganglioncellen eindigen in verschillende lagen van de LGN, die bij de kat uit zes lagen bestaat. De cellen in de LGN hebben eenzelfde type RV-structuur als die in het netvlies, omdat ze input krijgen van 2 tot 6 retinale ganglioncellen met grotendeels overlappende receptieve velden. Vanaf de LGN vertonen de uitlopers van axonen eveneens een geordend patroon: cellen uit bepaalde lagen van de LGN hebben uitlopers naar specifieke lagen van diverse visuele hersencentra, die op hun beurt vaak ook weer uitlopers terug naar de LGN hebben.

De primaire visuele cortex (area 17) is waarschijnlijk het meest bestudeerde hersenschorsgebied. Grote hoeveelheden uitlopers van de LGN eindigen daar. In area 17 vertonen de cellen voor het eerst bewegingsspecifieke responsen. Deze cellen hebben geen circulair-symmetrische opbouw, maar zijn onder te verdelen in twee hoofdtypen: simpele en complexe cellen. De eerste geven de voorkeur aan georiënteerde visuele prikkels zoals lange, lichte of donkere lijntjes die al dan niet in

een bepaalde richting bewegen. Hun RV is opgebouwd uit twee of meer parallelle langwerpige subvelden die op licht of donker reageren. De receptieve velden van complexe cellen hebben daarentegen geen gescheiden licht-donker domein: zij reageren overal in het RV op lichte of donkere stimuli. Deze cellen reageren nauwelijks op korte geflitste stimuli, maar des te meer op bewegende visuele prikkels. Afhankelijk van hun voorkeur voor specifieke bewegende stimuli kunnen verschillende typen complexe cellen worden onderscheiden. Zo zijn er speciale complexe cellen die vooral reageren op stimuli die bestaan uit vele korte lijnstukjes, balkjes, of puntjes. Dit type cel vuurt met hoge frequenties bij bewegende textuurpatronen, zoals de in dit proefschrift gebruikte Random Pixel Array (RPA).

De hogere hersencentra verwerken steeds specifiekere eigenschappen van visuele stimuli. De receptieve velden van hun cellen hebben daarom ingewikkelder structuren dan die in de primaire visuele cortex, maar kunnen nog steeds worden verdeeld in de twee basisgroepen van simpele en complexe cellen. Deze hogere centra krijgen veel van hun input van de primaire visuele cortex, maar ook rechtstreeks van subcorticale tussenstations. Net als de verbindingen tussen de LGN en area 17 zijn bijna alle verbindingen tussen area 17 of subcorticale gebieden met de hogere centra ook wederkerig.

Belangrijke hogere hersengebieden in de kat die betrokken zijn bij de verwerking van bewegende beelden, zijn area 18 en de Postero-Mediale-Laterale-Supraslyviane cortex (PMLS), de twee gebieden die in dit onderzoek werden bestudeerd. De eigenschappen van de speciale complexe cellen die richtingsgevoelig reageren op de beweging van willekeurige (random) texturen werden onderzocht. Waarom is zo'n respons-eigenschap belangrijk voor het zien van beweging?

In een random textuurpatroon als de RPA (zie Fig. 1 in Hoofdstuk 1) bevinden donkere en lichte elementen zich op willekeurige plaatsen in het patroon. Op een monitor beweegt zo'n patroon niet continu, maar bij elke presentatie worden de elementen een stukje verschoven in positie. Wanneer deze verschuiving snel genoeg plaatsvindt, wordt het beeld als continu bewegend ervaren. Dit is de schijnbare beweging die ook ten grondslag ligt aan de waargenomen beweging in televisiebeelden. In tegenstelling tot simpele cellen zijn complexe cellen in staat om beweging in complexe (random) texturen te detecteren. Ze kunnen, met andere woorden, het zogenaamde 'correspondentie-probleem' oplossen. Een RPA bevat geen vorm die de cellen zouden kunnen herkennen in opeenvolgende verplaatste beelden. Ze zijn dus afhankelijk van hun vermogen om elementen (afzonderlijke pixels of groepen van pixels) met elkaar te correleren. Dat betekent dat deze cellen zeer geschikt zijn om de basismechanismen van bewegingsdetectie (waaronder de correlatiestap) te bestuderen.

In dit proefschrift wordt vaak gerefereerd naar de zogenaamde bilocale bewegingsdetector (Fig. 2 in de Introduction). Deze detector signaleert de correlatie tussen twee opeenvolgende, maar verschoven presentaties van hetzelfde beeld. In het proces van de verwerking van bewegende stimuli zal deze detectie door een of

meer complexe cellen uitgevoerd kunnen worden, omdat zij richtingsgevoelig zijn en het correspondentieprobleem voor bewegende texturen kunnen oplossen. Waarschijnlijk convergeren er grote aantallen bilocale detectoren op iedere cel om de beweging van ieder textuurelelementje door te kunnen geven. De bilocale detector wordt alleen in deze context gebruikt; complexere modellen van bewegingsdetectie worden hier niet getoetst, noch worden nieuwe modellen uiteengezet.

In **hoofdstuk 1** wordt de snelheidsdetectie van complexe cellen in area 18 bestudeerd. Cellen die richtingsgevoelig zijn voor bepaalde stimuli, hebben ook een voorkeur voor een bepaalde bewegingssnelheid. Sommige cellen zijn pure snelheidsdetectoren, andere temporele frequentiedetectoren: hun respons hangt af van de spatiële structuur van de stimulus. Om te onderzoeken of complexe cellen van area 18 afgestemd zijn op temporele frequentie of op snelheid, is gebruik gemaakt van bewegende RPAs. Wat betreft temporele en spatiële frequentie zit een bewegende RPA ingewikkelder in elkaar dan een bewegend, in luminantie sinusoidaal gemoduleerd rasterpatroon, dat maar één spatiële en één temporele frequentie bevat. Desalniettemin is een bewegend RPA een geschikte stimulus om de eventuele snelheidsgevoeligheid van complexe cellen te bestuderen. Door de cellen te stimuleren met bewegende RPAs van verschillende snelheden en pixelgroottes, kan men hun respons in het tweedimensionale domein van snelheid en pixelgrootte beschrijven. Daarbij is het belangrijk te weten dat de kleinste pixel de zogenaamde hoge spatiële afsnijfrequentie bepaalt. De hoogste snelheid waarmee een RPA beweegt bepaalt de hoogste temporele afsnijfrequentie. Dit betekent dat er bij verschillende pixelgroottes en snelheden overlappende spatiële en temporele frequentiedomeinen zullen zijn, maar dat de hoge afsnijfrequenties het bereik afbakenen. Wanneer de cellen temporeel frequentiegevoelig zijn, zouden ze hun snelheid bij groter wordende pixels derhalve moeten verhogen. Dit zou resulteren in een georiënteerd responsprofiel in het tweedimensionale pixelgrootte-snelheidsdomein. Wanneer zij, aan de andere kant, niet voor temporele frequentie coderen, zullen de responsen langs één van de assen (pixelgrootte of snelheid) georiënteerd zijn. In bijna alle gevallen werd het laatste responsprofiel gevonden en waren de responsen langs de snelheid-as georiënteerd. Dit betekent dat deze cellen scherp zijn afgestemd op pixelgrootte en iets breder op snelheid.

In **hoofdstuk 2** werden de latentieperioden en de temporele dynamiek van de complexe celresponsen bestudeerd in area 18 en PMLS. Hierbij werden de cellen eveneens met bewegende RPAs gestimuleerd, maar met een nieuw ontwikkelde stimulatiemethode, die het mogelijk maakte om het responsverloop van de cellen tot op enkele milliseconden nauwkeurig te bestuderen. We wilden weten of complexe cellen in beide gebieden tegelijk hun bewegingsgevoeligheid ontwikkelen en of het verloop van de bewegingsgevoelige periode dezelfde is of niet. Omdat deze gebieden onderling sterk verbonden zijn en omdat beide gebieden door hetzelfde type ganglioncellen hun informatie binnenkrijgen, zouden ze een vergelijkbare

responsdynamiek in de tijd kunnen vertonen. Onze observaties bevestigden dat bewegingsgevoeligheid zich in beide gebieden ongeveer op hetzelfde moment ontwikkelt en dat ook het verloop van de bewegingsgevoelige periode vergelijkbaar is. Een kleine groep cellen in PMLS vertoonde een andersoortige responsdynamiek, die niet gevonden werd in area 18: deze cellen wisselden van voorkeursrichting in de tijd. Onze hoofdresultaten suggereren dat bewegingsdetectie tegelijkertijd wordt verwerkt in beide gebieden en dat de daartoe benodigde signalen door het gemeenschappelijke type ganglioncellen worden doorgegeven.

In **hoofdstuk 3** wordt teruggekeerd naar de bestudering van de elementaire bewegingsmechanismen van complexe cellen in area 18 en PMLS. De hoofdvraag was hier of de spatiotemporele beperkingen van de schijnbaar bewegende RPAs hetzelfde zijn in de twee gebieden en of die overeenkomen met die van area 17. Veel cellen in area 17 zijn afgestemd op een bepaalde stap en vertraging van de schijnbaar bewegende RPA. Voor elke complexe cel werden de optimale stimulusparameters zoals richting en snelheid bepaald. Ook werd gebruik gemaakt van de kleinste pixelgrootte die nog tot richtingsspecifieke respons leidde. De stimuli waren RPAs die met de voorkeurssnelheid ofwel in de voorkeursrichting, ofwel in tegenovergestelde richting bewogen. De voorkeurssnelheid werd in verschillende presentaties met steeds andere combinaties van stap en vertraging opgebouwd. De kleinste stap en vertraging gaf de gladste beweging. Alle bestudeerde PMLS cellen gaven de voorkeur aan deze gladde beweging. In area 18 reageerden veel cellen echter het beste op een stap-vertragingswaarde die een minder gladde beweging voorstelde. In area 18 was de gebruikte pixelgrootte medebepalend voor het al dan niet de voorkeur geven aan de gladste beweging: patronen met kleinere pixelgroottes leidden vaker tot een voorkeur voor niet-gladde beweging. In PMLS leidden zelfs kleine pixelgroottes tot een voorkeur voor de gladste beweging. Sommige area 18 cellen werden getest op stapgrootte en vertragingswaarden, die niet alleen de voorkeurssnelheid van de cel representeerden, maar ook een reeks hogere en lagere snelheden. De optimale stap bleek onafhankelijk te zijn van de vertraging, hetgeen suggereert dat de relatief brede snelheidsafstemming van deze cellen (zie Hoofdstuk 1) niet afhangt van de covariatie van stap- en vertragingswaarde.

Hoofdstuk 4 beschrijft de temporele interacties van celresponsen op bewegingsprikkels van verschillende richtingen voor complexe cellen van area 18 en PMLS. Hoewel beide gebieden textuurrichtingsgevoelige complexe cellen tellen, betekent dit niet dat deze cellen alle eenzelfde functionele rol hebben. Eerder werd al bijvoorbeeld aangetoond dat PMLS cellen ingewikkelder spatiële RV-structuren hebben dan cellen in andere gebieden. Wij verwachtten daarom dat de eigenschappen van hun temporele RV ook ingewikkelder zouden zijn. Men kan bijvoorbeeld stellen dat de volgorde van stimulusrichtingen ook bepalend is voor de respons van de cel. In dit hoofdstuk hebben we gekeken of de celrespons wordt beïnvloed door de volgorde van telkens twee opeenvolgende bewegingsrichtingen. Uitgaande van acht richtingen hebben we voor elk van de 64 richtingscombinaties de responsen van de

cellen in de tijd bestudeerd. Met behulp van een simpele lineaire voorspelling van de celresponsen keken we naar de niet-lineaire eigenschappen van de cellen. Area 18 cellen vertoonden bevorderende niet-lineaire responseigenschappen voor twee vergelijkbare richtingen en remmende niet-lineaire responseigenschappen voor richtingen die een hoek van meer dan 90 graden met elkaar vormden. Verschillende PMLS cellen vertoonden verschillend gedrag. Die met een duidelijke niet-lineare eigenschap vertoonden het omgekeerde effect van area 18 cellen: vergelijkbare richtingen hadden een remmend, en verschillende richtingen een bevorderend effect. Het lijkt erop dat integratie van vergelijkbare richtingen in area 18 belangrijk is en dat deze cellen daarom makkelijk de rol van coherente bewegingsdetectoren kunnen vervullen. In PMLS hebben opponente richtingen echter een bevorderend effect en lijken cellen dus geschikt voor het verwerken en/of detecteren van ingewikkeldere stimuli of stimuliconfiguraties zoals plotselinge richtingsovergangen.

Dankwoord aan de collegae

Mijn dank gaat vooral uit naar Martin, Bart en Wim. Discussies met Martin waren altijd zeer motiverend, ook in moeilijke perioden zoals na een serie mislukte experimenten of na een pijnlijk geval van dataverlies. De samenwerking met hem was altijd zeer prettig en van mijn kant wil ik graag de hoop uitspreken dat we ooit nog eens kunnen samenwerken. Bart schreef de achteraf gezien onmisbaar gebleken 'reverse' correlatie-code. Ik heb daar gretig gebruik van gemaakt (zie hoofdstukken 2 en 4). Verder was hij mijn meest nabije collega en dan doel ik niet alleen op het feit dat we één werkkamer deelden. Ik hoop dat hij niet voorgoed naar Amerika is vertrokken en dat hij ooit in goede gezondheid zal terugkeren (naar zijn echte vrienden). Wim was mijn promotor en dat betekent dat ik weinig met hem te maken had, althans in het begin van mijn onderzoek. Na zijn pensionering, die hij zelf immer betreurt, had hij meer tijd voor mij en mijn manuscripten, die ik altijd in rood gedecoreerd terugkreeg. Wim is een wandelende encyclopedie en menig keer heb ik me verbaasd over zijn altijd parate kennis en zijn vermogen alle feiten op orde te houden. Bart en ik noemden hem achter zijn rug 'onze held'.

Maarten, Mieke, János, Ervin, Jaap, Tao Ran, Ignace, Frans: met jullie kon ik het zeer goed vinden. Dank voor alle disussies, praktische hulp en zwarte humor. Zonder Miriam en Angela had ik veel zaken niet zo snel kunnen regelen en zonder de Robben, Theo, Hans, Henk en Wim L. had ik al mijn experimenten nooit zo efficiënt kunnen uitvoeren. Ed en Gerard worden bedankt voor hun twee rechterhanden en hun onovertroffen inventiviteit. Wat minder frequente maar desalniettemin leerzame en leuke contacten had ik met Rob P., Frank, Richard, Bert en André. Graag wil ik Wiebe bedanken voor zijn hulp met statistische problemen en de Matlab code. Mijn twee stagestudenten Klaas en Tessa hebben onmisbaar werk geleverd. Beiden waren enthousiaste leerlingen met een groot uithoudingsvermogen – een zeer nuttige kwaliteit in dit vak. Mijn koffiepauzes werden door de aanwezigheid van Chris en Anne altijd veel aangenamer. De nieuwe promovendi in onze groep, Jacob, Jeanette, Roger, Wouter en Lonneke: ondanks de korte tijd dat we elkaar kennen hebben we toch een goede tijd gehad. Veel geluk en success met jullie promotieonderzoek!

Köszönetszó

Köszönettel elõszõr is a szüleimnek tartozom, akik lehetõvé tették, hogy Hollandiában folytassam tanulmányaimat. Õk a tudomány szeretetére tanítottak és jóllehet nem sokat értettek az elmúlt években folytatott kutatásaimból, mindig érdeklõdve hallgatták az azokról szóló beszámolóimat. Sok köszönettel tartozom Josnak, továbbá Zsuzsának és a barátaimnak is. Mindannyian megértõen támogattak a nehéz napokban és rendszeresen érdeklõdtek a kísérleteim kimenetele felõl.

Curriculum Vitae

De auteur van dit proefschrift behaalde haar middelbare school diploma in 1991 in Bácstopolya (voormalig Joegoslavië). Datzelfde jaar verhuisde ze naar Nederland, waar ze in 1992 begon aan haar studie Biologie aan de Vrije Universiteit te Amsterdam. Het propaedeutisch examen werd behaald in 1993, waarna ze zich specialiseerde in neurofysiologische technieken. Een eerste onderzoekstage werd op de Vrije Universiteit gedaan en betrof de hersenen van de verouderende poelslak. Onder leiding van Dr Cees Janse werden simultane intracellulaire afleidingen gemaakt van twee identificeerbare neuronen voor en na beschadiging van hun connectie. In 1996 begon ze aan haar tweede stage bij Dr Martin Lankheet aan de Universiteit van Utrecht. Daar heeft ze extracellulaire afleidingen gedaan aan neuronen in het primaire visuele centrum van de kat en bestudeerde ze hun bewegingsverwerkende mechanismen. In 1997 heeft ze een derde stage gelopen in Davis, Californië, onder leiding van Dr Richard van Wezel en Dr Ken Britten. Daar heeft ze niet alleen ervaring met psyschofysisch werk opgedaan, maar zich ook de programmeertaal C eigen gemaakt. De afstudeerscriptie werd onder begeleiding van Dr Nico Schellart geschreven op het Academisch Medisch Centrum in Amsterdam. Het onderwerp van de scriptie was de ontwikkeling van het visuele systeem van kinderen door middel van zogenaamde 'visual evoked potentials'. In 1998 keerde zij terug naar Utrecht waar ze in deeltijd begon te werken aan haar promotieonderzoek. Tijdens dit onderzoek heeft ze verschillende cursussen gevolgd, twee stagestudenten begeleid en deelgenomen aan verschillende internationale congressen in Europa en de Verenigde Staten. Vanaf juni 2003 is zij werkzaam op het Nederlandse Instituut voor Hersenonderzoek waar ze samen met Dr Jaap van Pelt en Dr Ger Ramakers werkt aan een Europees project onder de naam 'Neurobit'. Het onderzoek wordt gedaan in samenwerking met zes Europese academische en industriële projectgroepen en heeft tot einddoel het trainen op doelgericht gedrag van een mobiele robot, die gekoppeld is aan een gekweekt neuronaal netwerk.

The author of this PhD dissertation received her high school diploma in Bácstopolya (Former Yugoslavia) in 1991. That year she moved to the Netherlands, where she started her studies in Biology at the Vrije Universiteit in Amsterdam in 1992. She took her propaedeutic exams in 1993, after which she specialised in neurophysiological techniques. A first practical training period was conducted at the Vrije Universiteit and concerned the brains of ageing snails. Supervised by Dr Cees Janse, she made simultaneous intracellular recordings from two identifiable neurons before and after damaging their connection. In 1996 she started a second research project as a trainee under supervision of Dr Martin Lankheet at the Utrecht University. Here she conducted extracellular recordings on neurons in the primary visual cortex of the cat, studying their mechanisms of movement perception. In 1997

she participated in a third project in Davis, California, under supervision of Dr Richard van Wezel and Dr Ken Britten. Here she gained experience in psychophysical research and learnt to program in C. She wrote her final paper under supervision of Dr Nico Schellart at the Amsterdam Academic Medical Centre on the development of the visual system of children, using so-called 'visual evoked potentials'. In 1998 she returned to the Utrecht University to start her research for this thesis. In the meantime she took several training courses, supervised two trainee students, and took part in several international congresses in both Europe and the USA. In June 2003 she started working in a post-doctoral position at the Netherlands Institute for Brain Research, joining Dr Jaap van Pelt and Dr Ger Ramakers in a European research project called 'Neurobit'. This project involves six academic and industrial groups from different countries and aims at coupling a mobile robot to a cultured neuronal network and training the robot for purposeful behavior.

Publications

Articles

Vajda, I., Lankheet, M.J.M, van Leeuwen, T.M., van de Grind, W.A. (2002). On the velocity tuning of area 18 complex cell responses to moving textures. *Visual Neuroscience* **19**:651-659.

Borghuis, B. G., Perge, J. A., Vajda, I., van Wezel, R. J., van de Grind, W. A., Lankheet, M. J. (2003). The motion reverse correlation (MRC) method: A linear systems approach in the motion domain. *J Neurosci Methods*. **123**: 153-66.

Vajda, I., Lankheet, M.J.M, Borghuis, B. G., Perge, van de Grind, W. A (2003). Dynamics of directional selectivity in area 18 and PMLS of the cat. Submitted to *Cerebral Cortex*.

Vajda, I., Lankheet, M.J.M., van de Grind, W.A. (2003) Spatio-temporal requirements for direction selectivity in area 18 and PMLS complex cells., Submitted to *Vision Research*.

Vajda, I., Lankheet, M.J.M, Borghuis, B. G., Perge, van de Grind, W. A (2003). Temporal interactions in direction selective complex cells of area 18 and PMLS of the cat. *To be submitted.*

Abstracts

Lankheet, M.J.M., Przybyszewski, A.W., Vajda, I. (1998). Spatio-temporal integration of motion information by complex cells in cat area 17. Annual meeting of the Society for Neuroscience, Los Angeles. **28** (*suppl*).

Vajda, I., Lankheet, M.J.M., Huijsman, K. (2000). Summation and integration underlying complex cell receptive fields in cat area PMLS and area 18. Annual meeting of the Association for Research in Vision and Opthalmology, Fort Lauderdale. **41** (*suppl*).

Vajda, I. (2001). Motion reverse correlation. Oral presentation at the 8th Hungarian Vision Symposium, Szeged, Hungary.

Vajda, I., Borghuis, B.G., Lankheet, M.J.M. (2002). Dynamics of direction selectivity in area 18 and PMLS of the cat. Annual meeting of the Society for Neuroscience, Orlando. **32** (*suppl*).

Vajda, I., Lankheet, M.J.M. (2002). Tuning for step size and delay in directionally selective complex cells in cat area 18. *Perception*, **25** (*suppl*).